

# The role of Sphingosine-1-phosphate receptors in adipocytes and adipose tissues

Dissertation

zur

Erlangung des Doktorgrades (Dr. rer. nat.)

der

Mathematisch-Naturwissenschaftlichen Fakultät

der

Rheinischen Friederich-Wilhelms-Universität Bonn

vorgelegt von

**Laura Prünke**

aus

Unna, Deutschland

Bonn 2020

Angefertigt mit der Genehmigung der Mathematisch-Naturwissenschaftlichen Fakultät der Rheinischen Friedrich-Wilhelms-Universität Bonn

1. Gutachter: Prof. Dr. Alexander Pfeifer
  2. Gutachterin: Prof. Dr. Evi Kostenis
- Tag der Promotion: 09.12.2020  
Erscheinungsjahr: 2021



## Acknowledgements

- My first gratitude goes to Prof. Alexander Pfeifer for the opportunity to work in your lab, the great learnings, the trust and the support you provided me during my great PhD time in your lab.
- Thank you, Prof. Evi Kostenis, for supporting my project as a second supervisor with your advice throughout the entire PhD and for your expertise in DMR measurements together with Dr. Katharina Simon.
- I would like to acknowledge Prof. Markus Gräler and Tina Müller for the helpful and uncomplicated measurement of S1P levels.
- I would like to acknowledge the DFG (Deutsche Forschungsgemeinschaft) for funding this project in the framework of the Research Training Group 1873 (RTG1873).
- Thanks to Dominic for your invaluable scientific support and S1P-expertise, moreover for the time, effort and interest you put into my project. You always provided very clever answers and ideas to all of my questions!
- Further I want to thank Aga for the initiation of the project, Vicky for the Calcium expertise and Elisabeth for proofreading my thesis.
- Grazie Francesca per aver percorso dal primo giorno insieme il dottorato e per il profondo legame che ne è conseguito.
- To Debori and Ben, thank you for your delightful and amazing company far beyond the four walls of our office!
- Muchas gracias a Laia para toda su ayuda, su peritaje y su cordialidad en la casa de farmacología.
- Thank you for the amazing time on the Venusberg: Eleni, Suki, Leni, Dani, Jaspal, Karsti, Steffi, Jeleni, Birti, Juhee and every single lab member of the Pfeifer group for your help, support and connection.
- I am overflowing with gratitude for Leo who shared the academic journey with me since day one and supported me with every fiber of his being in the whirlwind of the PhD. It all started with the 'meso-cat' ;-)
- Tausend Dank Anni und Niko, dass Ihr mir seit jeher alle erdenkliche Unterstützung gebt und mir gleichzeitig immer den nötigen Freiraum zur Entfaltung lasst.
- Ich danke Jonas und Federica, Birgit und Frank, Brigitte, Reinhild und Horst für die herzliche Unterstützung und Ermutigung.
- Thank you to Melly, Christina, Sarah, Lina and Pico for your loving support and your friendship.
- I want to thank Adi, Steffi, Hildegard, Vera, Anja, Knut, Georg and Judith for your soulful support during my PhD.

## Table of contents

Acknowledgements.....	I
Table of contents .....	II
Abbreviations.....	V
<b>1 Introduction .....</b>	<b>1</b>
1.1 G protein-coupled receptors.....	1
1.2 Obesity.....	2
1.3 Adipose tissue .....	3
1.3.1 White adipose tissue (WAT).....	4
1.3.2 Brown adipose tissue (BAT) .....	5
1.3.3 Beige adipose tissue .....	6
1.4 Sphingosine-1-phosphate (S1P) .....	7
1.4.1 S1P metabolism .....	7
1.4.2 S1P receptors.....	8
1.4.3 S1P in metabolism and adipose tissues .....	10
<b>2 Aim of the thesis .....</b>	<b>13</b>
<b>3 Material and Methods.....</b>	<b>14</b>
3.1 Chemicals and Materials .....	14
3.2 Animal experiments .....	14
3.2.1 Housing .....	14
3.2.2 Immunohistochemistry .....	14
3.2.3 Serum preparation.....	16
3.2.4 S1P determination in serum and tissue .....	16
3.2.5 Exposure to 30°C, 23°C and 4°C .....	17
3.2.6 Metabolic phenotyping in metabolic cages .....	17
3.2.7 Body composition .....	17
3.2.8 Pharmacological injections .....	18
3.3 Cell culture .....	19
3.3.1 Isolation and cultivation of brown adipocytes.....	21
3.3.2 Expansion of brown adipocytes .....	22
3.3.3 Differentiation of brown adipocytes .....	23
3.3.4 Isolation and cultivation of white adipocytes .....	24
3.3.5 Differentiation of white adipocytes .....	25
3.3.6 Browning of white adipocytes.....	25

3.4	Oil Red O Staining .....	26
3.5	RNA analysis .....	27
3.5.1	RNA-Isolation .....	27
3.5.2	cDNA Synthesis.....	27
3.5.3	RT-qPCR.....	28
3.6	Protein analysis.....	29
3.6.1	Protein Isolation .....	30
3.6.2	Bradford assay.....	30
3.6.3	Protein preparation .....	31
3.6.4	SDS-PAGE .....	31
3.6.5	Western blotting.....	32
3.6.6	Development of Western Blot.....	33
3.7	Lipolysis .....	34
3.8	Calcium Measurements .....	35
3.9	IP <sub>1</sub> -Assay .....	37
3.10	Dynamic Mass Redistribution Measurements [DMR].....	38
3.11	<i>In silico</i> .....	38
3.11.1	Analysis of data from the Genotype-Tissue Expression (GTEx) project.....	38
3.11.2	Statistical analysis.....	39
<b>4</b>	<b>Results .....</b>	<b>40</b>
4.1	Overview of S1PR distribution.....	40
4.2	Sphingosine-1-phosphate in brown adipocytes.....	42
4.2.1	S1P in lipolysis of brown adipocytes.....	43
4.2.2	S1P in brown adipogenesis .....	44
4.3	Downstream signaling of S1P in brown adipocytes .....	46
4.3.1	DMR measurements in brown adipocytes.....	47
4.3.2	Calcium measurements in brown adipocytes .....	48
4.3.3	Inositol monophosphate measurements in brown adipocytes .....	50
4.3.4	CYR61 mRNA measurements in brown adipocytes .....	52
4.4	The role of individual Sphingosine-1-phosphate receptors in brown adipocytes .....	53
4.4.1	The role of Sphingosine-1-phosphate receptors in differentiation of BAs .....	53
4.4.2	The role of Sphingosine-1-phosphate receptors in calcium signaling in brown adipocytes .....	57
4.5	Sphingosine-1-phosphate in white adipocytes .....	59
4.6	The role of S1P and S1PRs in mice and humans .....	61
4.7	<i>In vivo</i> : Injection of S1PR-Agonists and Antagonists in C57Bl/6J mice .....	66

<b>5</b>	<b>Discussion .....</b>	<b>71</b>
5.1	Sphingosine-1-phosphate in brown adipocytes.....	71
5.2	Downstream signaling of S1P in brown adipocytes .....	72
5.3	The role of S1PRs in brown adipocytes .....	75
5.4	Sphingosine-1-phosphate in white adipocytes.....	77
5.5	The role of S1P and S1PRs in mice and humans .....	77
5.6	<i>In vivo</i> : Injection of S1PR-Agonists and Antagonists in C57Bl/6J mice .....	79
5.7	Outlook: Fat tissue specific knockout of S1PR1 <i>in vitro</i> and <i>in vivo</i> .....	79
<b>6</b>	<b>References .....</b>	<b>81</b>
	<b>Summary.....</b>	<b>90</b>
	<b>Abstracts.....</b>	<b>91</b>

## Abbreviations

°C	Degrees Celsius
μL	Microliter
μm	Micrometer
μM	Micromolar
AC	Adenylyl cyclase
Akt	Proteinkinase B
AMPKα	5'AMP activated protein kinase
ANCOVA	Analysis of covariance
ANOVA	Analysis of variance
aP2	Adipocyte Protein 2 (synonym for FABP4)
ApoE	Apolipoprotein E
ApoM	Apolipoprotein M
APS	Ammonium peroxodisulfate
AT	Adipose tissue
BA	Brown adipocyte
BAT	Brown adipose tissue
BMI	Body mass index
bp	Base pair
BSA	Bovine serum albumin
BW	Body weight
C3T	C3 Transferase
C/EBPα	CCAAT/enhancer binding protein alpha
Ca <sup>2+</sup>	Calcium ion
cAMP	Cyclic adenosine monophosphate
CD	Control diet
CD31	Cluster of differentiation 31 = Platelet endothelial cell adhesion molecule
CDH5	Cadherin 5
CL	CL-316,243
CO <sub>2</sub>	Carbon dioxide
Cre	Cre recombinase protein
Cre ERT	Tamoxifen-dependent Cre recombinase
CTRL	Control
CYR61	Cysteine-rich protein 61
DAG	Diacylglycerol
Dig. Ph. Cont.	Digital Phase Contrast
DIO	Diet-induced obesity
DM	Differentiation Medium
DMEM	Dulbecco's Modified Eagle Medium
DMR	Dynamic mass redistribution
DMSO	Dimethyl sulfoxide
DNA	Desoxyribunucleic acid
E	Embryonic day
EDG	Endothelial-differentiation-gene
EDTA	Ethylenediaminetetraacetic acid
EGTA	Ethyleneglycoltetraacetic acid

EE	Energy expenditure
ELISA	Enzyme-linked Immunosorbent Assay
ELPHO	Electrophoresis
et al.	And others ("et alii")
ET-1	Endothelin 1
ET <sub>A</sub>	Endothelin receptor type A
FABP4	Fatty acid-binding protein 4
FACS	Fluorescence-activated cell sorting
g	gravity
GAP	GTPase-activating protein
GDP	Guanosine diphosphate
GM	Growth Medium
GTE <sub>x</sub>	Genome-tissue expression
GTP	Guanosine triphosphate
GTT	Glucose tolerance test
HBSS	Hanks balanced salt solution
HDL	High density lipoprotein
HE	Hematoxylin / Eosin
HEK 293	Human embryonic kidney cell line
HFD	High fat diet
Hprt	Hypoxanthine-guanine phosphoribosyltransferase
HSL	Hormone-sensitive lipase
IBMX	3-isobutyl-1-methylxanthine
IL-6	Interleukin-6
IM	Induction Medium
IP <sub>1</sub>	Inositol monophosphate
IP <sub>3</sub>	Inositol trisphosphate
kDA	Kilodalton
kg	Kilogram
LiCl	Lithium chloride
LPA	Lysophosphatidic acid
mA	Miliampere
Mfsd2b	Major facilitator superfamily transporter 2b
mM	Milimolar
mRNA	messenger RNA
msec	Miliseconds
Na	Sodium
ND	Normal diet
NE	Norepinephrine
NFAT	Nuclear factor of activated T-cells
nM	Nanomolar
O <sub>2</sub>	Oxygen
ob/ob	Obese mouse
ORO	Oil red O
P	Passage
p	phospho
PAGE	Polyacrylamide gel electrophoresis
PASMC	Pulmonary artery smooth muscle cells

PBS	Phosphate-Buffered Saline
PDE	Phosphodiesterase
PDGFR $\alpha$	Platelet-derived growth factor receptor $\alpha$
PFA	Paraformaldehyde
PGC1 $\alpha$	PPAR $\gamma$ co-activator-1 $\alpha$
p-GSK3 $\alpha/\beta$	Phospho Glycogen synthase kinase 3 alpha/beta
PIP <sub>2</sub>	Phosphatidylinositol 4,5-bisphosphate
PKC	Protein kinase C
PLC- $\beta$	Phospholipase C $\beta$
PPAR $\gamma$	Peroxisome proliferator-activated receptor gamma
PRDM16	PR domain zinc-finger protein 16
preBA	Brown preadipocytes
preWA	white preadipocyte
PTEN	Phosphatase and tensin homolog
PTX	Pertussis toxin
PZN	Pharmazentralnummer
qPCR	Real-time quantitative polymerase chain reaction
RER	Respiratory exchange ratio
RH7777	Rat hepatoma cell line
Rho	Ras homologue
RhoGEF	Rho guanine nucleotide exchange factors
RNA	Ribonucleic acid
ROCK	Rho-associated protein kinase
Rpm	Revolutions per minutes
RT	room temperature
s.e.m	standard error of the mean
S1P	Sphingosine-1-phosphate
S1PR	Sphingosine-1-phosphate receptor
S1PR1 <sup>0/0</sup>	S1PR1 <sup>fl/fl</sup> x AdipoQ-Cre <sup>wt/cre</sup>
S1PR1 <sup>fl/fl</sup>	S1PR1 <sup>fl/fl</sup> x AdipoQ-Cre <sup>wt/wt</sup>
scWAT	Subscapular white adipose tissue
SDS	Sodium dodecyl sulfate
SHIP	Study of Health in Pomerania
SM	Sphingo myelin
SphK	Sphingosine Kinase
Spns2	Protein spinster homolog 2
SVF	Stromal vascular fraction
TC	Tissue culture
TEMED	N,N,N',N'-Tetramethyl ethylenediamine
Tie2	TEK tyrosine kinase
TNF $\alpha$	Tumor necrosis factor alpha
TPM	Transcripts per million
Tris	Tris(hydroxymethyl)aminomethane
TRP	Transient receptor potential
UCP1	Uncoupling protein-1
USA	United States of America
V	Volt

VWF	Von Willebrand factor
WA	White adipocyte
WATg	Gonadal white adipose tissue
WATi	Inguinal white adipose tissue
WHO	World Health Organization
WT	Wild type

# 1 Introduction

## 1.1 G protein-coupled receptors

G protein-coupled receptors (GPCRs) are proteins located in the cellular membrane transferring extracellular signals into the inside of a cell. The protein consists of seven transmembrane helices winding through the membrane therefore the description seven-transmembrane receptor is used synonymously for GPCR (Neves et al., 2002; Trzaskowski et al., 2012).

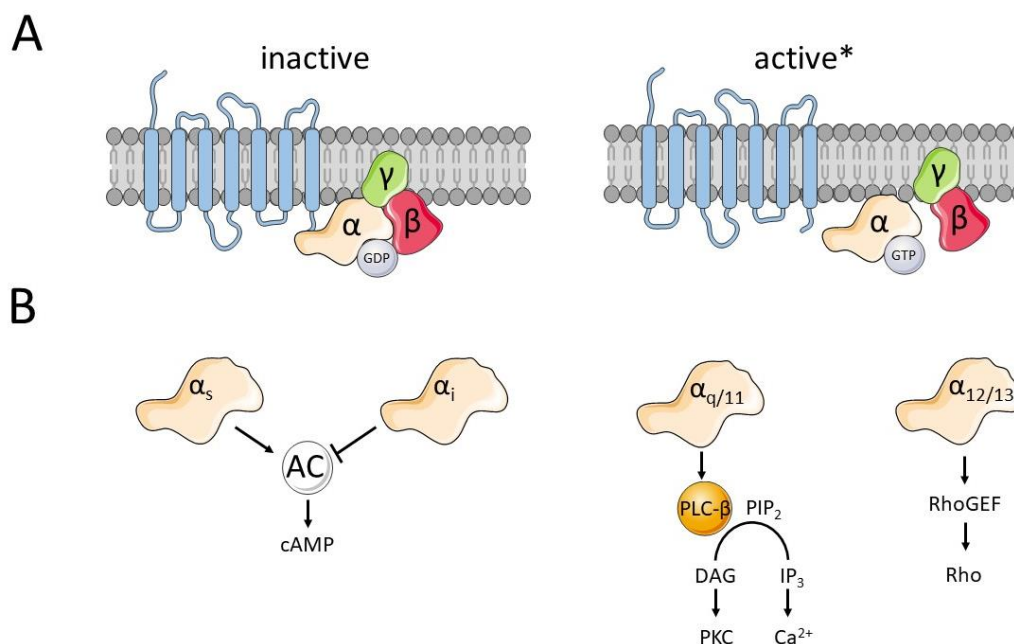


**Figure 1 | GPCR downstream signaling**

(A) Active\* and inactive state of the GPCR (B) Downstream signaling pathways of the different G $\alpha$  subunits. Abbreviations: GDP: Guanosine diphosphate, GTP: Guanosine triphosphate, AC: Adenylyl cyclase, cAMP: Cyclic adenosine monophosphate, PLC- $\beta$ : Phospholipase C- $\beta$ , PIP<sub>2</sub>: Phosphatidylinositol 4,5-bisphosphate, DAG: Diacylglycerole, PKC: Protein kinase C, IP<sub>3</sub>: Inositol trisphosphate, Ca<sup>2+</sup>: Calcium, RhoGEF: Rho guanine nucleotide exchange factors. This image was produced using templates of Servier Medical Art by Servier which are licensed under a Creative Commons Attribution 3.0 Unported License, <https://smart.servier.com>. (26.10.2019).

The signal is initiated by the binding of a ligand molecule to the extracellular moiety of the GPCR. Upon this stimulus the receptor changes its conformation leading to an activation of the G protein which is located at the cytosolic side of the plasma membrane and is bound to the seven transmembrane helices. The G protein is composed of three different subunits: the alpha ( $\alpha$ ), beta ( $\beta$ ) and gamma ( $\gamma$ ) subunit. Due to receptor activation guanosine diphosphate (GDP) is replaced by guanosine triphosphate (GTP) at the  $\alpha$  subunit of the G protein. As a consequence, the G protein destabilizes and the  $\alpha$  subunit diffuses from the  $\beta\gamma$  subunit. In this state the G $\alpha$  subunit is able to activate or inhibit enzymes (Trzaskowski et al., 2012). The G $\alpha$  subunit is subclassified by its downstream targets. G $\alpha_s$  proteins activate the Adenylyl cyclase (AC) leading to an increase in intracellular cyclic adenosine

monophosphate (cAMP) whereas  $G_{\alpha i}$  proteins inhibit the AC leading to a decrease of cAMP. The initiation of  $G_{\alpha q/11}$  signaling leads to an activation of Phospholipase C- $\beta$  (PLC- $\beta$ ) resulting in the cleavage of phosphatidylinositol 4,5-bisphosphate into inositol trisphosphate ( $IP_3$ ) and the membrane bound diacylglycerole (DAG). When  $IP_3$  binds to its receptor on the endoplasmatic reticulum, calcium ( $Ca^{2+}$ ) is released into the cytosol.  $G_{\alpha 12/13}$  activates the small GTPase Rho (Buhl et al., 1995; Neves et al., 2002) (Figure 1B). The activation of the GPCR is terminated by the GTPase activity of the  $\alpha$  subunit, supported by other proteins such as GTPase-activating protein (GAP), leading to a dephosphorylation of the bound GTP to GDP (Trzaskowski et al., 2012). Thereupon, the  $\alpha$  and  $\beta\gamma$  subunits associate again to form the inactive state of the receptor (Figure 1A). Some GPCRs are also active without a ligand binding to them. Still, the ligand can additionally enhance the activity of these so called constitutively active receptors (Trzaskowski et al., 2012).

GPCRs are also able to build oligomers. These oligomers can either consist of two or more receptors of the same type (Homomers) or they are composed of different types (Heteromers) (Smith and Milligan, 2010). Besides their usual location in the cellular membrane, GPCRs are also prone to be internalized by proteins called  $\beta$ -Arrestins (Grundmann et al., 2018). Due to this internalization the GPCRs are either degraded or recycled and rebuilt into the plasma membrane. The underlying cause of this effect is to regulate and modulate delicately the GPCR activity. The genetic superfamily of GPCRs is grouped into six different classes: A-F. Receptors in class A are most abundantly targeted by drugs on the market (Basith et al., 2018). In 2018, approximately 35% of the approved drugs on the pharmaceutical market target GPCRs (Sriram and Insel, 2018). This fact makes GPCRs an interesting and valuable target for future drug discovery.

## 1.2 Obesity

The incidence of obesity has reached alarming proportions worldwide. According to latest data of the World Health Organization (WHO) 1,9 billion adults worldwide were classified overweight in 2016, 35% of them were obese (World Health Organization (WHO), 2020). In 2019, 38 million children under 5 years were either overweight or obese (World Health Organization (WHO), 2020). Commonly, the body mass index (BMI) is used to categorise body weight of human beings. It is calculated by division of the body mass [kg] by the square of the body length [ $m^2$ ] (World Health Organization (WHO), 2020). Obesity is characterised by an excess accumulation of fat mass leading to an increased bodyweight. It occurs when calorie intake is higher than calorie usage which is a sum of the basal and the active metabolic rate (Jéquier and Schutz, 1988). The underlying causes are diverse: obesity can be caused by overnutrition, due to mental health issues, hypothyroidism, congenital leptin deficiency, consumption of mainly ultra-processed food, genetic predisposition and adverse effects of drugs

(Sharma and Padwal, 2010; Salviato Balbão et al., 2014; Sanyal and Raychaudhuri, 2016; Poti et al., 2017; Yupanqui-Lozno et al., 2019), just to name a few.

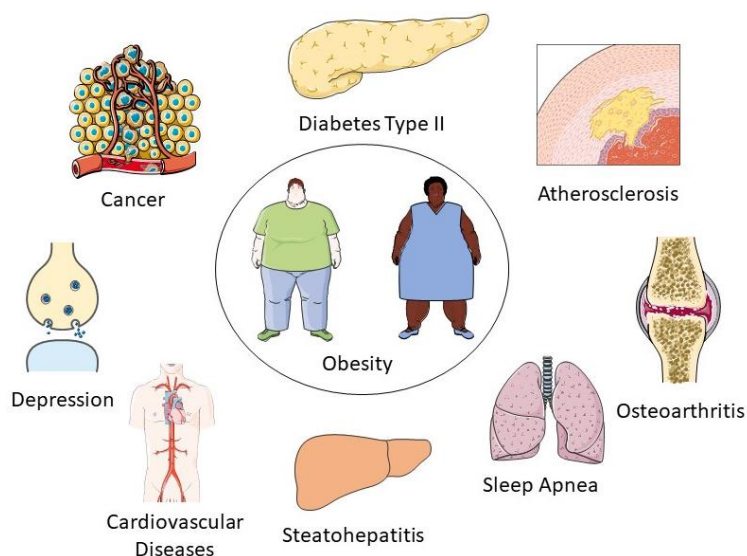


**Figure 2 | Obesity and its comorbidities**

This image was produced using templates of Servier Medical Art by Servier which are licensed under a Creative Commons Attribution 3.0 Unported License, <https://smart.servier.com>. (26.10.2019).

Adiposity is associated with a plethora of comorbidities such as diabetes mellitus, atherosclerosis, osteoarthritis, sleep apnea, non-alcoholic fatty liver disease, cardiovascular diseases, depression and some types of cancer (Figure 2) (King et al., 2013; Pergola and Silvestris, 2013; Al-Goblan et al., 2014; Lovren et al., 2015; Csige et al., 2018; Ouakinin et al., 2018; Sarwar et al., 2018). Moreover, the mortality is increased in obese individuals (Abdelaal et al., 2017). The rising number of obese patients confronts health systems world-wide with enormous economic problems and many individuals suffer the loss of quality of life (Khaodhiar et al., 1999; Lobstein et al., 2015).

### 1.3 Adipose tissue

There exist two main types of adipocytes which differ explicitly in their function, morphology and precursor cells: White and brown adipocytes. White adipocytes (WA) are morphologically characterized by a large intracellular lipid droplet and few mitochondria (Figure 3A). On the contrary, brown adipocytes (BA) carry plenty of small lipid droplets and a high mitochondrial density (Figure 3C) (Trayhurn and Beattie, 2001; Seale et al., 2008). A third type of adipocytes, called beige adipocytes, contains multilocular lipid droplets and several mitochondria (Figure 3B) (Pfeifer and Hoffmann, 2015).

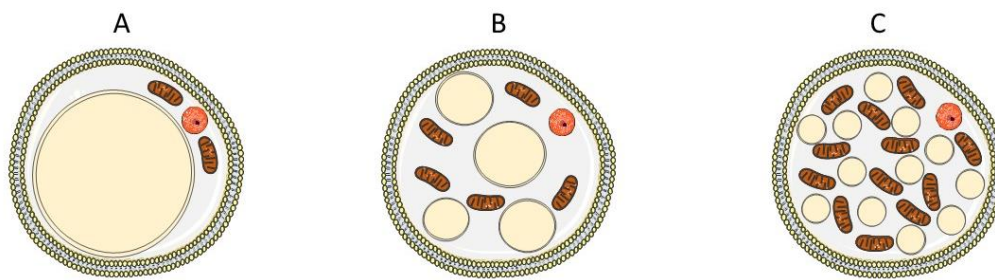


**Figure 3 | Morphology of white, beige and brown adipocytes**

(A) White adipocyte (B) Beige adipocyte (C) Brown adipocyte. This image was produced using templates of Servier Medical Art by Servier which are licensed under a Creative Commons Attribution 3.0 Unported License, <https://smart.servier.com>. (26.10.2019).

### 1.3.1 White adipose tissue (WAT)

The major purpose of white adipose tissue (WAT) is the storage of triglycerides which serve as energy source in times of starvation (Trayhurn and Beattie, 2001; Seale et al., 2008).

WAT consists not only of adipocytes but also of immune cells, stromal-vascular cells, blood vessels, sympathetic and parasympathetic nerves (Frayn et al., 2003; Kershaw and Flier, 2004). Furthermore, WAT is a hormonally active endocrine organ which produces and releases a broad range of hormones and other substances called adipokines. The secretion can be performed in an autocrine, paracrine or endocrine manner. Two major adipokines are adiponectin and leptin. Adiponectin acts in favor of insulin sensitivity, increases glucose uptake into adipocytes and skeletal muscle and further promotes fatty acid oxidation. Leptin is encoded by the *ob* gene in adipocytes. Among the regulation of various physiological functions, the most prominent task of leptin is the regulation of appetite and enhancement of energy expenditure. Whereas leptin levels increase with rising body weight, adiponectin levels decrease inversely proportional. Inflammatory cytokines such as tumor necrosis factor  $\alpha$  (TNF $\alpha$ ) and interleukin-6 (IL-6) also derive from adipocytes, especially from those, resident in the visceral area rather than from subcutaneous adipocytes. It has to be mentioned that TNF $\alpha$  can derive from macrophages which also infiltrate the adipose tissue (Coelho et al., 2013).

Besides BMI, distribution of the WAT throughout the body influences the severity of comorbidities in obese patients. WAT is mainly located in abdominal and subcutaneous fat depots. Increased abdominal adipose tissue is associated closely with a higher cardiovascular risk, atherosclerosis and diabetes. In contrast, accumulation of subcutaneous adipose tissue is considered to display milder symptoms and course of disease. The subcutaneous adipose tissue is less susceptible to metaflammation and more prone to browning (Ibrahim, 2010; Neeland et al., 2013; Cohen et al., 2014). Furthermore, the presence of brown adipose tissue (BAT) in obese subjects correlates with a better metabolic profile and

improved cardiometabolic health (Becher et al., 2020). The murine gonadal white adipose tissue (WATg) which resembles the human visceral adipose tissue exhibits a pro-inflammatory phenotype in obese mice. In murine inguinal white adipose tissue (WATi) which is comparable to human subcutaneous adipose tissue less inflammation is observed (Sanyal et al., 2017). WAT can expand in a hypertrophic fashion by increasing the storage of triglycerides or in a hyperplastic way by differentiation of pre-adipocytes into mature fat cells (Coelho et al., 2013).

#### 1.3.1.1 *Transcriptional regulation*

The nuclear receptor peroxisome proliferator-activated receptor  $\gamma$  (PPAR $\gamma$ ) is often referred to as the master transcription factor of brown and white adipogenesis. PPAR $\gamma$  transcriptionally regulates around 5300 genes, many of them are crucial for and involved in adipogenesis as well as adipocyte function. Interestingly, PPAR $\gamma$  and the transcription factor CCAAT/enhancer-binding protein  $\alpha$  (C/EBP $\alpha$ ) share many target genes, work synergistically and control adipogenesis (Lefterova et al., 2008; Yu et al., 2012). In the course of adipocyte differentiation C/EBP $\beta$  and C/EBP $\gamma$  are early expressed and induce PPAR $\gamma$  and C/EBP $\alpha$  expression (Lefterova et al., 2008; Yu et al., 2012). Fatty acid-binding protein 4 (FABP4), also known as adipocyte Protein 2 (aP2) is another important protein marker for adipocyte differentiation. By binding to hydrophobic molecules FABP4 influences fatty acid storage and lipolysis (Furuhashi et al., 2015; Hotamisligil and Bernlohr, 2015; Floresta et al., 2017). PPAR $\gamma$  activation enhances FABP4 expression, which in turn is reported to negatively influence PPAR $\gamma$  activity (Hotamisligil and Bernlohr, 2015; Floresta et al., 2017). Thiazolidinediones pharmacologically activate PPAR $\gamma$  and thereby lead to a higher insulin sensitivity and improved glucose tolerance in diabetes mellitus type II patients. The thiazolidinedione Rosiglitazone is used to induce differentiation of primary WAs *in vitro* (Sanyal et al., 2017; Quintanilla Rodriguez and Correa, 2019).

#### 1.3.2 **Brown adipose tissue (BAT)**

Brown adipose tissue is characterized by the ability to perform a process called non-shivering thermogenesis in order to produce heat. Upon exposure to cold, norepinephrine (NE) is released from sympathetic nerves and activates the  $\beta_3$  adrenergic receptor of brown adipocytes. Agonizing the  $G_s$  coupled  $\beta_3$  adrenergic receptor leads to activation of the enzyme hormone-sensitive lipase (HSL) which splits triglycerides into free fatty acids and glycerol. The procedure of triglyceride cleavage is called lipolysis. Both BAT and WAT are able to perform this process however the lipolysis rate of WAT is three times lower than of BAT (Blackburn, 2011). The free fatty acids (FFA) are further enzymatically processed and shuttled into the mitochondria. Uncoupling protein-1 (UCP1) is a mitochondrial carrier protein and serves as a proton shuttle at the inner mitochondrial membrane. It can also be referred to as Thermogenin. UCP1 expression is unique to brown and beige adipocytes. Functionally, UCP1

disrupts the proton gradient needed for formation of ATP. As a consequence energy which is normally transformed into ATP during oxidative phosphorylation is instead released as heat (Cannon and Nedergaard, 2004; Fenzl and Kiefer, 2014). This physiological process is important for the maintenance of the body temperature of neonates (Blackburn, 2011).

In literature there are approximately 50 transcription factors described which are involved in enhancing or attenuating brown and beige adipocyte formation (Inagaki et al., 2016). It is stated that PPAR $\gamma$  co-activator-1 $\alpha$  (PGC1 $\alpha$ ), PR domain zinc-finger protein 16 (PRDM16), C/EBP $\beta$  and PPAR $\gamma$  control most of these transcription factors and their expression positively influences the development of brown and beige adipocytes (Inagaki et al., 2016).

In 2009 it was shown by Virtanen et al. that also adult human beings possess active supraclavicular BAT (Virtanen et al., 2009). The activity of brown adipose tissue (BAT) in humans was shown to inversely correlate with the incidence of obesity. The research group around Wouter van Marken Lichtenbelt found that subjects with an BMI of 37 kg/m<sup>2</sup> or higher displayed almost no BAT activity (Vijgen et al., 2011; Yoneshiro et al., 2011). Another group investigated that even the epigenetic programming such as paternal cold exposure influences BAT abundance (Sun et al., 2018). As the activation of brown adipose tissue enhances energy expenditure by the production of heat, it is a promising target to combat obesity (Gnad et al., 2014). However, despite the extensive research in the field of BAT and obesity, no drug exists on the market targeting brown adipocytes for combating the growing number of patients suffering from obesity (Fenzl and Kiefer, 2014).

### 1.3.3 Beige adipose tissue

Beige or brite ('brown-in-white') adipocytes are characterized by multilocular lipid droplets, several mitochondria and the expression of UCP1 protein (Figure 3B). Even though beige and brown adipocytes share many similarities, they derive from different origins (Pfeifer and Hoffmann, 2015). Beige adipocytes appear within depots of WAT in mice after certain stimuli such as cold exposure or  $\beta$ 3-adrenergic receptor agonist (CL-316,243) stimulation (Loncar, 1991; Shin et al., 2019). It has been recently proposed that beige adipocytes derive prevalingly from beige precursor cells upon a cold stimulus (Shao et al., 2019). Afterwards these cells switch between an 'active' and a 'dormant' state depending on the surrounding temperature (Shao et al., 2019). In male rodents, beige adipocytes are predominantly recruited within WAT<sub>i</sub> whereas beige adipocyte development within WAT<sub>g</sub> depots is not regularly observed (Okamatsu-Ogura et al., 2013; Kim et al., 2016). Among scientists the interest in activating beige adipocytes in humans is tremendous as beige adipocytes arise from WAT depots which are very abundant especially in obese subjects (Vijgen et al., 2011; Bartelt and Heeren, 2014).

## 1.4 Sphingosine-1-phosphate (S1P)

### 1.4.1 S1P metabolism

Sphingosine-1-phosphate (S1P) is a lysophospholipid and serves as a bioactive mediator (Rivera and Chun, 2008). It influences many physiological processes such as proliferation, migration, cell survival and adhesion (Mendelson et al., 2014; Proia and Hla, 2015). S1P is primarily produced by blood and endothelial cells (Venkataraman et al., 2008; Tukijan et al., 2018).

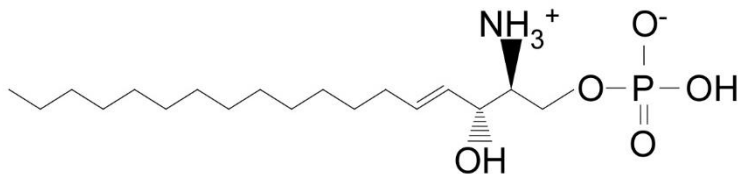


Figure 4 | Skeletal formula of Sphingosine-1-phosphate

Sphingomyelin (SM) is an integral part of the eukaryotic extracellular plasma membrane (Ramstedt and Slotte, 2002). It can be further degraded to ceramides by sphingomyelinases. Ceramides are then enzymatically degraded to sphingosine via ceramidases. Sphingosine Kinase (SphK) 1 and 2 phosphorylate sphingosine to S1P (Figure 5) (Hla and Dannenberg, 2012; Gosejacob et al., 2016). The differential distribution of SphKs in the circulation system and tissues leads to a S1P gradient. Compared to high S1P levels in the blood [approx. 1  $\mu$ M] and medium levels in the lymph [approx. 100s nM], the S1P concentrations in interstitial fluids are estimated rather low [nm range] (Hla et al., 2008; Cyster and Schwab, 2012). Furthermore the SphK1 is preferentially expressed in the cytosol whereas SphK2 is mainly found in the nucleus and in mitochondria (Spiegel et al., 2019).

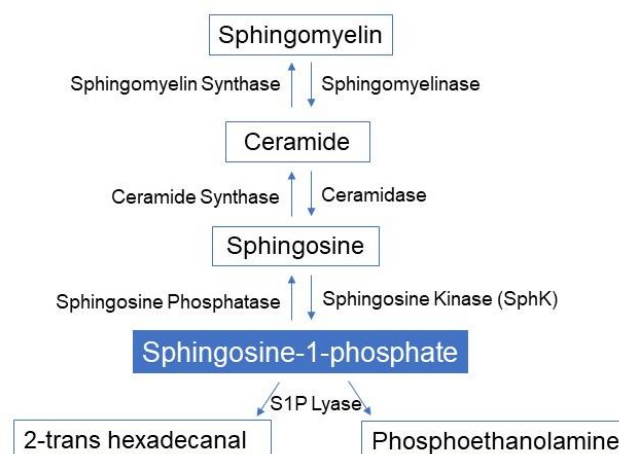


Figure 5 | Sphingolipid metabolism

Modified after Hla and Dannenberg, 2012 (Hla and Dannenberg, 2012)

S1P can either be dephosphorylated by sphingosine phosphatase resulting in the formation of sphingosine or cleaved by Sphingosine-1-phosphate lyase into phosphoethanolamine and 2-trans hexadecanal (Hla and Dannenberg, 2012).

As S1P is an amphiphilic molecule it cannot diffuse through the plasma membrane. In fact, S1P secretion is driven by different transporters. One of them is the protein spinster homolog 2 (Spns2) which was firstly discovered in zebra fish (Kawahara et al., 2009). Spns2 exerts its function particularly via control of S1P egression from endothelial cells (Fukuhara et al., 2012). A recent study by the group of Tsuyoshi Nishi discovered a new S1P transporter in erythroid cells called 'major facilitator superfamily transporter 2b' (Mfsd2b) (Kobayashi et al., 2018). Mfsd2b is involved in S1P secretion out of the cell and accounts for approximately half of the S1P circulating in the blood (Vu et al., 2017). S1P is transported throughout the blood mainly via two chaperones. The lysophospholipid is either bound to apolipoprotein M (apoM) which is associated with HDL (~65%) or tied to albumin (~35%) (Christoffersen et al., 2011; Wilkerson et al., 2012).

#### 1.4.2 S1P receptors

S1P functions as a ligand binding to five different G protein-coupled receptors. Nowadays these receptors are designated Sphingosine-1-phosphate receptors (S1PRs). Formerly, these receptors were called 'endothelial-differentiation-gene' and EDG1 was the first S1PR described, even though S1P was not identified as a ligand yet (Hla and Maciag, 1990). In 1998, two independent groups allocated S1P as a ligand for EDG1 (Lee et al., 1998; Zondag et al., 1998). In 2002, the nomenclature of the eight EDG receptors was harmonized and altered, as three of the EDGs are activated by lysophosphatidic acid (LPA) whereas the other five are stimulated by S1P (Table 1) (Chun et al., 2002).

**Table 1 | EDG nomenclature vs. IUPHAR nomenclature**

Modified after Chun et al., 2002 (Chun et al., 2002)

EDG name	IUPHAR nomenclature	Ligand
EDG 1	S1P <sub>1</sub> receptor	S1P
EDG 2	LPA <sub>1</sub> receptor	LPA
EDG 3	S1P <sub>3</sub> receptor	S1P
EDG 4	LPA <sub>2</sub> receptor	LPA
EDG 5	S1P <sub>2</sub> receptor	S1P
EDG 6	S1P <sub>4</sub> receptor	S1P
EDG 7	LPA <sub>3</sub> receptor	LPA
EDG 8	S1P <sub>5</sub> receptor	S1P

The S1PR1 is a G<sub>i</sub>-coupled receptor (Spiegel and Milstien, 2003; O'Sullivan and Dev, 2013; Mendelson et al., 2014; Patmanathan et al., 2017). S1PR1 regulates the lymphocyte egress from the lymphoid organs into the blood. This effect was harnessed to develop a drug called FTY720 which binds to S1PR1

on the lymphocytes. Since 2010 FTY720 is accredited for the treatment of multiple sclerosis targeting the S1PR system. After an oral uptake, FTY720 is metabolized by SphKs, preferably Sphk2 to its bioactive form FTY720-P. FTY720-P acts as a functional antagonist on S1PR1s of lymphocytes leading to an internalization of S1PR1. Consequently, lymphocytes are not able to egress from the lymphoid organs which causes lymphopenia resulting in immunosuppressant effects in patients (Brinkmann et al., 2004; Matloubian et al., 2004).

S1PR1 is prone to internalization. However, the known S1PR1-ligands induce internalization and ubiquitination to different extents. Only AFD-R, the chiral analog of FTY720-P, down-regulates S1PR1 significantly in HEK 293 cells. S1P and the specific S1PR1-agonist SEW 2871 induce ubiquitin binding to S1PR1 but to a lower extent than AFD-R and without promoting S1PR1-downregulation (Gonzalez-Cabrera et al., 2007).

S1PR1 is crucial for embryonic development. When the S1PR1 is genetically knocked out in mice, either globally or endothelial cell specifically via Tie2-Cre, the murine embryos die between E12.5 and E14.5 due to insufficient vascular maturation (Liu et al., 2000; Allende et al., 2003).

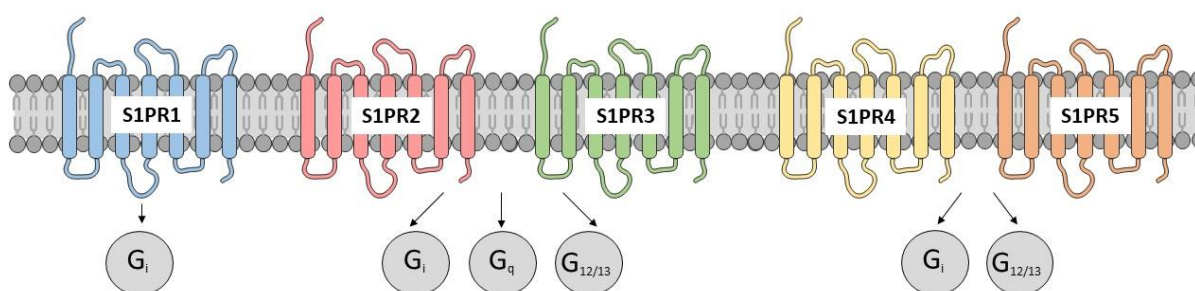


**Figure 6 | G protein-coupling of the five different S1PRs**

Modified from Spiegel and Milstien 2003 (Spiegel and Milstien, 2003), Mendelson et al. 2014 (Mendelson et al., 2014), Patmanathan et al. 2017 (Patmanathan et al., 2017). This image was produced using templates of Servier Medical Art by Servier which are licensed under a Creative Commons Attribution 3.0 Unported License, <https://smart.servier.com>. (26.10.2019).

The S1PR2 and S1PR3 are reported to be coupled to  $G_i$ ,  $G_q$  and  $G_{12/13}$  (O'Sullivan and Dev, 2013). S1PR2 signaling is associated with various functions and effects both of physiological and pathophysiological nature (Adada et al., 2013). Within the first four weeks of age S1PR2-null mice develop deafness (Herr et al., 2007; Kono et al., 2007). In human endothelial cells it was found that S1PR2 enhances paracellular permeability via the Rho-ROCK-PTEN pathway (Sanchez et al., 2007). Mice lacking the S1PR2 are more resistant to streptozotocin-induced pancreatic  $\beta$ -cell apoptosis (a mouse model of diabetes) than WT mice (Imasawa et al., 2010). Unlike S1PR1 which is in favor of lymphocyte migration, S1PR2 attenuates inflammation-driven macrophage recruitment via contribution of cAMP and repression of AKT phosphorylation. Even though an AC mediated increase in cAMP levels is generally associated with an activation of  $G_s$ , it is stated that an S1PR2 induced cAMP elevation can also be

rooted in the stimulation of  $G_{12/13}$  (Jiang et al., 2007; Jiang et al., 2008; Michaud et al., 2010). The study of an ApoE knockout model for atherosclerosis and the simultaneous S1PR3 knockout leads to the conclusion that S1PR3 promotes the recruitment of monocytes and macrophages in atherosclerosis and inflammation (Keul et al., 2011). A comprehensive *in vitro* and *in vivo* study with murine and human plasma samples designated the nitrated form of S1PR3 in the circulation as a biomarker for severity of sepsis-induced acute lung injury (Sun et al., 2012).

While S1PR1, S1PR2 and S1PR3 are abundantly expressed throughout the body, S1PR4 is mostly present in airway smooth muscle cells and the lymphoid system whereas S1PR5 is predominantly found in the central nervous system and in natural killer cells (Gräler et al., 1998; Im et al., 2000; Graeler and Goetzl, 2002; Jolly et al., 2002; Terai et al., 2003; Obinata and Hla, 2012; Adada et al., 2013). Both, S1PR4 and S1PR5, are known to be coupled to  $G_i$  and  $G_{12/13}$  (Watters et al., 2011).

#### 1.4.3 S1P in metabolism and adipose tissues

Compared to the field of immunology, little is known yet about S1P in the field of metabolic diseases, especially about S1P in obesity. Two studies display examination of S1P blood levels in human subjects dependent on the body mass index (BMI). An investigation of 25 human patients by Kowalski et al. reveals that S1P plasma levels increase simultaneously with an enhanced BMI (Kowalski et al., 2013). The research group around Bodo Levkau screened data, gathered from the SHIP-Trend study, for metabolic parameters in conjunction with S1P. It is found that dependent on the BMI, S1P levels increase, but this effect occurs only up to a BMI of approximately  $30 \text{ kg/m}^2$ . In human subjects whose BMI exceeds  $30 \text{ kg/m}^2$  decreasing S1P serum concentrations are measured the higher the BMI gets (Weske et al., 2018).

Previous *in vitro* studies have shown that chronic S1P treatment [ $0.5\text{-}10 \mu\text{M}$ ] of 3T3-L1 fibroblasts which underwent a white adipocyte differentiation protocol lead to decreased PPAR $\gamma$  mRNA and protein levels or to declined lipid contents. This effect is abolished by simultaneous addition of the specific S1PR2 antagonist JTE 013, but not by the specific S1PR1 antagonist W 146 (Moon et al., 2014; Moon et al., 2015; Weske et al., 2018). When 3T3-F442A preadipocytes were differentiated in the presence of S1P [ $10 \mu\text{M}$ ] a significant decrease of aP2, adiponectin and lipoprotein lipase mRNA occurs. These effects are reversible by addition of the dual S1PR1 and S1PR3 antagonist VPC-23019, whereas the S1PR2 antagonist JTE 013 does not influence the S1P effect (Kitada et al., 2016a). All the studies presented have seen a decrease of differentiation indicators after chronic S1P treatment, whereas there is still discordance about the receptor responsible for this effect. These incongruent observations may emerge since two different cell lines have been used for these investigations.

The siRNA mediated knockdown of S1PR1 and S1PR2 in 3T3-F442A adipocytes implicates that cells lacking S1PR1 proliferate less but accumulate more triglycerides. A higher proliferation rate but a lower triglyceride accumulation is detectable for the S1PR2 knockdown in these cells (Kitada et al., 2016b). The same study found that treatment of 3T3-L1 preadipocytes with S1P [10  $\mu$ M] enhances proliferation of the cells which can be reversed by the addition of VPC-23019, but not by JTE 013 (Kitada et al., 2016b). These data allow the conclusion that S1P enhances proliferation of adipocytes via S1PR1.

Moreover, it is reported in literature that FTY720 owes antiobesity properties. Mice which were injected intraperitoneally with FTY720 twice a week during a 10 week-long HFD gained significantly less bodyweight. The proposed mechanism behind this effect, investigated in 3T3-L1 adipocytes treated with FTY720-P, is the decrease of PPAR $\gamma$ , C/EBP $\alpha$  and adiponectin mRNA. Furthermore, *in vitro* and *in vivo* protein analysis revealed that FTY720-P treatment increases phosphorylation of Akt and AMPK $\alpha$  whereas phosphorylation of GSK3 $\alpha/\beta$  is attenuated (Moon et al., 2012).

In another prior study the impact of genetic S1PR2 deletion on mice subjected to an HFD for 4 weeks was explored. Even though the body weight was not different, the S1PR2<sup>-/-</sup> mice displayed significantly lower plasma glucose levels compared to the WT group. In the knockout mice the WATg weight, as well as the fat cell diameter were significantly decreased. A similar trend was observed when *ob/ob* mice were fed the specific S1PR2 antagonist JTE 013 for four weeks. *Ob/ob* mice serve as a model for obesity as well as diabetes and are characterized by leptin deficiency leading to an immense food intake (Lindström, 2007). The four week JTE 013 feeding period resulted in significantly lower body weights, WATg weights, plasma glucose levels and improved insulin sensitivity compared to the control group (Kitada et al., 2016b). Overall, these data suggest that blockade of S1PR2 could be beneficial for the treatment of obesity.

The knockout of ApoM in female mice leads to a higher BAT mass, improved postprandial triglyceride clearance, protection from DIO and amelioration of glucose tolerance. The proposed mechanism by the authors is a reduction of S1PR1 signaling in the ApoM<sup>-/-</sup> mice because it was found that the injection of the specific S1PR1 antagonist W 146 in WT mice showed similar results as the genetic ApoM knockout (Christoffersen et al., 2018). In the same study flow cytometry analysis of BAT and WATi was performed and the different cellular fractions underwent mRNA analysis. S1PR1 was highly expressed in CD31<sup>+</sup> cells extracted from BAT (Christoffersen et al., 2018). CD31<sup>+</sup> is commonly used as an endothelial cell marker (Liu and Shi, 2012). Because of the S1PR1 abundance in CD31<sup>+</sup> cells in BAT the authors conclude that S1PR1 has an important role in endothelial barrier function of BAT (Christoffersen et al., 2018).

Recent research shows that male and female mice lacking the SphK2 are protected from age-related weight gain and display improved glucose tolerance compared to WT mice. The energy expenditure (EE), as well as the food intake are significantly increased in male SphK2<sup>-/-</sup> subjects. Plasma leptin levels of the SphK2<sup>-/-</sup> knockout mice are attenuated whereas the 'opponent' adiponectin is enriched in the plasma (Ravichandran et al., 2019). The adipokine adiponectin binds to two receptors called adipoR1 and adipoR2. It is hypothesised that upon stimulation of these receptors, the S1P formation is initiated due to ceramidase activity of these receptors (Holland et al., 2011).

In human endothelial cells it was found that S1P can serve as a direct ligand and activator of PPAR $\gamma$ . This observation could potentially be relevant for further investigation in adipose tissues as PPAR $\gamma$  is a master transcription factor of adipogenesis (Farmer, 2006; Parham et al., 2015).

## 2 Aim of the thesis

As stated in chapter 1.4.3 not much is known yet about the influence of S1P on adipose tissue and obesity. The research conducted so far in this field still leaves many open questions and is sometimes contradictory, probably also due to the presence of five different receptors which impedes the investigation of S1P mediated effects. Especially the role of S1P and its receptors in brown adipocytes is barely investigated and understood until today. Preliminary S1PR expression analysis performed in our lab, revealed that the receptors are present in brown and white adipocytes. In order to shed light on the impact of S1P on adipocytes, the following questions are addressed in this thesis:

1. Does S1P have an impact on brown adipocyte adipogenesis or function *in vitro*?
2. What is the influence of S1PRs in brown adipocyte differentiation and activation *in vitro*?
3. Does S1P have an impact on adipogenesis and function of primary white adipocytes *in vitro*?
4. Is there any effect of a pharmacological treatment of mice with S1PR agonists or antagonists on brown fat activation at 23°C or at 4°C?

Different biochemical techniques and specific agonists and antagonists of the S1PRs were used to investigate the role of S1P and its downstream signaling in adipocytes. The serum levels of S1P and its precursors were measured in samples of mice exposed to different temperatures. To near a future treatment approach, pharmacological injections with agonists and antagonists of S1PRs were performed.

## 3 Material and Methods

### 3.1 Chemicals and Materials

Most chemicals applied were obtained from Tocris (Bristol, United Kingdom), Sigma-Aldrich (München, Germany), Carl Roth GmbH (Karlsruhe, Germany), Calbiochem (Darmstadt, Germany), VWR (Darmstadt, Germany) und Merck KGaA (Darmstadt, Germany). For water purification purposes the Milli-Q Water Purification System from Merck EMD Milipore is utilized. The majority of labware is obtained from Sarstedt AG & Co. KG (Nümbrecht, Germany).

### 3.2 Animal experiments

#### 3.2.1 Housing

Mice are bred and housed in a specific-pathogen-free (SPF) animal facility prior to performance of the experiments. The animals are daily exposed to twelve hours of light (6:00 AM – 6:00 PM) and twelve hours of darkness (6:00 PM - 6:00 AM) and a room temperature of  $24 \pm 1^\circ\text{C}$ . Moreover, the mice have *ad libitum* access to food and water.

#### 3.2.2 Immunohistochemistry

##### *Equipment and materials*

Ethanol ROTIPURAN®  $\geq 99,8\%$  (Roth), Cat. No. 9065

Leica EG1160 (Embedding machine)

Microm SB 80 (Warm bath)

Microm HM 335 E (Cutting machine)

Paraplast® (Roth), Cat. No. X880.1

Paraformaldehyde (Roth), Cat. No. 0335.3

Xylol < 98% (Roth), Cat. No. 9713.3

- **PBS**

Sodium chloride 137 mM

Potassium chloride 2.7 mM

Disodium hydrogenphosphate dodecahydrate 8mM

Potassium dihydrogen phosphate 1.4 mM

→ Dissolve the salts in water and adjust pH to 7.4 with NaOH, autoclave at  $121^\circ\text{C}$  for 20 minutes.

- **PBST**  
 Tween 20 1 mL  
 PBS 1000 mL  
 → Dissolve Tween 20 in PBS and store the solution at room temperature under exclusion from light
  
- **PFA 4%**  
 Paraformaldehyde 40 g  
 PBS 1000 mL  
 5 M NaOH 20 µL  
 → Let solution stir at 60°C overnight and keep it in the fridge at 4°C.

### **Procedure**

After dissection of murine tissues, the tissue pieces were fixed at 4°C for 24-48 hours in a 4% paraformaldehyde (PFA) solution in phosphate-buffered saline (PBS). Afterwards dehydration of the tissues was performed by bathing the tissues consecutively in increasing concentrations of ethanol (50%, 70%, 95%, 100%). The dehydration in each concentration of ethanol was repeated three times for 20 minutes, each time in a fresh solution of the respective concentration. This step was followed by a ten-minute incubation in xylol which was repeated three times. Subsequently the tissues were kept twice in liquid paraffin for one hour at 60°C, followed by an overnight incubation. On the next day the tissues were embedded in liquid paraffin and solidified on ice or at room temperature. The precooled embedded tissues were cut into 6 µm thick sections, mounted on microscope glass slides and were left to dry at 37°C for 24 hours.

#### *3.2.2.1 Hematoxylin / Eosin (HE) staining*

##### **Equipment and materials**

Hematoxylin solution A acc. to Weigert (Roth), Cat. No. X906.1  
 EOSIN Y SOLUTION AQUEOUS (Sigma-Aldrich), Cat. No. HT110216  
 Roti®-Histokitt (Roth), Cat. No. 6638.2

### **Procedure**

For removal of paraffin, the tissue sections were washed three times for five minutes in xylol. Afterwards the samples were rehydrated by exposure to decreasing concentrations of ethanol (100%, 95%, 75%, 50%). The step was repeated twice for two minutes for each concentration, followed by incubation in water for five minutes (twice). The staining with hematoxylin was performed for two seconds, immediately followed by a washing step applying distilled water. Subsequently the sections were stained in an eosin solution for one minute and washed in distilled water for four minutes. The

dehydration of the tissues was performed immersing them in increasing ethanol compositions (50%, 70%, 90%, 95%, 100%) for two minutes per concentration. The procedure was finalized by washing the slides twice for two minutes in xylol and mounting them applying the Roti®-Histokitt. Staining of the histological slices was kindly supported by Patricia Zehner.

### 3.2.3 Serum preparation

#### *Equipment and materials*

Sterican® cannula 27 G x ½", 0.40 x 12 mm (B. Braun Melsungen AG, Germany)

Omnifix®-F solo syringe 1 mL (B. Braun Melsungen AG, Germany)

Centrifuge 5430 R (Eppendorf AG, Hamburg, Germany)

#### *Procedure*

After cervical dislocation, the heart is punctured and blood is taken with a syringe. Then the needle is removed and blood is transferred into an eppi and left at RT for 20 minutes for clotting. Afterwards the blood is centrifuged at 4°C at 1000 rpm for 10 minutes. The supernatant is taken and the resulting serum is shock frozen in liquid nitrogen. The serum is further used for leptin ELISA or S1P measurements.

### 3.2.4 S1P determination in serum and tissue

#### *Equipment and materials*

Hammer

Profissimo Wassereis-Tüten (plastic bag), (DM, Karlsruhe, Germany)

#### *Procedure*

The serum is prepared as described in chapter 3.2.3. The fat tissues are excised, shock frozen in liquid nitrogen and stored at -80°C. On day of preparation the tissue is cut on dry ice and then put into the described plastic bag (DM). This type of bag is favourable because it does not become porous when exposed to liquid nitrogen. Then the tissue in the bag is dipped into liquid nitrogen and the tissue is pulverised with a hammer. This procedure is repeated several times, then the pulverised tissue is weighted into an eppi and the samples were sent on dry ice to the research group of Professor Markus Gräler where isolation and measurement of the samples occurred according to the methods described in the following publication: Bode, C. & Gräler, M. H. Quantification of sphingosine-1-phosphate and related sphingolipids by liquid chromatography coupled to tandem mass spectrometry. *Methods in molecular biology* (Clifton, N.J.) 874, 33–44; 10.1007/978-1-61779-800-9\_3 (2012) (Bode and Gräler, 2012).

### 3.2.5 Exposure to 30°C, 23°C and 4°C

#### ***Equipment and materials***

PhenoMaster (TSE Systems, Bad Homburg, Germany)

(Cool)incubator MKK 600 (Flohr Instruments, Nieuwegein, Netherlands)

#### ***Procedure***

The mice are housed from the age of eight weeks either for seven days at 23°C or 30°C in a mouse hotel and if required the animals are metabolically characterized in the TSE PhenoMaster (Chapter 3.2.6). The 4°C cold exposure occurs for seven days as well either in the mouse hotel or in the TSE PhenoMaster, but prior to cold exposure the mice are acclimatized for three days at 16°C. The animals are daily exposed to twelve hours of light (6:00 AM – 6:00 PM) and twelve hours of darkness (6:00 PM - 6:00 AM) and food and water are provided *ad libitum*. After treatment mice are sacrificed and organs are taken.

### 3.2.6 Metabolic phenotyping in metabolic cages

#### ***Equipment and materials***

PhenoMaster (TSE Systems, Bad Homburg, Germany)

#### ***Procedure***

Male mice are weighted and then measured in the TSE PhenoMaster for at least 24 hours. The measurement occurs from 6 PM till 6 PM the next day with a twelve hours dark-light rhythm. From 6 PM till 6 AM the lights are switched off, from 6 AM till 6 PM daylight is mimicked. The animal wellbeing is controlled twice a day. The TSE PhenoMaster measures oxygen (O<sub>2</sub>) consumption, carbon dioxide (CO<sub>2</sub>) production and motility. Mice obtain food and water *ad libitum*.

### 3.2.7 Body composition

#### ***Equipment and materials***

NMR minispec device (Bruker Corporation)

#### ***Procedure***

In order to determine lean mass, fat mass and water content of mice, the body weight of the animals is measured. Then the mouse is put into a restrainer which is then put into the NMR minispec device (Bruker Corporation). The non-invasive body composition measurement lasts for approximately two minutes.

### 3.2.8 Pharmacological injections

#### *Equipment and materials*

Sterican® cannula 27 G x ½", 0.40 x 12 mm (B. Braun Melsungen AG, Germany)

Omnifix®-F solo syringe 1 mL (B. Braun Melsungen AG, Germany)

Kochsalzlösung 0.9% Miniplasco connect 5 mL (B. Braun Melsungen AG, Germany), PZN: 03040980

CYM 5520 (Tocris), Cat. No. 5418

JTE 013 (Tocris), Cat. No. 2392

SEW 2871 (Tocris), Cat. No. 2284

#### *Procedure*

During the seven day long 4°C cold exposure or the one week long 23°C exposure (in accordance with chapter 3.2.5) mice are daily intraperitoneally injected with the following compounds: S1PR1 agonist SEW 2871 [5 mg/kg body weight (BW)] or S1PR2 agonist CYM 5520 [5 mg/kg BW] or S1PR2 antagonist JTE 013 [4 mg/kg body BW] or the respective vehicle control. A volume of 100 µL is injected daily for seven consecutive days. The side of injection is alternated daily. The mice are checked two times a day. In accordance with the '3 R principle of humane animal research' (Russell and Burch, 1992) there is no separate, independent vehicle control group for each compound injected. All three compounds share the same control group (Figure 30, Figure 31, Figure 32). By this means the animal numbers needed for this experiment can be reduced by one third.

**Table 2 | Composition of pharmacological injections**

Compound	Dosage	Amount DMSO per injection	Amount NaCl 0.9% per injection
Vehicle control	50%	50 µL	50 µL
SEW 2871 (S1PR1-Agonist)	5 mg / kg BW	50 µL	50 µL
CYM 5520 (S1PR2-Agonist)	5 mg / kg BW	50 µL	50 µL
JTE 013 (S1PR2-Antagonist)	4 mg / kg BW	50 µL	50 µL

### 3.3 Cell culture

#### *Equipment and materials*

##### Labware

6-well tissue culture plates (Sarstedt AG & Co. KG), Cat. No. 83.3920  
 6-well TPP plates (TPP Techno Plastic Products AG), Cat. No. 92406  
 10 cm TC dishes [58 cm<sup>2</sup>], Standard (Sarstedt), Cat. No. 83.3902  
 12-well TPP plates (TPP Techno Plastic Products AG), Cat. No. 92412  
 12-well TC plates, Standard (Sarstedt), Cat. No. 83.3921  
 BD Discardit II, 5 mL syringe, (Becton Dickinson, Franklin Lakes, USA), PZN: 03626817  
 Conical tubes, 15 ml and 50 ml volume (Sarstedt), Cat. No. 62.554.502, 62.547.254  
 Cryogenic vials (Sarstedt), Cat. No. 72.379.992  
 Micro Tube 1.5 mL, SafeSeal (Sarstedt), Cat. No. 72.706.400  
 Nylon Net Filter, pore size: 30 µm (Merck Millipore, Burlington, USA), Cat. No. NY3002500  
 Nylon Net Filter, pore size: 100 µm (Merck Millipore, Burlington, USA), Cat. No. NY1H00010  
 Reaction tube 1.5 mL (Sarstedt), Cat. No. 72706  
 Serological pipette, sterile 5 ml (Sarstedt), Cat. No. 86.1253.001  
 Serological pipette, sterile 10 mL (Sarstedt), Cat. No. 86.1254.001  
 Serological pipette, sterile 25 mL (Sarstedt), Cat. No. 86.1685.001  
 Sterican® cannula 20 G x ½", 0.9 x 40 mm (B. Braun Melsungen AG, Germany), PZN: 02050798  
 Syringe filter 0.22 µm (VWR), Cat. No. 514-0061  
 T175 tissue culture flasks (Sarstedt) Cat. No. 83.3912.002

##### Compounds Part I

3,3',5-Triiodo-L-thyronine sodium salt (Sigma-Aldrich), Cat. No. T6397  
 3-Isobutyl-1-methylxanthine [IBMX], (Sigma-Aldrich), Cat. No. I5879  
 Albumin Fraktion V [BSA] (Roth), Cat. No. 8076.3  
 Bovine Serum Albumin fatty acid free (Sigma-Aldrich), Cat. No. A7030  
 Calcium chloride (Roth), Cat. No. CN93.1  
 Calcium chloride dihydrate (Roth), Cat. No. T885.1  
 Collagenase Type II (Worthington Biochemical Corporation, Lakewood, USA), Cat. No. CLS2  
 CYM 5520 (Tocris), Cat. No. 5418  
 CYM 5541 (Tocris), Cat. No. 4891  
 Dexamethasone (Sigma-Aldrich) Cat. No. D4902  
 Dimethyl sulfoxide [DMSO], (Roth), Cat. No. A994  
 Dulbecco's Modified Eagle's Medium [DMEM], high glucose, GlutaMAX(TM) (Gibco), Cat. No. 61965  
 Dulbecco's Modified Eagle's Medium [DMEM], high glucose, GlutaMAX(TM) (Gibco), Cat. No. 61966  
 Endothelin 1 [ET-1] (Tocris), Cat. No. 1160  
 Ethanol ROTIPURAN® ≥99,8 % (Roth), Cat. No. 9065  
 Fetal Bovine Serum [FBS], (Biochrom), Cat. No. S0015  
 FR900359, G<sub>q</sub> inhibitor (Kindly provided by AG Kostenis, University of Bonn, Germany)  
 FTY720 phosphate [FTY720P], (Cayman Chemicals), Cat. No. 10008639  
 Glucose, waterfree (Roth), Cat. No. X997.2  
 HEPES (Sigma-Aldrich), Cat. No. H4034  
 Insulin solution human (Sigma-Aldrich), Cat. No. I9278  
 Isopropanol ROTIPURAN® ≥99,8 % (Roth), Cat. No. 6752  
 JTE 013 (Tocris), Cat. No. 2392

**Compounds Part II**

L-(-)-Norepinephrine (+)-bitartrate salt monohydrate [NE] (Sigma-Aldrich), Cat. No. A9512  
L-ascorbic acid (Sigma), Cat. No. A-4034  
Magnesium chloride hexahydrate (Roth), Cat. No. A-537.1  
Oil Red O (Sigma-Aldrich), Cat. No. O0635  
Paraformaldehyde (Roth), Cat. No. 0335.3  
Penicillin/Streptomycin, [Pen/Strep], (Merck), Cat. No. A2213  
Pertussis Toxin from *Bordetella pertussis* (Sigma-Aldrich), Cat. No. P7208  
Potassium chloride (Roth), Cat. No. 6781.1  
Rho Inhibitor 1 [C3T, C3 Transferase] (Cytoskeleton, Inc., Denver, USA), Cat. No. CT04-A  
Rosiglitazone (Sigma-Aldrich), Cat. No. R2408  
SEW 2871 (Tocris), Cat. No. 2284  
Sphingosine-1-phosphate [S1P] (Tocris), Cat. No. 1370  
Sodium ascorbate (Sigma-Aldrich), Cat. No. A7631  
Sodium chloride (Roth), Cat. No. 3957.1  
Thapsigargin (Tocris), Cat. No. 1138  
Trypan Blue Solution 0.4%, (Gibco), Cat. No. 15250-061  
Trypsin-EDTA (0.05 %), phenol red (Gibco) Cat. No. 25300054  
TY 52156 (Tocris), Cat. No. 5328  
W146 (Avanti polar lipids), Cat. No. 857390P  
Y-27632 dihydrochloride (Tocris), Cat. No. 1254

**Machines**

Centrifuge, Biofuge Primo (Heraeus)  
Autoclave, Varioklav 135 T (Faust, Meckenheim)  
Countess Automated Cell Counter (Invitrogen), Cat. No. C10227  
Incubator, HERAcell® 150 (Heraeus)  
Laminar air flow, HERAsafe™ (Heraeus)  
Microscope, LEICA DMIL (Leica Microsystems, Wetzlar, Germany)  
PURELAB classic (ELGA LabWater, Celle, Germany)  
Surgical instruments (scissors, forceps)  
Epson Perfection V370 Photo Scanner (Epson)

### 3.3.1 Isolation and cultivation of brown adipocytes

- **PBS**  
Sodium chloride 137 mM  
Potassium chloride 2.7 mM  
Disodium hydrogenphosphate dodecahydrate 8mM  
Potassium dihydrogen phosphate 1.4 mM  
→ Dissolve the salts in water and adjust pH to 7.4 with NaOH, autoclave at 121°C for 20 minutes.
- **Isolationbuffer**  
Sodium chloride 123 mM  
Potassium chloride 5 mM  
Calcium chloride 1.3 mM  
Glucose 5 mM  
HEPES 100 mM  
BSA 1.5%  
Collagenase II 2mg/mL  
→ all five first named compounds are dissolved together in H<sub>2</sub>O and pH is adjusted to 7.4 with a 5M sodium hydroxide solution and the buffer is filtered sterilely. Before usage BSA and Collagenase II are added, the solution is heated up in the warm bath at 37°C and the solution is filtered sterilely again.
- **HEPES-solution 0.1 M**  
HEPES (H4034) 11.92 g  
DMEM (Cat. No. 61965) ad 500.0 mL
- **T<sub>3</sub>-solution**  
3,3',5-Triiodo-L-thyronine sodium salt 2.0 mg  
Sodium hydroxide solution 1M 1.0 mL  
DMEM (Cat. No. 61965) 49.0 mL
- **Sodium ascorbate-solution**  
Sodium ascorbate 100 mg  
Ad 10 mL PBS
- **Culture medium**  
DMEM (Cat. No. 61965) 396.2 mL  
Pen/Strep 5.0 mL  
FBS, heat inactivated 50.0 mL  
HEPES solution 0.1 M 50.0 mL  
Insulin (Cat. No. I9278) 1.16 µL  
T<sub>3</sub>-solution 33.7 µL  
Sodium ascorbate solution 1.25 mL

### ***Procedure***

Interscapular BAT is excised from newborn pups, transferred into a 1.5 mL micro tube containing 0.5 mL of isolation buffer. The tissue is chopped with surgical scissors into fine pieces. Afterwards the tissue suspension is transferred into a 15 mL falcon containing 2.5 mL isolation buffer and heated in a 37°C warm water bath for a period of 30 minutes while shaking thoroughly every five minutes. Then the suspension is filtered through a 100 µm Nylon filter and stored on ice for 30 minutes. The middle phase (approximately 2 mL) is taken and filtered through a 30 µm Nylon filter following a centrifugation at 700g for 10 minutes. The supernatant is sucked up and the pellet is resuspended in 2 ml of culture medium. The isolations of at least three pups are pooled and then seeded on a six well plate (one well per pup). After 24 hours the brown preadipocytes are immortalized with a Simian Virus 40 (SV40) large T-antigen under the control of phosphoglycerate kinase (PGK) promoter. 200 ng of virus are used per one 6 well.

### **3.3.2 Expansion of brown adipocytes**

- **Brown adipocyte growth medium [GM]**
  - DMEM (Cat. No. 61965) 450.0 mL
  - Pen/Strep 5.0 mL
  - FBS, heat inactivated 50.0 mL

### ***Procedure***

When the immortalized brown preadipocytes (Chapter 3.3.1) reach around 90% confluency they are split. Therefore, the cells are washed twice with PBS and then incubated for 5 min. at 37°C with 0.5 mL Trypsin-EDTA per well. When the cells detach 2 mL of brown adipocyte growth medium is added to the wells. The presence of FBS leads to an inactivation of the trypsin enzyme. The cells are centrifuged at 1000 rpm for 10 minutes. Supernatant is removed and the cells are resuspended in brown adipocyte growth medium, pooled and seeded on a 10 cm round tissue culture dish. The content of one 6 well is seeded into two 10 cm dishes. This passage is defined as P1. The cells are further split 1:10 when reaching 90% confluence and are later frozen at P4. Prior to freezing, cells are stained with trypan blue solution and counted by Countess Automated cell counter. Either one or three million cells are frozen per one cryogenic vial. Intermediate freezing at P2 and P3 for later expansion is also possible. The immortalized brown preadipocytes are stored at -150°C and used at P4 for brown adipocyte experiments.

### 3.3.3 Differentiation of brown adipocytes

- **Brown adipocyte differentiation medium [DM]**  
DMEM (Cat. No. 61965) 450.0 mL  
FBS, heat inactivated 50.0 mL  
Pen/Strep 5.0 mL  
T<sub>3</sub> solution 8.43 µL [see chapter 3.3.1]  
Insulin solution [9.5-11.5mg/mL] 5.83 µL, Cat. No. I9278
- **Dexamethasone-solution**  
Dexamethasone 1 .0 mg  
Ethanol 99%
- **IBMX-solution**  
3-Isobutyl-1-methylxanthine [IBMX], (Sigma-Aldrich), Cat. No. I5879 5.56 mg  
DMSO 50 µL  
→ Heat up the IBMX solution to 70°C, until the solution is clear
- **Brown adipocyte induction medium [IM]**  
Brown adipocyte differentiation medium 50 mL  
IBMX solution 50 µL  
Dexamethasone solution 20 µL

#### *Procedure*

Brown preadipocytes at P4 are seeded in brown adipocyte growth medium at a density of 166.000 cells per one well of a 6 well plate or at a density of 83.000 cells per one well of a twelve well plate. This day is considered day -4 which means that cells are four days prior to induction. At day-2 cells are usually confluent and the medium is switched from growth to brown adipocytes differentiation medium. For the induction of the adipogenic program, cells are induced at day 0 with adipocyte differentiation medium containing an induction cocktail of IBMX and dexamethasone. Afterwards the medium is replaced every second day (day 2, 4, 6) with adipocyte differentiation medium. Whenever chronic treatment is described in this thesis, it occurred from day -2 until day 7 and the compounds are added freshly together with each medium change.

**Table 3 | Procedure of *in vitro* brown adipocyte differentiation and chronic treatment**

Day -4	Day -2	Day 0	Day 2	Day 4	Day 6	Day 7
Seeding	Confluency	Induction				
GM	DM	IM	DM	DM	DM	Experiment
	T3, Insulin	T3, Insulin, IBMX, Dexa	T3, Insulin	T3, Insulin	T3, Insulin	
Chronic Treatment together with each medium change						

### 3.3.4 Isolation and cultivation of white adipocytes

- **Collagenase digestion solution**

Collagenase Type II 75 mg  
 BSA fatty acid free (Sigma-Aldrich), Cat. No. A7030 250 mg  
 DMEM (Cat. No. 61966) 50.0 mL  
 → The solution is filtered sterilely through a 0.45 µm filter.

- **White adipocyte growth medium [GM]**

DMEM (Cat. No. 61966) 450.0 mL  
 Pen/Strep 5.0 mL  
 FBS, heat inactivated 50.0 mL

#### **Procedure**

Inguinal white adipose tissue is excised from eight to twelve-week old mice. The lymph node is removed. Until the collection of all tissues is finished, the tissues are stored in a falcon containing PBS on ice. The tissues of two mice serve as one “n”. Afterwards the tissues are minced with small sharp scissors in an 1.5 mL micro tube and the tissue pulp is moved to a 15 mL falcon tube containing 5 mL of collagenase digestion solution. The falcon is heated at 37°C in the water bath and shaken thoroughly every five minutes. After approximately 20 minutes, 5 mL of fresh collagenase solution is added additionally to each falcon and the shaking and warming process goes on until no bigger tissue parts are visible after a total digestions time of 30 - 45 minutes. Five mL of the GM are added to the falcon and the digested tissue is centrifuged at 500g for 10 minutes at room temperature (RT). The supernatant is discarded and the pellet is resuspended in GM and filtered through a 100 µm Nylon filter. More GM is added to the cell filtrate to obtain a total volume of 25 mL which is seeded on a T175 tissue culture flask. The white adipocytes are grown in the incubator and when they reach 95-100% confluency they are frozen. Therefore, the cells are washed twice with PBS and 2 mL Trypsin-EDTA is added to the flask which is incubated for 5 minutes at 37°C, 5% CO<sub>2</sub>. After detachment of the cells, GM is added and a representative amount of cells is stained with Trypan Blue Solution and counted with Countess Automated Cell Counter. One million cells are frozen in one cryogenic vial. The cells are stored at -150°C.

### 3.3.5 Differentiation of white adipocytes

- White adipocyte maintenance medium [MM]**  
 DMEM (Cat. No. 61966) 470.0 mL  
 FBS, heat inactivated 25.0 mL [5%]  
 Pen/Strep 5.0 mL [1%]  
 D-biotin 1 mM  
 Insulin 0.172 mM  
 L-ascorbate 50 mg / mL  
 Panthothenate 17 mM  
 T<sub>3</sub> 1 nM
- White adipocyte induction medium [IM]**  
 IBMX 0.5 mM  
 Dexamethasone 0.25 mM  
 Rosiglitazone 1 μM  
 → all compounds are added to the white adipocyte maintenance medium.

#### Procedure

Primary white adipocytes are seeded on a 12-well TPP plate with approximately 83.000 cells per well. The day of confluency is considered day -2 and induction of the cells with white adipocyte induction medium occurs 48 hours after confluency (day 0). Afterwards the medium is changed every second day to white adipocyte maintenance medium. The chronic treatment of the cells occurs from day of confluency (day -2) and the compounds are administered together with each medium change. Experiments are performed on day 7 and day 8.

**Table 4 | Procedure of *in vitro* white adipocyte differentiation and chronic treatment**

	Day -2	Day 0	Day 2	Day 4	Day 6	Day 7/8
Seeding	Confluency	Induction				
GM	GM	IM	MM	MM	MM	
		IBMX, Dexa, Rosiglitazone, T3, Insulin, D-biotin, L-ascorbate, Panthothenate	T3, Insulin, D- biotin, L- ascorbate, Panthothenate	T3, Insulin, D- biotin, L- ascorbate, Panthothenate	T3, Insulin, D- biotin, L- ascorbate, Panthothenate	Experiment
		Chronic Treatment together with each medium change				

### 3.3.6 Browning of white adipocytes

White adipocytes are cultured according to the protocol in chapter 3.3.5. On day seven the cells are incubated for 16 hours with the compounds whose influence on browning is of interest. Norepinephrine in a concentration of 1 μM serves as a positive control. After 16 hours of treatment RNA is isolated from these cells and browning markers are measured.

### 3.4 Oil Red O Staining

- **PFA 4% solution**  
Paraformaldehyde 4.0 g  
PBS 1000.0 mL  
1M NaOH 1.0 mL  
→ The solution is stirred over night and then stored at 4°C.
- **Oil Red O Stock solution [5 mg / ml]**  
Oil Red O 5.0 g  
Isopropanol 99% 1000.0 mL  
→ The Oil Red O Stock solution is stirred for 24 hours and is stored at room temperature.
- **Oil Red O solution**  
Oil Red O Stock solution 60 mL  
Water 40 mL  
→ The solution is filtered through a double layer of filter paper

#### *Procedure*

Brown and white adipocytes are washed twice with PBS. Afterwards, the PFA 4% solution is added in order to fix the cells. After 15 minutes of incubation the cells are washed again twice with PBS and the cells are incubated with the Oil Red O solution for 2-3 hours. The cells are washed with distilled water and the plate is left to dry at room temperature. Afterwards the plate is scanned with an Epson Perfection V370 Photo scanner.

### 3.5 RNA analysis

#### *Equipment and materials*

InnuSOLV RNA Reagent (Analytik Jena AG), Cat. No. 845-SB-2090100  
 7900HT Fast Real-Time PCR System (Applied Biosystems), Cat. No. 4330966  
 Micro Tube 1.5 mL, SafeSeal (Sarstedt), Cat. No. 72.706.400  
 Centrifuge (Eppendorf), Cat. No. 5415R  
 Diethyl pyrocarbonate [DEPC] (Roth), Cat. No. K028.1  
 Nanodrop200 Spectrophotometer (ThermoScientific)  
 SYBR-Green PCR master mix (Applied Biosystems), Cat. No. 4309155  
 Thermomixer comfort (Eppendorf), Cat. No. 2050-120-04  
 ProtoScript® II First Strand cDNA Synthesis Kit (New England Biolabs), Cat. No. E6560S  
 Thermocycler Biometra TProfessional Trio 30 (Analytik Jena)

#### 3.5.1 RNA-Isolation

InnuSOLV RNA reagent is applied for the isolation of RNA from cells or tissues. Cells are washed with PBS followed by addition of 1 mL of InnuSOLV RNA reagent per well which induces lysis of the cells. The resulting suspension is then transferred into an 1.5 mL micro tube. 200 µL of chloroform are added and the microtube is shaken thoroughly for 15 seconds. After five minutes at room temperature the micro tube is centrifuged at 13.000 rpm at a temperature of 4°C for ten minutes. Afterwards the upper clear phase (approximately 500 µL) is transferred into a fresh micro tube and for precipitation of the RNA 500 µL of isopropanol are added. The RNA is pelleted by centrifugation (4°C, 10 min., 13.000 rpm). The supernatant is discarded and 1 mL of cold Ethanol 75% (in DEPC water) is added followed by a centrifugation (4°C, 5 min., 13.000 rpm). This step is performed three times. Afterwards the pellet is air dried and dissolved in nuclease free water. To improve the solubility of the RNA, ten-minute-long heating at 50°C can be performed optionally. When dissolved, the concentration of the RNA is measured with the help of a Nanodrop Spectrophotometer.

#### 3.5.2 cDNA Synthesis

For transcription of RNA into cDNA the ProtoScript® II First Strand cDNA Synthesis Kit is used.

**Table 5 | Recipe for cDNA reaction mix**

Substance	Amount
RNA	1000 ng
ProtoScript II® Reaction Mix (2X)	10 µL
ProtoScript II® Enzyme Mix (10X)	2 µL
Random Primer Mix	2 µL
Nuclease free water	ad 20.0 µL

After pipetting all substances together thermocycling is performed. Afterwards the cDNA is diluted to a concentration of 2.5 ng /  $\mu$ L.

**Table 6 | Thermocycling program for cDNA Synthesis**

Step #	Temp °C	Time [s]
1	25	5
2	42	60
3	80	5

### 3.5.3 RT-qPCR

In order to determine mRNA expression of specific target genes real-time quantitative PCR (RT-qPCR) was performed using the 7900HT Fast Real-Time PCR System (Applied Biosystems). The second derivative maximum method is used to quantify the resulting mRNA levels. The Hypoxanthine-guanine phosphoribosyltransferase (*Hprt*) gene is used as an internal control. The recipe for the RT-qPCR reaction mix, the RT-qPCR program, as well as the primer sequences can be found in Table 7-Table 9.

**Table 7 | Recipe for RT-qPCR reaction mix**

Compound	Volume
SYBR-Green PCR master mix	5 $\mu$ L
Primer forward 5 $\mu$ M	0.5 $\mu$ L
Primer reverse 5 $\mu$ M	0.5 $\mu$ L
cDNA [2.5 ng / $\mu$ L]	4 $\mu$ L

**Table 8 | RT-qPCR program**

Step #	Temp °C	Time [s]	Notes
1	95	600	
2	95	15	Step 2 and 3 are repeated 40 times
3	60	60	
Melting Curve			
4	95	1	
5	65	15	
6	95	/	

**Table 9 | Real-time PCR primer sequences**

Gene	Forward sequence (5' → 3')	Reverse Sequence (5' → 3')
S1pr1	AAGTCTCTGGCCTTGCTGAA	GATGATGGGGTTGGTACCTG
S1pr2	CAGCTTTTGTCACTGCCGTA	TCTCAGGGCATGTCACTCTG
S1pr3	GCCCCTAGACGGGAGTCTTA	ATAGGCTCTCGTTCTGCAAGG
S1pr4	TCCAGCATTTCCAGCGTC	TCATGTTCTCAGTCACCATCAG
S1pr5	CCAACAGCTTGACGCGATCCCC	GGTTGCTACTCCAGGACTGCCG
Shk1	TGTGAACCACTATGCTGGGTA	CAGCCCAGAAGCAGTGTG
Shk2	AGACGGGCTGCTTTACGAG	CAGGGGAGGACACCAATG
Hprt	GTCCCAGCGTCGTGATTAGC	TCATGACATCTCGAGCAAGTCTTT
aP2	GCGTGGAATTTCGATGAAATCA	CCCGCCATCTAGGGTTATGA
Ppargamma	ACAAGACTACCTTTACTGAAATTACCAT	TGCGAGTGGTCTTCCATCAC
Ucp1	TAAGCCGGCTGAGATCTTGT	GGCCTCTACGACTCAGTCCA
Cyr61	CAGCTCACTGAAGAGGCTTCTCT	GCGTGCAGAGGGTTGAAAA

### 3.6 Protein analysis

#### *Equipment and materials*

Albumin Fraction V (Roth), Cat. No. 8076.3

Ammonium peroxydisulphate [APS] (Roth), Cat. No. 9592.2

Bandelin SONOPLUS HD 2070 (BANDELIN electronic GmbH & Co. KG, Berlin, Germany)

BioPhotometer D30 (Eppendorf)

Centrifuge 5430R (Eppendorf)

Color Prestained Protein Standard, Broad Range (11–245 kDa) (New England Biolabs), Cat. No. P7719

Complete protease inhibitor cocktail (Roche), Cat. No. 04693116001

Coomassie brilliant blue G-250 (Merck), Cat. No. 1.15444.0025

Glycine (Roth), Cat. No. 3908.3

Methanol ROTIPURAN® (Roth), Cat. No. 4627.1

Minispin centrifuge (Sigma-Aldrich), Cat. No. Z606235

Mini-PROTEAN Tetra Cell electrophoresis system (BioRad)

Nitrocellulose membrane, Amersham Protran 0.45 NC (GE Healthcare Life Sciences),  
Cat. No. 10600002

N, N, N', N'-Tetramethylethylenediamine [TEMED] (Sigma), Cat. No. T7024

Nonfat dried milk powder (AppliChem GmbH, Darmstadt, Germany), Cat. No. A0830,1000

Nonident™ P 40 Substitute [NP-40], (Fluka BioChemika), Cat. No. 74385

PageRuler Prestained Protein Ladder (Thermo Scientific), Cat. No. 26616

Power supply, Consort EV 202 (Sigma-Aldrich), Cat. No. Z654418

Roller Mixer SRT6 (Stuart)

Rotiphorese®Gel 30 "Acrylamide" (Roth), Cat. No. 3029

Sodium dodecyl sulfate [SDS] (Roth), Cat. No. 2326.2

Sodium chloride (Roth), Cat. No. 3957.1

Sodium orthovanadate (Sigma), Cat. No. S6508

Syringe filter 0.22 µm (VWR), Cat. No. 514-0061

Thermomixer comfort (Eppendorf), Cat. No. 2050-120-04

Tween® 20 (Roth), Cat. No. 9127.2

Whatman® Gel Blot Paper GB003 (Sigma-Aldrich), Cat. No. 10426892

### 3.6.1 Protein Isolation

- **RIPA Buffer**

NaCl 150 mM

Tris HCl (pH 7.5) 50 mM

NP-40 1 %

SDS 0.1 %

→ All compounds are dissolved in Millipore water, the buffer is sterilely filtered and stored at 4°C

- **Lysis Buffer**

NaF 10 mM

Na<sub>3</sub>VO<sub>4</sub> 1 mM

Complete 40 µL / mL

→ The protease inhibitors are added prior to protein isolation to the RIPA buffer.

#### *Procedure*

Cells are washed twice with PBS. Then 200 µL of Lysis buffer is added to each well of a 6 well plates. The plate is kept on ice and the cell layer is carefully peeled off with the tip of a pipette and the cell suspension is transferred into a microtube. Afterwards the mixture is sonicated for four cycles with Bandelin SONOPLUS sonicator. The micro tube is kept on ice for 30 minutes followed by a centrifugation for 20 minutes at 13.000 rpm at a temperature of 4°C. Afterwards the supernatant is carefully taken, considering not transfer any fat into the new micro tube. The fat could disturb the Western blot procedure. The protein concentration in the lysate is quantified via Bradford assay (chapter 3.6.2)

### 3.6.2 Bradford assay

- **Coomassie solution**

Phosphoric acid 8.5 %

Ethanol 5 %

Coomassie brilliant blue G-250 0.01 %

→ The ingredients are prepared with water and the solution is stored at 4°C.

#### *Procedure*

The lysate from chapter 3.6.1 is thoroughly mixed and 2 µL are pipetted into a new microtube containing 98 µL of a sodium chloride solution [0.15 M]. 1 mL of Coomassie solution is added and the absorption is photometrically measured with help of the BioPhotometer D30 at a wavelength of 595 nm. A standard curve was determined by measurement of different known BSA concentrations. According to this standard curve the protein content in the lysate is measured. The lysate is stored at -80°C.

### 3.6.3 Protein preparation

- **Lämmli solution (6x)**  
Tris (pH 6.8) 1.5 M 7 mL  
Glycerol 3 mL  
SDS 1.0 g  
Dithiothreitol 0.93 g  
Bromophenol blue 1.2 mg

#### *Procedure*

The protein lysates are diluted with lysis buffer and lämmli solution in order to achieve the same amount of protein per volume among all protein samples of one experimental batch and a lämmli concentration of 1x. Afterwards the mixture is cooked at 98°C for five minutes. The preparation can be stored at -20°C or immediately used for SDS-PAGE.

### 3.6.4 SDS-PAGE

- **Tris (pH 8.8) 1.5 M**  
Tris base 91.0 g  
SDS 2.0 g  
Water 500.0 mL  
→ set the pH to 8.8 using 37% hydrochloric acid. Store at 4°C.
- **Tris (pH 6.8) 1.5 M**  
Tris base 60.4 g  
SDS 2.0 g  
Water 500.0 mL  
→ set the pH to 6.8 using 37% hydrochloric acid. Store at 4°C.
- **ELPHO buffer (10x)**  
Glycine 2 M  
Tris 250 mM  
SDS 0.1 %  
→ The components are dissolved in water and the pH is appointed to 8.3. For SDS Page the ELPHO buffer is diluted 1:10 with water to obtain a 1x solution.

**Table 10 | Recipe for 10.0 mL of resolving gel**

Components	Gel percentage		
	10%	12%	15%
H <sub>2</sub> O	4.0 ml	3.3 ml	2.3 ml
30% acrylamid mix	3.3 ml	4 ml	5 ml
1.5 M Tris (pH 8,8)	2.5 ml	2.5 ml	2.5 ml
20% APS	0.05 ml	0.05 ml	0.05 ml
TEMED	0.004 ml	0.004 ml	0.004 ml

**Table 11 | Recipe for 10.0 mL of stacking gel**

Components	Amount
H <sub>2</sub> O	6.8 ml
30% acrylamid mix	1.7 ml
1.0 M Tris (pH6,8)	1.25 ml
20% APS	0.05 ml
TEMED	0.01 ml

### **Procedure**

The gel is casted according to recipes in Table 10 and Table 11 with a thickness of 1.5 mm. The SDS-PAGE (Sodium dodecyl sulfate polyacrylamide gel electrophoresis) is performed in order to separate proteins according to their size. In the upper part of the gel, the 'stacking' part the proteins are gathered and concentrated followed by a separation in the resolving gel. The electrophoresis is carried out in 1x ELPHO buffer with the help of the Mini-PROTEAN Tetra Cell electrophoresis system at 100 V until the protein reaches the resolving gel, then the voltage is increased to 140 V.

### **3.6.5 Western blotting**

- **Transfer buffer**  
Water 70%  
Methanol 20%  
ELPHO buffer (10x) 10%
- **TBS (10x)**  
NaCl 1.4 M  
SDS 0.1 %  
Tris 100 mM  
→ The components are dissolved in water and the pH is appointed to 8.0.
- **TBST**  
Water 89.9%  
TBS 10%  
Tween-20 0.1 %
- **BSA solution 5%**  
BSA 2.5 g  
Sodium azide [10%] 250 µL  
TBST 50.0 mL
- **Milk blocking solution**  
TBS (10x) 10%  
Milk powder 5 %  
→ blocking solution is freshly prepared with water right before usage.

### Procedure

After the gel electrophoresis western blotting is performed. This technique leads to the transfer of the proteins from the resolving gel onto a nitrocellulose membrane. The process is executed on ice in ice cold transfer buffer together with a cool pack inside the transfer chamber. The current is kept constant at 300 mA for 1 hour and 45 minutes. After the transfer, the membrane is washed twice with TBST and then blocked for at least one hour in milk blocking solution at room temperature under constant movement. Afterwards the membrane is transferred into a 50 mL falcon tube and 5 mL of BSA 5% solution is added together with the primary antibody (Table 12). The incubation of the membrane occurs over night at 4°C.

**Table 12 | List of primary antibodies**

Target protein	Species	Company	Cat. No.	Dilution factor	Gel percentage
FABP4 (aP2)	rabbit	Cell Signaling Technologies	2120S	1:1000	15%
PPAR $\gamma$	rabbit	Cell Signaling Technologies	2430S	1:500	10-12%
Tubulin	mouse	Dianova	DLN-009993	1:2500	10-15%
UCP1	rabbit	Homemade AB		1:1000	10-12%

### 3.6.6 Development of Western Blot

Odyssey® Fc Imaging System (Li-cor Biosciences, Lincoln, USA)

Image Studio™ Lite Quantification Software (Li-cor Biosciences, Lincoln, USA)

- **BSA solution 5%**  
BSA 5 %  
→ The solution is prepared freshly at the day of usage.

**Table 13 | List of secondary antibodies**

Antibody	Company	Car. No.	Dilution	Used for detection of
Anti-rabbit IgG (H+L) (DyLight™ 800 4X PEG Conjugate)	Cell Signaling Technologies	5151s	1 : 30.000	FABP4, aP2, UCP1
Anti-mouse IgG (H+L) (DyLight™ 680 Conjugate)	Cell Signaling Technologies	5470s	1 : 15.000	Tubulin

### Procedure

After primary antibody incubation over night the nitrocellulose membrane is washed three times for five minutes with TBST. Then it is incubated for one hour in 5 mL of BSA 5% solution (no NaN<sub>3</sub>) enriched with the secondary fluorescence antibody (Table 13) at room temperature. It is important to cover the falcon with aluminum foil in order to protect from light. Afterwards the membrane is washed three times for five minutes in TBST and then detected at a wavelength of 700 and 800 nm with the Odyssey®

Fc Imaging System. The Image Studio™ Lite Quantification Software is used to quantify the protein bands.

### 3.7 Lipolysis

#### *Equipment and materials*

DMEM [Dulbecco's Modified Eagle Medium] (Gibco®), Cat. No. 21063

Bovine Serum Albumin fatty acid free (Sigma-Aldrich), Cat. No. A7030

96-well plate (Sarstedt), Cat. No. 83.3924

L-(-)-Norepinephrine (+)-bitartrate salt monohydrate [NE] (Sigma-Aldrich), Cat. No. A9512

S1P (Tocris), Cat. No. 1370

Incubator, HERAcCell® 150 (Heraeus)

Free glycerol reagent (Sigma-Aldrich), Cat. No. F6428

Glycerol standard (Sigma-Aldrich), Cat. No. G7793

Perkin Elmer EnSpire® microplate reader, Cat. No. 23000902

- **Lipolysis medium [LM]**

DMEM (Cat. No. 21063) 100 mL

BSA (fatty acid free) 0.2 g

#### *Procedure*

Mature adipocytes are washed twice with LM. Then 800 µL (6 well plate) or 400 µL (12 well plate) of LM including compounds are added to each well. The plate is incubated for two hours at 37°C, 5% CO<sub>2</sub>. After two hours 40 µL of the conditioned lipolysis medium is taken from each well and pipetted into a 96 well plate. 60 µL of free glycerol reagent is added additionally to each well. 40 µL of pure LM plus 60 µL of glycerol serves as blank. The standard consists of 5 µL of Glycerol standard solution and 95 µL of glycerol free reagent. The 96 well plate is incubated for five minutes at 37°C, 5% CO<sub>2</sub>. Afterwards the adsorption is measured at 540 nm in the Perkin Elmer EnSpire® microplate reader, the measurement at the wavelength of 600 nm serves as a reference. The blank and the standard are obtained to calculate the absolute glycerol release of each well which is normalized to the protein abundance which is measured on the lines of chapter 3.6.2.

### 3.8 Calcium Measurements

#### *Equipment and materials*

LSM 700 VRGB (445), ZEN 2010, laser scanning confocal microscope (Carl Zeiss Microscopy GmbH, Jena, Germany), Cat. No. 000000-1865-957

Immersol™ 518 F/30°C (Carl Zeiss Microscopy GmbH, Jena, Germany), Cat. No. 444970-9000-000

Fluo-4 Direct™ Calcium Assay Kit (Invitrogen™, Eugene, USA), Cat. No. F10471

HBSS, Calcium, magnesium, no phenol red (Invitrogen™, Eugene, USA), Cat. No. 14025092

Lonza™ BioWhittaker™ HEPES Buffer 1 M (Lonza™, Wakersville, USA), Cat. No. 17-737E

S1P (Tocris, Bristol, UK), Cat. No. 1370

W 146 (Avanti Polar Lipids, Alabaster, USA), Cat. No. 857390P

JTE 013 (Tocris, Bristol, UK), Cat. No. 2392

TY 52156 (Tocris, Bristol, UK), Cat. No. 5328

Thapsigargin (Tocris, Bristol, UK), Cat. No. 1138

FR 900359 (Prof. Kostenis, Prof. König, Bonn, Germany)

μ-Slide 8 well ibiTreat (ibidi GmbH, Gräfelfing, Germany), Cat. No. 80826

ImageJ Software including Add-on Fiji

Gelatine solution 0.5%

Calcium chloride dihydrate (Roth), Cat. No. T885.1

Glucose, waterfree (Roth), Cat. No. X997.2

HEPES (Sigma-Aldrich), Cat. No. H4034

Magnesium chloride hexahydrate (Roth), Cat. No. A-537.1

Potassium chloride (Roth), Cat. No. 6781.1

EGTA (Roth), Cat. No. 3054.2

Ionomycin (Cayman Chemical, Ann Arbor, USA), Cat. No. Cay10004974

**Table 14 | Recipe for Ringer solution for measurements in Figure 13 and Figure 14**

	stock	final concentration	for Ca <sup>2+</sup> Buffer [mL]	for Ca <sup>2+</sup> free Buffer [mL]
NaCl	5 M	140 mM	2,8	2,8
KCl	1 M	2.8 mM	0,28	0,28
MgCl <sub>2</sub> 6 x H <sub>2</sub> O	1 M	2 mM	0,2	0,2
CaCl <sub>2</sub> 2 x H <sub>2</sub> O	1 M	1 mM	0,1	----
EGTA pH 7.4	0.5 M	1 mM	----	0,2
Milipore H <sub>2</sub> O	/	/	96,62	96,52
add freshly			in [g]	in [g]
HEPES		10 mM	0,24	0,24
D+ Glucose		10 mM	0,18	0,18

→ Adjust pH to 7.3 with using 5 M NaOH solution. Prepare freshly before use.

**Table 15 | Microscope settings of LSM 700 (Zeiss) for calcium measurements**

Mode	Figure 13, Figure 14, Figure 21, Figure 22, Figure 23
Dimensions	x:512, y:512, time: 1200, 16-bit
Image size	x:319.46 $\mu\text{m}$ , y:319.46 $\mu\text{m}$
Zoom	1.0
Objective	EC Plan-Neofluar 20x/0.50 M27
Master gain	560
Filters	
Lasers	488 nm: 2%
Cycle length	0.481 s

### **Procedure**

Brown preadipocytes were seeded on a  $\mu$ -Slide 8 well plate by ibidi. For Figure 13 and Figure 14 the ibidi plates were coated before use. Therefore a 0.5% gelatine solution was preheated to 37°C and 100  $\mu\text{L}$  of the warm solution was pipetted into each well. After an hour incubation of the plate at 37°C, 5%  $\text{CO}_2$  the gelatine solution was aspirated and the brown preadipocytes were immediately seeded. One to two days after seeding the cells were incubated for one hour with the dye Fluo4 Direct™ in the incubator at 37°C, 5%  $\text{CO}_2$ . Subsequently, cells were washed with HBSS-HEPES or freshly prepared Ringer solution and fresh HBSS-HEPES or Ringer solution was added for the measurement. Intracellular calcium imaging was performed using the confocal laser scanning microscope (LSM 700, Zeiss). Drug application occurred manually with a pipette.  $G_q$  inhibition was achieved by one-hour preincubation with the inhibitor FR900359. The measurement regime is listed in Table 15. Regions of interest were selected using the ImageJ add on “Fiji”. Baseline correction was performed using  $\Delta F/F_0$ .  $F_0$  is defined as the mean fluorescence ( $F_0$ ) 60 seconds before the addition of the first compound with  $\Delta F$  corresponding to the fluorescence ( $F$ ) minus  $F_0$ . The Min/Max Peak ratio is calculated by the subtraction of the maximum  $\Delta F/F_0$  from the minimum  $\Delta F/F_0$  value within the time window of 60 seconds before and 60 seconds after the application of S1P or Ionomycin. All calculations were performed for each cell individually using the Excel Software.

### 3.9 IP<sub>1</sub>-Assay

#### *Equipment and materials*

Perkin Elmer EnSpire® microplate reader, Cat. No. 23000902  
384-well low volume white microplates, (Greiner Bio-One), Cat. No. 784075  
IP-One – G<sub>q</sub> kit (cisbio), Cat. No. 62IPAPEC

#### *Procedure*

Brown preadipocytes at P4 are seeded on a 10 cm tissue culture dish. After two days of growth cells are once washed with PBS and detached using 2 mL Trypsin-EDTA. 8 mL of brown adipocyte growth medium is added and cells are counted with Trypan blue stain and Countess Automated Cell Counter. Afterwards the cells are centrifuged at 1000 rpm for ten minutes. The supernatant is discarded and cells washed by resuspension in PBS followed by a second centrifugation time at 1.000 rpm for ten minutes. Subsequently the supernatant is discarded and 100.000 cells are resuspended in 7 µL of stimulation buffer from the IP-One – G<sub>q</sub> kit (cisbio). Then 7 µL of cell suspension are seeded per one well of the 384-well low volume white microplate. The plate is incubated for 10 minutes at 37°C, 5% CO<sub>2</sub> followed by addition of 7 µL of stimulation buffer containing compounds which are supposed to be investigated for their influence on IP<sub>3</sub> production. A one-hour incubation period (37°C, 5% CO<sub>2</sub>) is followed by an addition of 3 µL of IP1-d2 compound and 3 µL of Anti-IP1-Cryptate (both from IP-One – G<sub>q</sub> kit). The plate is incubated at room temperature at darkness for one hour before acceptor and donor emission signals are measured at 615 and 665 nm with the Perkin Elmer EnSpire® microplate reader. The amount of IP<sub>1</sub> released is calculated with help of standard curve measurements.

### 3.10 Dynamic Mass Redistribution Measurements [DMR]

#### *Equipment and materials*

Corning Epic system (Corning Incorporated, Corning, USA)  
CyBio® SELMA, semiautomatic pipettor (Analytik Jena AG, Jena, Germany)  
Compound plate, 384 well (Corning Incorporated, Corning, USA), Cat. No. 3657  
EPIC cell assay plate, 384 well (Corning Incorporated, Corning, USA), Cat. No. 9027.90.50  
HBSS containing 20 mM HEPES  
FR900359, G<sub>q</sub> inhibitor (Kindly provided by AG Kostenis, University of Bonn, Germany)  
Pertussis Toxin from *Bordetella pertussis* (Sigma-Aldrich), Cat. No. P7208  
Sphingosine-1-phosphate [S1P] (Tocris), Cat. No. 1370  
Y-27632 dihydrochloride (Tocris), Cat. No. 1254

#### *Procedure*

Dynamic mass redistribution (DMR) experiments were performed in kind cooperation and support of Professor Evi Kostenis and Dr. Katharina Simon. Brown preadipocytes are seeded on a 384 well fibronectin-coated EPIC cell assay plate. 3000 cells per well are seeded. The cells are incubated at 37°C, 5% CO<sub>2</sub> in brown adipocyte growth medium for 48 hours. The cells are washed twice with HBSS/HEPES solution and then 30 µL of HBSS/HEPES buffer is added to each well followed by a one-hour incubation at 28°C in the Corning EPIC DMR reader. The fourfold concentration of the applied compounds is prepared in HBSS/HEPES solution and pipetted to a 384 well compound plate which is also heated to 28°C for 20 minutes. After measurement of the basal DMR signal of the brown preadipocytes for one to two hours until the signal is not higher or lower than 10 pm, the compounds are pipetted onto the EPIC cell assay plate with help of the semiautomatic CyBio® SELMA pipettor. The measurement of the optical DMR changes takes 5.000 seconds. Pertussis toxin (PTX) [50 ng/mL] was added to the cells 16 hours prior to the experiment, FR900359 [10 µM] and Y-27632 [10 µM] were added to the cells together with the HBSS/HEPES buffer prior to the baseline measurement. The resulting DMR traces were buffer corrected.

### 3.11 *In silico*

#### 3.11.1 Analysis of data from the Genotype-Tissue Expression (GTEx) project

The data presented in Figure 29 are extracted from the open source Genotype-Tissue Expression (GTEx) portal (<https://gtexportal.org/home/> 27.10.2019, 06:54 AM) which is run by the Broad Institute of Massachusetts Institute of Technology (MIT) and Harvard. This data bank consists of RNA sequencing data from human patient samples analysed from a big variety of different tissues (The Genotype-Tissue Expression (GTEx) project, 2013). The data displayed in this study is taken from the

GTEX analysis V7 data set. Analysis was performed with kind help of Dr. Dominic Gosejacob using the software R. All data are presented as transcripts per million (TPM).

**Table 16 | Amount of independent samples (n) for each type of human tissue**

Tissue	n	Tissue	n
Adipose - Subcutaneous	442	Esophagus - Gastroesophageal Junction	244
Adipose - Visceral (Omentum)	355	Esophagus - Mucosa	407
Adrenal Gland	190	Esophagus - Muscularis	370
Artery - Aorta	299	Fallopian Tube	7
Artery - Coronary	173	Heart - Atrial Appendage	297
Artery - Tibial	441	Heart - Left Ventricle	303
Bladder	11	Kidney - Cortex	45
Brain - Amygdala	100	Liver	175
Brain - Anterior cingulate cortex (BA24)	121	Lung	427
Brain - Caudate (basal ganglia)	160	Minor Salivary Gland	97
Brain - Cerebellar Hemisphere	136	Muscle - Skeletal	564
Brain - Cerebellum	173	Nerve - Tibial	414
Brain - Cortex	158	Ovary	133
Brain - Frontal Cortex (BA9)	129	Pancreas	248
Brain - Hippocampus	123	Pituitary	183
Brain - Hypothalamus	121	Prostate	152
Brain - Nucleus accumbens (basal ganglia)	147	Skin - Not Sun Exposed (Suprapubic)	387
Brain - Putamen (basal ganglia)	124	Skin - Sun Exposed (Lower leg)	473
Brain - Spinal cord (cervical c-1)	91	Small Intestine - Terminal Ileum	137
Brain - Substantia nigra	88	Spleen	162
Breast - Mammary Tissue	290	Stomach	262
Cells - EBV-transformed lymphocytes	130	Testis	259
Cells - Transformed fibroblasts	343	Thyroid	446
Cervix - Ectocervix	6	Uterus	111
Cervix - Endocervix	5	Vagina	115
Colon - Sigmoid	233	Whole Blood	407
Colon - Transverse	274		

### 3.11.2 Statistical analysis

The data in this thesis are presented as mean  $\pm$  standard error of the mean (s.e.m.). Statistical analysis is performed using GraphPad Prism software Version 5 and 6. For single comparisons the two-tailed t-test is applied. For multiple comparisons of different treatments one-way analysis of variance (ANOVA) is used followed by the Dunnett post-hoc test if all treatments are supposed to be compared to the control treatment. For post-hoc comparison of all treatments among each other Tukey's post-hoc test is chosen. For determination of the influence of two independent variables (e.g. genotype and treatment) on the dependent variable two-way ANOVA is performed. "n" is defined as independent experiments from either different mice or individually seeded cells.

## 4 Results

### 4.1 Overview of S1PR distribution

In order to obtain an overview of S1PR expression in adipocytes, qPCR analysis of S1PRs in murine primary immortalized BAs and in murine primary WAs has been performed (Figure 7A,B). Preadipocytes (Day -2) as well as mature adipocytes (Day 7/8) have been analyzed. It occurs that S1PR1 and S1PR2 are significantly higher expressed in preadipocytes compared to mature adipocytes. This finding is true for both BAs and WAs. S1PR3 is significantly higher expressed in brown preadipocytes.

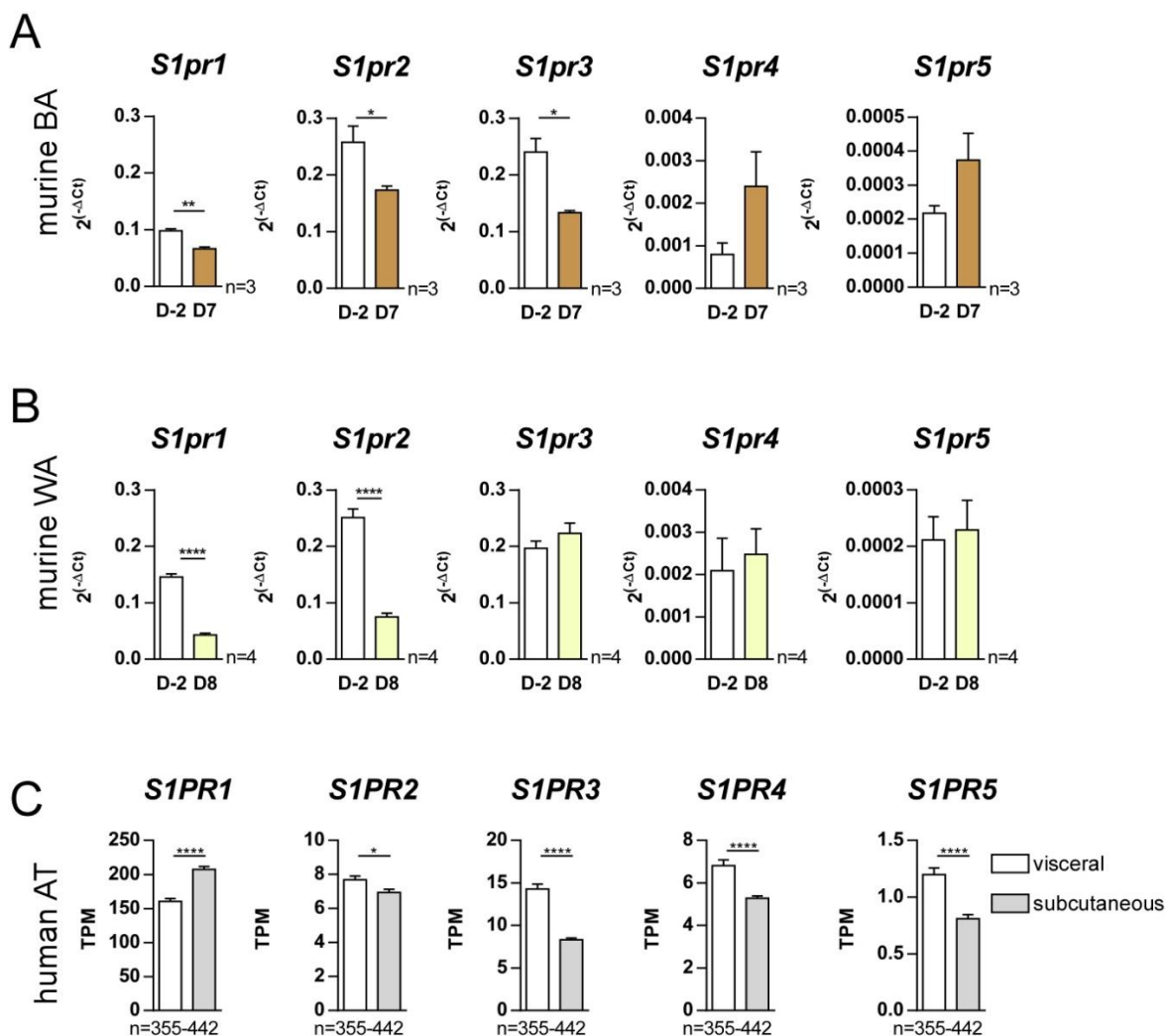


**Figure 7 | Expression of S1PRs in murine BAs, murine WAs and human adipose tissues**

mRNA expression of *S1pr1*, *S1pr2*, *S1pr3*, *S1pr4*, *S1pr5* in murine primary immortalized brown adipocytes (A) and murine primary white adipocytes (B) at preadipocyte (D-2) and mature adipocyte stage (D7/D8). Expression data are normalized to Hprt. (C) RNA sequencing data presented as transcripts per million (TPM) of *S1PR1*, *S1PR2*, *S1PR3*, *S1PR4*, *S1PR5* in visceral and subcutaneous human adipose tissue (AT). Data in Figure 7C are extracted from the data bank of the Genotype-Tissue Expression (GTEx) project. T-test, \*\*\*\*p < 0.0001, \*\*\*p < 0.001, \*\*p < 0.01, \*p < 0.05. All data are represented as means ± s.e.m. Note: Data from this Figure are also used in Figure 8, Figure 24 and Figure 29.

Moreover, the analysis of human RNA sequencing data gathered from the Genotype-Tissue Expression (GTEx) project data bank reveals that all S1PRs are expressed in human visceral and subcutaneous adipose tissues (AT) however at different magnitudes (Figure 7C) (The Genotype-Tissue Expression (GTEx) project, 2013). Most transcripts per million (TPM) were found for S1PR1.

S1PR2, S1PR3, S1PR4 do not differ much in regards of their transcriptional profile. In human ATs, the lowest amount of transcripts per million (TPM) has been found for S1PR5. S1PR1 is significantly higher expressed in human subcutaneous AT compared to visceral AT. The opposite is found for the other four receptors: S1PR2-5 are significantly more abundant in visceral than in subcutaneous human AT.

## 4.2 Sphingosine-1-phosphate in brown adipocytes

To date the role of S1P in BAs has not yet been broadly investigated. When I started my research on S1P back in 2016 there was no previous research linking S1P and BA. Since 2017 only two papers involving S1P and BAs have been published (Christoffersen et al., 2018; Gohlke et al., 2019). To overcome this gap of knowledge the expression levels of the S1PRs and SphKs in primary immortalized BA were examined via qPCR (Figure 8).

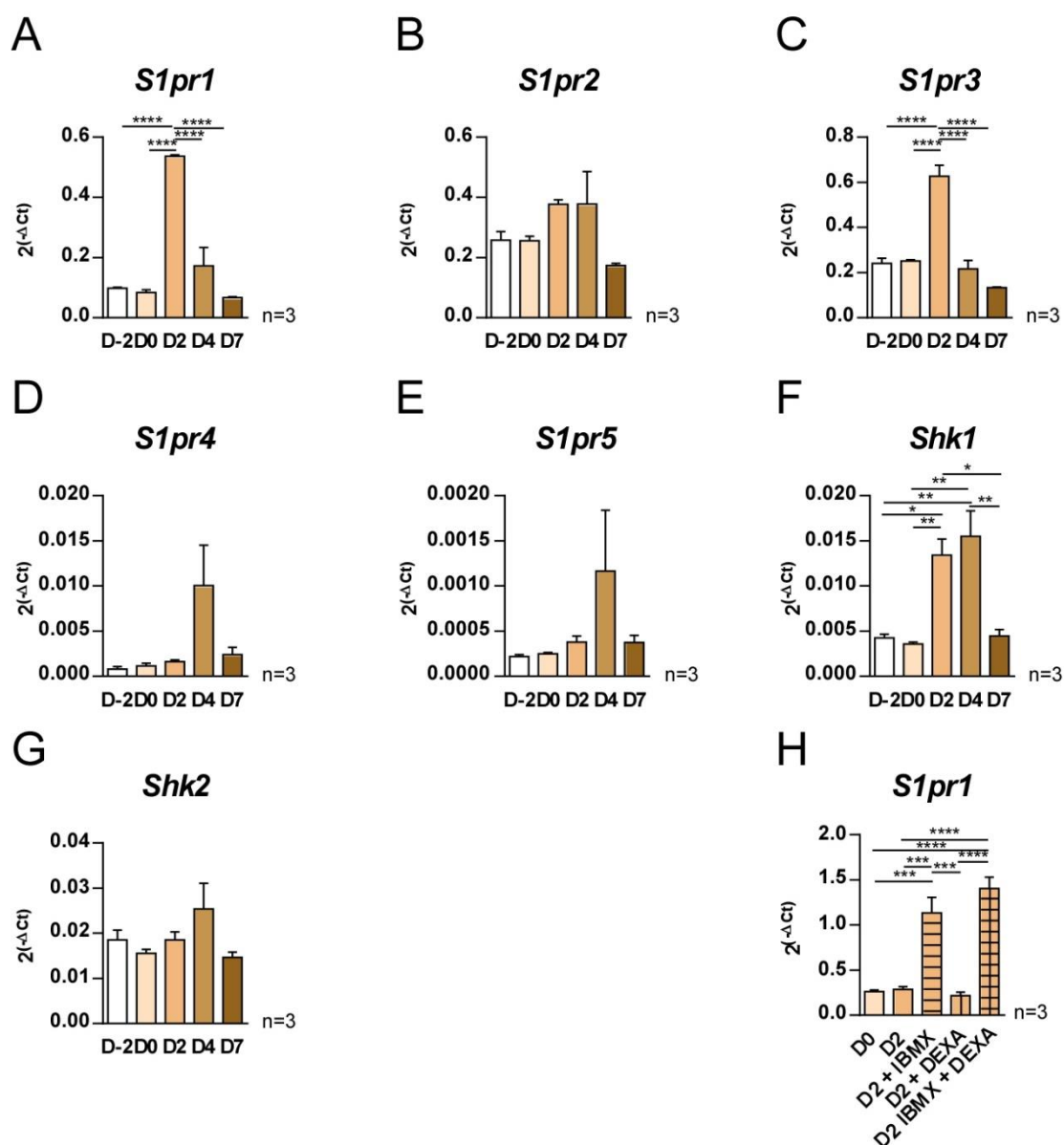


**Figure 8 | Expression of S1PRs and SphKs in BA**

mRNA expression of *S1pr1* (A), *S1pr2* (B), *S1pr3* (C), *S1pr4* (D), *S1pr5* (E), *Shk1* (F), *Shk2* (G), in murine primary immortalized brown adipocytes (BA) throughout differentiation from confluent preadipocytes (d-2), via preadipocytes on day of induction (D0), two days after induction (D2), four days after adipogenic induction (D4) to mature adipocytes (D7) (H) mRNA expression of *S1pr1* on day of confluency (D0) and two days after induction with different induction cocktails. Expression data are normalized to *Hprt*. One-way ANOVA, post-hoc test: Tukey, \*\*\*\*p < 0.0001, \*\*\*p < 0.001, \*\*p < 0.01, \*p < 0.05. All data are represented as means  $\pm$  s.e.m.

All five S1PRs, as well as the two SphKs are expressed. Among the five S1PRs, S1PR1, S1PR2 and S1PR3 mRNA levels are most abundant. The three receptors are expressed to a similar extent and the receptor mRNA levels are 32%-45% higher in preadipocytes (d-2) than in mature adipocytes (d7). In contrast to S1PR1-3, S1PR4 and S1PR5 are lower expressed. S1PR4 is three-fold and S1PR5 is 1.7-fold increased in mature adipocytes (d7) compared to preadipocytes (d-2).

Strikingly, S1PR1 and S1PR3 levels are significantly increased on day 2 of differentiation. Day 2 is the first reading point after the addition of an induction cocktail containing IBMX and dexamethasone. In order to detect the compound responsible for this increase in S1PR1 expression, BAs were induced on day 0 in the presence and absence of IBMX and/or dexamethasone (Figure 8H) and S1PR1 expression was determined via qPCR after two days of compound incubation. IBMX as well as the combination of IBMX and dexamethasone caused a significant elevation of S1PR1 mRNA levels whereas dexamethasone treatment alone had no effect on S1PR1 mRNA expression levels. According to the literature the non-selective PDE inhibitor IBMX increases cAMP levels in differentiated BA (Kraynik et al., 2013).

This fact leads to the conclusion that the S1PR1 mRNA levels are increased in response to enhanced cAMP levels in BA. Similar to S1PR1 and S1PR3, also SphK1 mRNA levels are elevated after induction of BA on day 0 and remain significantly elevated on day 4 as well.

#### **4.2.1 S1P in lipolysis of brown adipocytes**

For this study, it was of interest whether S1P exhibits acute effects on BA function. An *in vitro* read out for BA function is the lipolysis assay. Treating BAs acutely with norepinephrine leads to an activation of  $\beta$ -3 adrenergic receptors. These receptors mediate the degradation of triglycerides into glycerol and free fatty acids. The free fatty acids are further degraded and the resulting products activate UCP1 which induces thermogenesis (Cannon and Nedergaard, 2004). An indirect measurement for the ability of BAs to perform thermogenesis is the lipolysis assay in which the release of glycerol deriving from triglycerides is measured. Hence, mature BA were treated for two hours with either S1P [10  $\mu$ M], NE [1  $\mu$ M] or a combination of both compounds and glycerol release was measured as a read out for lipolysis (Figure 9). As anticipated the NE treatment increased the glycerol release significantly, which is also true for the treatment with both compounds together. S1P treatment elevated basal glycerol levels by 50% ( $p=0.0504$ ).

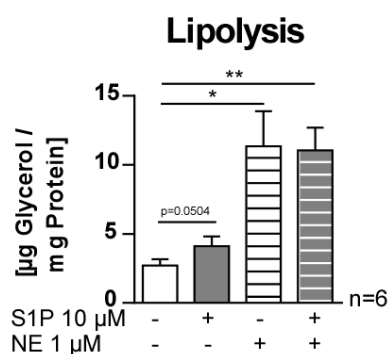


**Figure 9 | S1P-mediated lipolysis in mature brown adipocytes**

µg Glycerol release per mg Protein in mature brown adipocytes after a two-hour treatment with S1P 10 µM and/ or NE 1 µM. One-way ANOVA, post-hoc test: Dunnett. \*\*p < 0.01, \* p < 0.05. All data are represented as means ± s.e.m.

#### 4.2.2 S1P in brown adipogenesis

As we observed a differential expression of the S1PRs during different days of brown adipogenesis it was of interest whether chronic S1P treatment affects differentiation of brown adipocytes. Therefore, BAs were treated chronically every second day with 1 µM of S1P, starting from day -2 (Figure 10). After the differentiation process, on day 7, ORO, qPCR and Western Blot analysis were performed. In S1P treated BAs the ORO staining of lipid droplets is diminished compared to the control treatment (Figure 10A). A further novel finding is that the chronic exposition of BAs to S1P leads to significantly attenuated levels of the adipogenic markers aP2 and PPARγ as well as of the thermogenic marker UCP1 in both mRNA and protein analysis (Figure 10B-D). These data reveal that S1P decreases the differentiation of BAs.

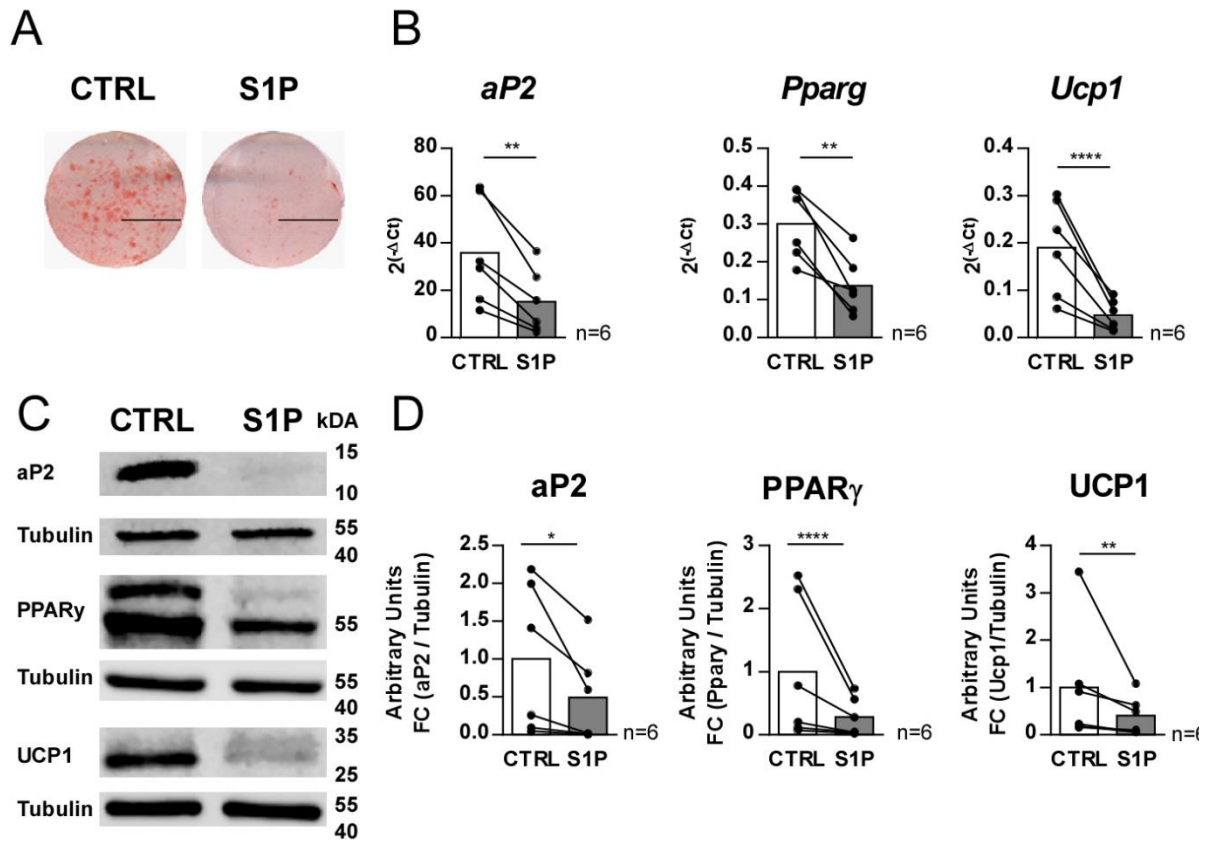


**Figure 10 | S1P decreases differentiation of brown adipocytes**

(A) ORO of brown adipocytes treated chronically with S1P [1 $\mu$ M] from day -2. (B) Relative mRNA expression of *Ucp1*, *aP2* and *Pparg* after chronic treatment of BA with S1P [1 $\mu$ M] from day -2. (C), (D) Representative immunoblots and quantification of UCP1, aP2 and PPAR $\gamma$  after chronic treatment of BA with S1P [1 $\mu$ M] from day -2. Expression data are normalized to *Hprt*. T-test, \*\*\*\*p < 0.0001, \*\*\*p < 0.001, \*\* p < 0.01, \* p < 0.05. All data are represented as means  $\pm$  s.e.m.

### 4.3 Downstream signaling of S1P in brown adipocytes

It has been previously reported by our lab that the activation of  $G_q$  signaling pathways inhibits differentiation of BAs whilst the blockade of  $G_q$  signaling pathways enhances differentiation of BAs (Klepac et al., 2016). In order to investigate whether the earlier observed inhibition of differentiation via chronic S1P treatment of BAs (Figure 10) is due to an activation of  $G_q$  signaling, BAs were treated chronically from day -2 with S1P or Vehicle in the presence and absence of the specific  $G_q$  inhibitor FR900359 (FR) (Schrage et al., 2015) (Figure 11). On day 7 of differentiation ORO staining and protein analysis were performed.

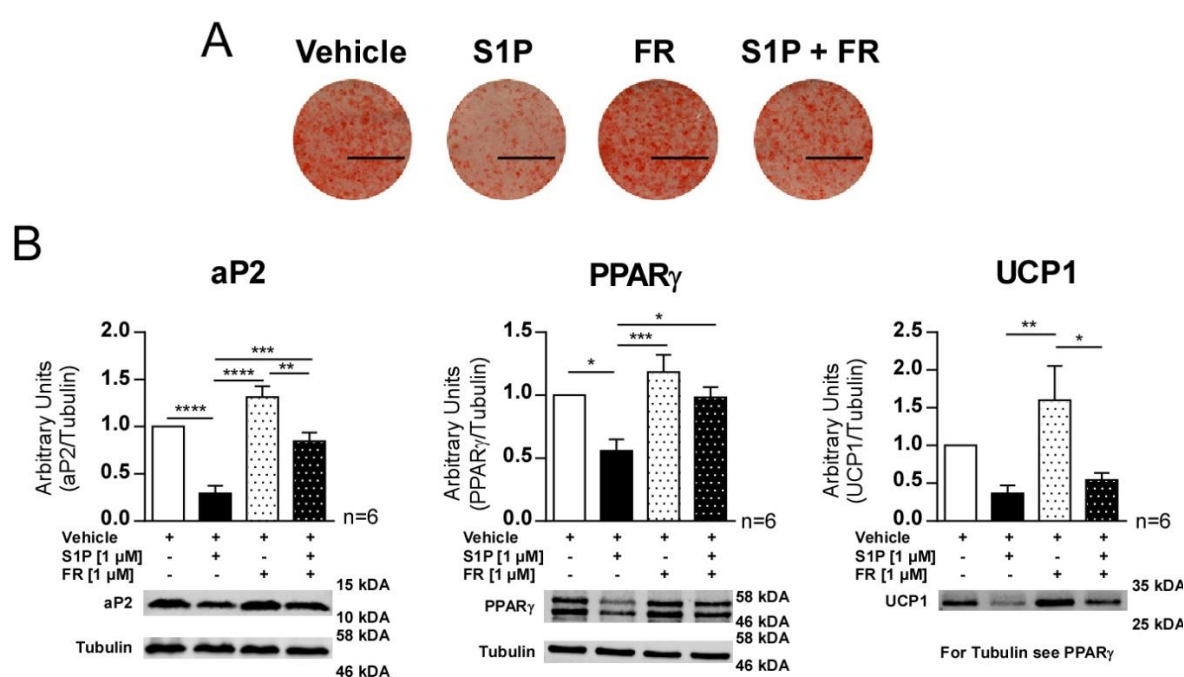


**Figure 11 | S1P decreases differentiation partially by  $G_q$  activation**

(A) ORO of brown adipocytes treated chronically with S1P [1 μM] and/ or FR900359 [1 μM] from day -2. (B) Representative immunoblots and quantification of Ucp1, aP2 and PPAR $\gamma$  after chronic treatment of BA with S1P [1 μM] and/ or FR900359 [1 μM] from day -2. One-way ANOVA, post-hoc test: Tukey, \*\*\*\* $p < 0.0001$ , \*\*\* $p < 0.001$ , \*\* $p < 0.01$ , \* $p < 0.05$ . All data are represented as means  $\pm$  s.e.m.

As anticipated the chronic S1P treatment reduces aP2 [-71%] and PPAR $\gamma$  [-55%] protein levels significantly. UCP1 protein levels are attenuated for 64%. Chronic FR treatment of BA alone leads to an increase of aP2 [+31%], PPAR $\gamma$  [+19%] and UCP1 [+59,8%] protein levels, however these changes are not statistically significant. PPAR $\gamma$  protein levels are not altered between the FR and the S1P + FR treated group indicating that the inhibitory effect of S1P on PPAR $\gamma$  protein can be rescued by a  $G_q$  inhibition. However, a significant difference in aP2 and UCP1 levels between the FR treatment and the FR + S1P treatment group was observed. Hence, in this case  $G_q$  inhibition was not able to fully rescue

the inhibiting S1P effects. These results suggest that the S1P mediated inhibition of BA differentiation occurs partially, however not exclusively, due to a  $G_q$  activating signaling property.

#### 4.3.1 DMR measurements in brown adipocytes

A holistic approach to learn more about downstream signaling of certain compounds is the label-free measurement of DMR (Schröder et al., 2011). In order to find out more about S1P mediated signaling in BAs DMR measurements were performed (Figure 12). For this purpose, preBAs were treated with different concentrations of S1P during the DMR assay in presence and absence of the  $G_i$  inhibitor pertussis toxin, the  $G_q$  inhibitor FR and the ROCK inhibitor Y-27632. The representative traces show a dose dependent signal for S1P treated preBAs (Figure 12A). However, the signal is not abolished by pretreatment with neither pertussis toxin, FR or Y-27632 (Figure 12B-D), nor by a combination of all three inhibitors (Figure 12E). These results indicate the complexity of S1P signaling in preBAs, not at least due to the presence of the five different S1PRs (Figure 8).

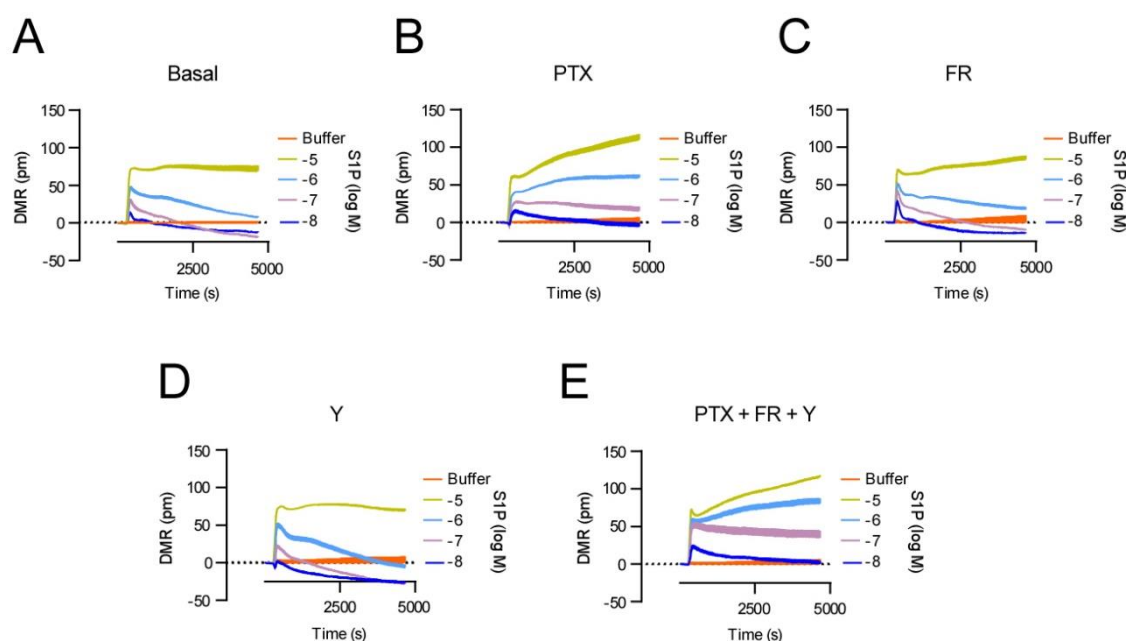


**Figure 12 | S1P derived DMR response in brown preadipocytes is not abolished by the inhibitors pertussis toxin, FR900359 and Y-27632**

Representative DMR traces of S1P mediated cellular responses of brown preadipocytes treated with vehicle (A), with  $G_i$ -inhibitor pertussis toxin [PTX] (50 ng / mL) (B),  $G_q$ -inhibitor FR900359 [FR] (10  $\mu$ M) (C), Rock-inhibitor Y-27632 [Y] (10  $\mu$ M) (D) and a combination of all three inhibitors (E).

### 4.3.2 Calcium measurements in brown adipocytes

In order to gain further insight into S1P signaling in preBA, I performed calcium ( $[Ca^{2+}]$ ) measurements in preBA using the fluorescent dye Fluo-4-Direct™ (Figure 13, Figure 14). S1P induces an increase in intracellular calcium ( $[Ca^{2+}]_i$ ) levels in the presence of 1 mM  $[Ca^{2+}]_{ex}$  in the ringer solution (Figure 13A). In order to find out whether the  $[Ca^{2+}]_i$  derives from intracellular stores or enters extracellularly, the measurements were repeated in a  $[Ca^{2+}]$ -free ringer solution (Figure 13B). In  $[Ca^{2+}]$ -free ringer solution a similar S1P peak is observable (Figure 13B). The Min/Max Peak ratio for S1P is significantly higher for the  $[Ca^{2+}]_{ex}$ -free buffer experiment indicating that S1P triggers a  $[Ca^{2+}]$  release from intracellular stores (Figure 13C). For this experiment Ionomycin serves as a positive control (Figure 13D-F). Ionomycin is an ionophore and thereby able to facilitate  $[Ca^{2+}]_i$  release from intracellular stores and  $[Ca^{2+}]_i$  influx from extracellular space (Kao et al., 2010). The application of Ionomycin after S1P stimulation triggers a  $[Ca^{2+}]_i$  response. In the presence of 1 mM  $[Ca^{2+}]_{ex}$  the calcium response to Ionomycin does not return back to baseline after the initial increase. In  $[Ca^{2+}]$ -free medium the Ionomycin-induced calcium signal drops down to baseline (Figure 13E), indicating a lack of extracellular calcium in the solution (Figure 13D). Taken these results into account the increase of  $[Ca^{2+}]_i$  upon a S1P stimulus is mediated via release from  $[Ca^{2+}]_i$  stores.

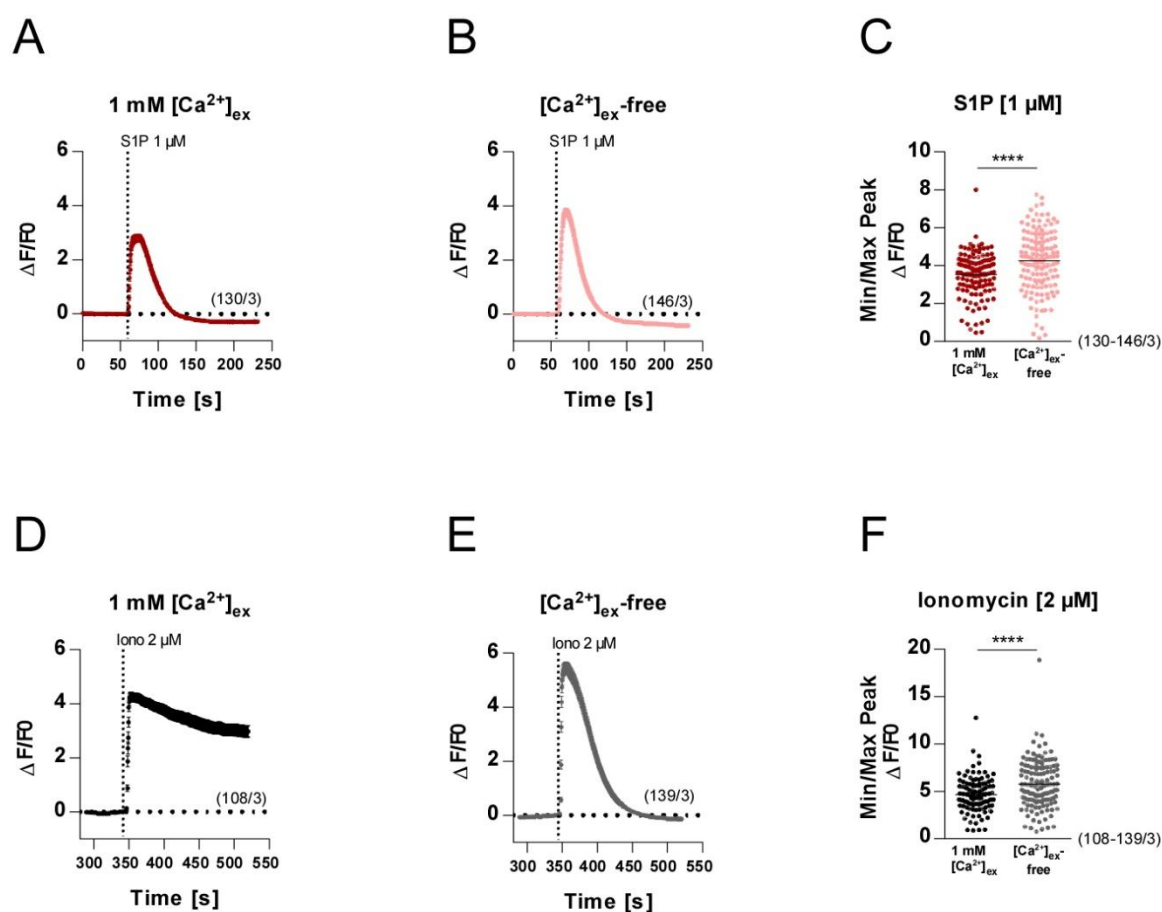


**Figure 13 | Stimulation of brown preadipocytes with S1P induces an increase of  $[Ca^{2+}]_i$**

Measurement of  $[Ca^{2+}]_i$  changes in preBAs incubated for one hour with the fluorescent dye Fluo-4 Direct™. Acute stimulation with S1P [1  $\mu M$ ] and subsequently Ionomycin (Iono) [2  $\mu M$ ] occurred in 1 mM  $[Ca^{2+}]_{ex}$ -containing (A, D) or  $[Ca^{2+}]_{ex}$ -free ringer solution (B, E). (C, F) Min/Max Peak ratio of S1P and Ionomycin peaks from (A), (B), (D) & (E). T-test, \*\*\*\* $p < 0.001$ . All data are represented as means  $\pm$  s.e.m. of n cells from x experiments (n/x).

In order to investigate whether the S1P-induced  $[Ca^{2+}]_i$  release from intracellular stores is due to  $G_q$  activation,  $[Ca^{2+}]_i$  imaging experiments were performed in the presence of the  $G_q$  inhibitor FR. S1P application resulted in an instant calcium increase (Figure 14A, D). In contrast, a pretreatment with the  $G_q$  inhibitor FR abolished the S1P-mediated calcium increase (Figure 14B, D). Vehicle treatment did not alter the calcium levels in preBAs (Figure 14C, D). According to these data it can be stated that S1P increases  $[Ca^{2+}]_i$  in preBA in a  $G_q$ -dependent manner. Ionomycin was applied at the end of each experiment as a positive control for cell viability. Independent of the previous treatments (Figure 14A-C), Ionomycin addition evokes similar  $[Ca^{2+}]_i$  traces (Figure 14E-G). The Min/Max Peak values after Ionomycin application are highly similar. Despite the high “n”-number there is no significant Min/Max Peak difference observable, making Ionomycin a reliable positive control (Figure 14H).

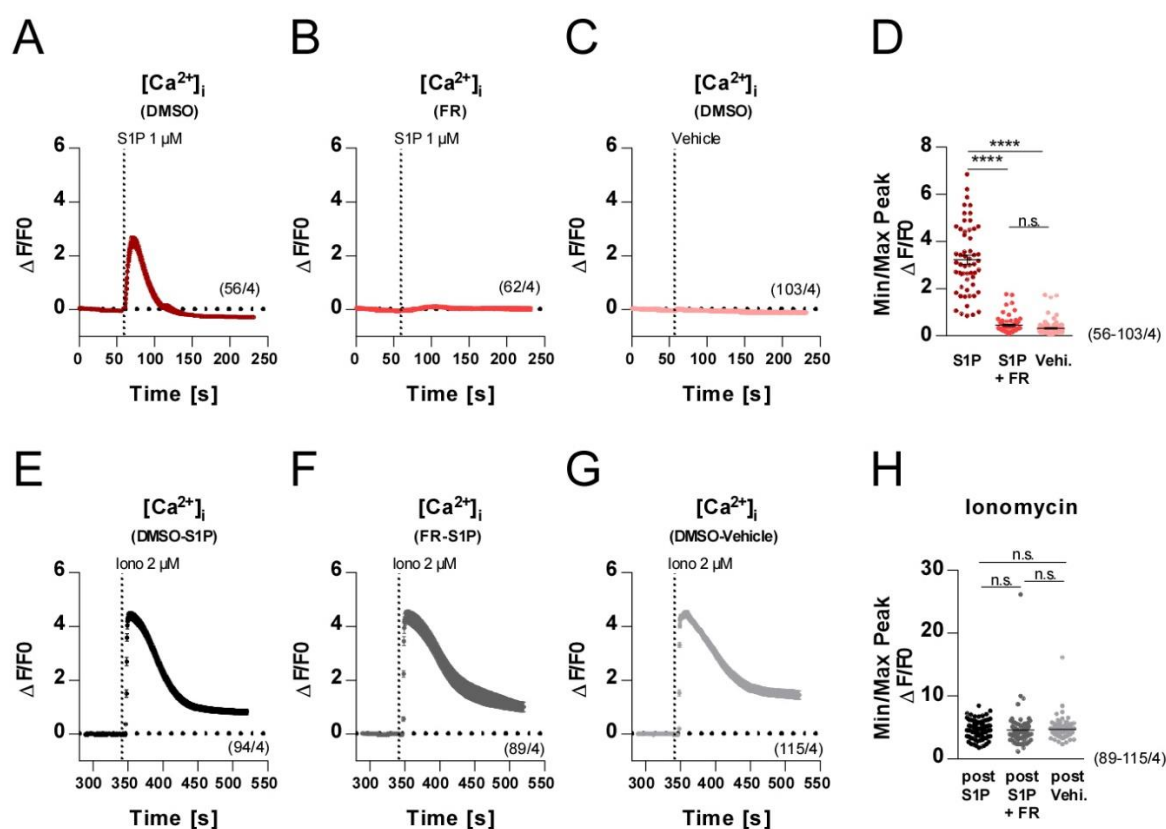


**Figure 14 | Stimulation of brown preadipocytes with S1P induces a  $G_q$  dependent intracellular  $Ca^{2+}$  increase**  
 Measurement of intracellular calcium changes  $[Ca^{2+}]_i$  in preBAs incubated for one hour with the fluorescent dye Fluo-4 Direct™ in presence of either DMSO (A,C) or FR900359 (B), followed by acute stimulation with Vehicle (C) or S1P 1  $\mu$ M (A, B). The respective S1P or Vehicle stimulation was always followed by an Ionomycin [2  $\mu$ M] injection as control (E, F, G). Min/Max Peak ratio of S1P (D) and Ionomycin (H) peak. One-way ANOVA, post-hoc test: Tukey, \*\*\*\* $p < 0.001$ , n.s. (not significant)  $p \geq 0.05$ . All data are represented as means  $\pm$  s.e.m. of n cells from x experiments (n/x).

#### 4.3.3 Inositol monophosphate measurements in brown adipocytes

The canonical  $G_q$  downstream signaling pathway involves upon  $G_q$  protein activation a hydrolysis of  $PIP_2$  into DAG and  $IP_3$  via PLC- $\beta$ .  $IP_3$  binds to the  $IP_3$  receptor at the endoplasmatic reticulum and thereby causes the release of calcium into the cytoplasm (Steinhilber et al., 2010; Sánchez-Fernández et al., 2014). Under physiological conditions  $IP_3$  is quickly degraded to  $IP_1$ . Therefore the measurement of  $IP_1$  which accumulates in the cells when LiCl is added to the assay serves as an indicator for earlier  $IP_3$  formation upon activation of a  $G_q$  protein-coupled receptor (Trinquet et al., 2006). To investigate whether S1P induces an increase in  $IP_1$  in preBA the  $IP_1$  assay was performed (Figure 15). ET-1 which binds to the  $G_q$ -coupled receptor  $ET_A$  serves as a positive control and leads to a significant elevation of  $IP_1$  levels (Klepac et al., 2016; D'Orléans-Juste et al., 2019). Unexpectedly, various concentrations of S1P did not influence  $IP_1$  levels compared to vehicle (BSA). Contrary to the former findings that S1P exhibits  $G_q$  signaling properties in BA I could not find evidence for this hypothesis using the  $IP_1$  assay.

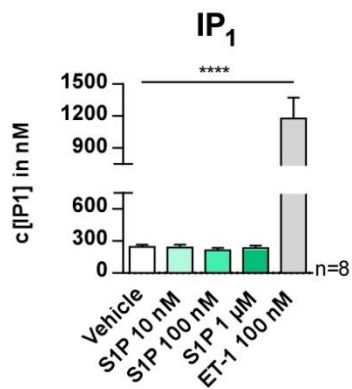


**Figure 15 | IP<sub>1</sub>-release after stimulation of brown preadipocytes with S1P**

IP<sub>1</sub>-levels of brown preadipocytes which were treated with S1P. ET-1 serves as positive control. One-way ANOVA, post-hoc test: Dunnett, \*\*\*\* $p < 0.0001$ . All data are represented as means  $\pm$  s.e.m.

#### 4.3.4 CYR61 mRNA measurements in brown adipocytes

Previous studies have shown that S1P is a potent Rho activator (Donati and Bruni, 2006). Generally, the activation of  $G_{12/13}$  leads to an increase in CYR61 mRNA expression. The binding of S1P to its receptors can also enable  $G_{12/13}$  activation with a subsequent increase in mRNA levels of CYR61 (Walsh et al., 2008; Kim et al., 2011). To unravel whether S1P activates  $G_{12/13}$  in preBAs in a Rho dependent manner, but independent of  $G_q$ , preBAs were pretreated for 6 hours with vehicle, the Rho inhibitor C3 transferase (C3T) or the  $G_q$  inhibitor FR, following a two-hour treatment with S1P or vehicle (Figure 16). S1P treatment augments CYR61 levels significantly compared to vehicle in all three groups despite of the inhibitor applied. However, either vehicle or FR pretreated preBAs exhibit upon S1P stimulation 6fold higher CYR61 mRNA levels compared to vehicle stimulated cells, whereas the C3T pretreated group shows a 3fold elevation of CYR61 expression. The S1P response in preBAs pretreated with C3T is significantly decreased compared to vehicle or FR pretreatment. These findings suggest that S1P has a Rho activating moiety in BA which is mediated rather via  $G_{12/13}$  than via  $G_q$ .

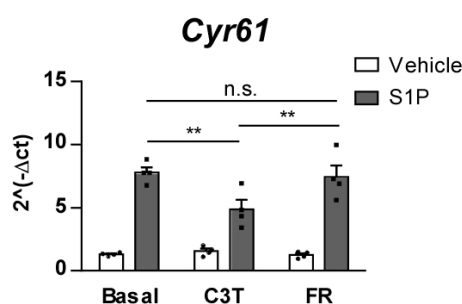


**Figure 16 | S1P mediated *Cyr61* expression in brown preadipocytes is decreased after Rho inhibition via C3T**

*Cyr61* expression of brown preadipocytes which were treated with either S1P [1  $\mu$ M] or vehicle for two hours after incubation with the selective  $G_q$ -inhibitor FR900359 [1  $\mu$ M] or the Rho-inhibitor C3 Transferase (C3T) [1  $\mu$ g/ml] (n=4). Expression data are normalized to *Hprt*. Two-way ANOVA, \*\*  $p < 0.01$ . All data are represented as means  $\pm$  s.e.m.

## 4.4 The role of individual Sphingosine-1-phosphate receptors in brown adipocytes

### 4.4.1 The role of Sphingosine-1-phosphate receptors in differentiation of BAs

In chapter 4.3, it is shown that S1P decreases differentiation of BAs (Figure 10). The question arose whether 'FTY720' the only approved S1PR targeting drug on the market possesses similar effects on BA differentiation as S1P (Figure 10). For this purpose, BAs were treated chronically from day of confluency (d-2) with 1  $\mu$ M of FTY720-P (Figure 17). The bioactive phosphorylated form of FTY720 was used deliberately to circumvent the necessary activation by the SphKs. Moreover, FTY720-P is assumed to target mainly S1P receptors, whereas FTY720 also serves additionally as an inhibitor of ceramide synthases (Berdyshev et al., 2009). The ORO of the BAs treated with FTY720-P reveals a reduction of lipid droplets compared to the control treated cells. Furthermore, aP2, PPAR $\gamma$  and UCP1 protein levels of BAs are significantly diminished when exposed to FTY720-P chronically. This allows for the conclusion that FTY720-P decreases differentiation of BAs.

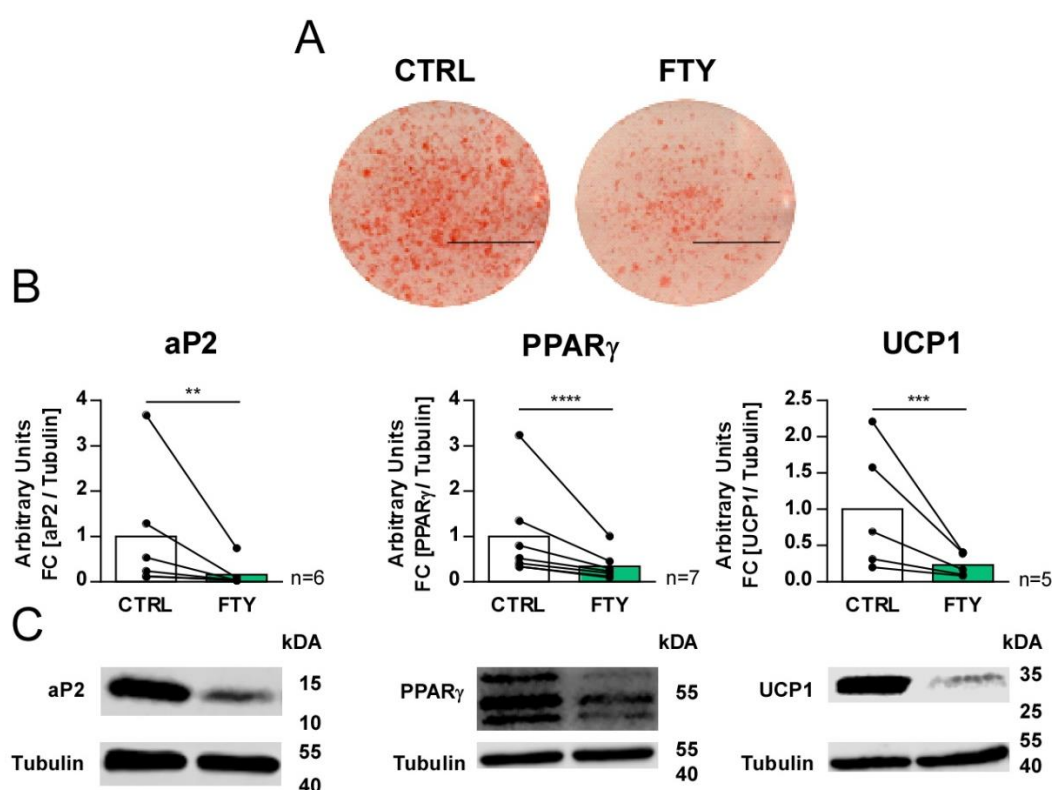


**Figure 17 | FTY720-P decreases differentiation of brown adipocytes**

(A) ORO of brown adipocytes treated chronically with FTY720-P [1  $\mu$ M] from day -2. (B), (C) Representative Immunoblots and quantification of aP2, PPAR $\gamma$  and UCP1 after chronic treatment of BA with FTY720-P [1  $\mu$ M] from day -2. T-test, \*\*\*\*p < 0.0001, \*\*\*p < 0.001, \*\*p < 0.01.

As FTY720-P does not bind specifically to S1PR1 alone but also targets S1PR3, S1PR4 and S1PR5 (Brinkmann et al., 2002), recent literature even states that FTY720-P could potentially activate S1PR2 (Al Alam and Kreydiyyeh, 2016), more specific S1PR agonists have to be applied to determine the main receptor/s responsible for the S1P mediated inhibition of BA differentiation. Hence, BAs were treated chronically with specific agonists for S1PR1, S1PR2 and S1PR3. These three receptors were chosen in accordance with the data presented in Figure 8 due to their high expression.

To assess the effect of S1PR1 on BA differentiation, BAs were treated chronically from day -2 with 10  $\mu$ M of the specific S1PR1 agonist SEW 2871 (Figure 18). S1PR1 treated BAs demonstrated on day 7 a smaller amount of lipid droplets compared to the control group (Figure 18A). Moreover, aP2 and PPAR $\gamma$  protein levels were significantly decreased after S1PR1 treatment (Figure 18B). UCP1 protein levels of the S1PR1 agonist treated cell moiety are 17,5% decreased, however this effect is not significant.

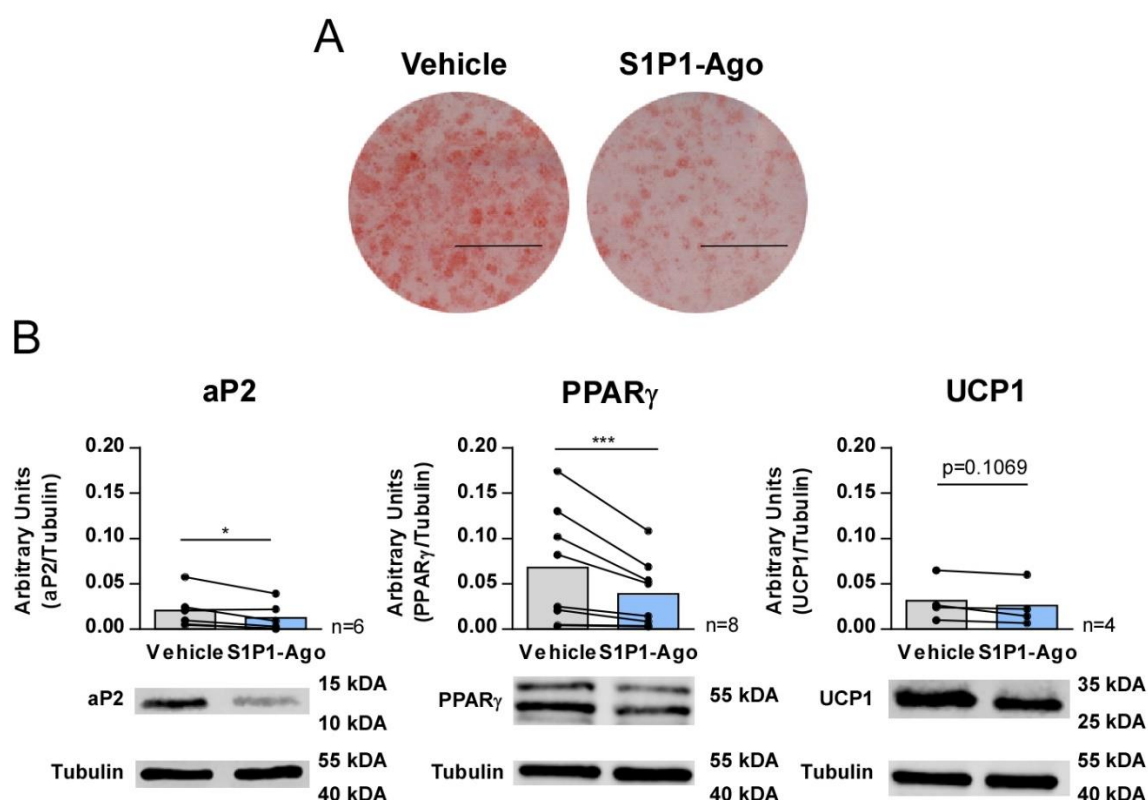


**Figure 18 | Agonism of S1PR1 decreases differentiation of brown adipocytes**

(A) ORO of brown adipocytes treated chronically with SEW 2871 [specific S1PR1-Agonist, 10  $\mu$ M] from day -2. (B), Representative immunoblots and quantification of aP2, PPAR $\gamma$  and UCP1 after chronic treatment of BA with SEW 2871 [specific S1PR1-Agonist, 10  $\mu$ M] from day -2. T-test, \*\*\*p < 0.001, \*\* p < 0.01, \* p < 0.05.

Applying 10  $\mu\text{M}$  of the S1PR2 specific allosteric agonist CYM 5520 chronically to BAs from day of confluency (d-2) throughout differentiation leads to diminished lipid droplets in the ORO staining compared to control treated cells (Figure 19A). Beyond that the chronic treatment leads to significantly lower aP2, PPAR $\gamma$  and UCP1 protein levels in BAs when analysed by Western blot at the end of the differentiation time course on day 7 (Figure 19B). Taken the findings gained from experiments presented in Figure 10, Figure 18 and Figure 19 together, it can be assumed that S1P decreases differentiation of BAs via agonism of S1PR1 and S1PR2.

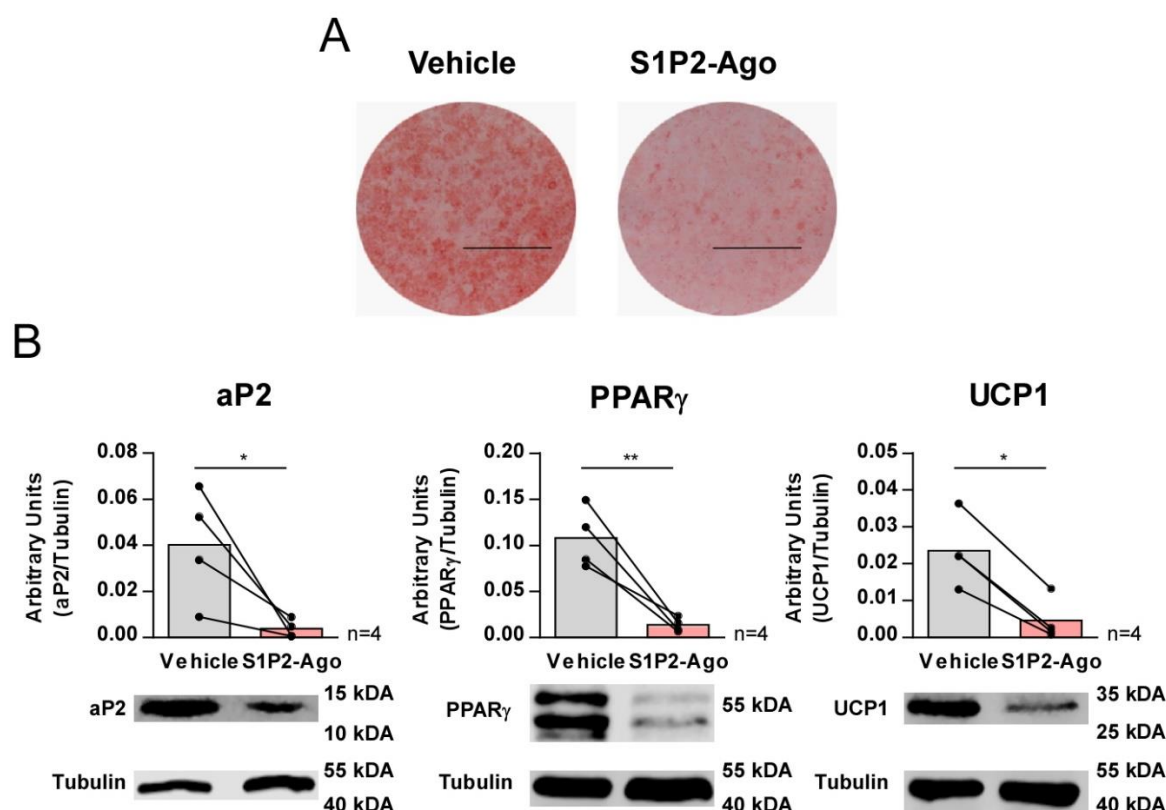


**Figure 19 | Agonism of S1PR2 decreases differentiation of brown adipocytes**

(A) ORO of brown adipocytes treated chronically with CYM 5520 [specific S1PR2-Agonist, 10  $\mu\text{M}$ ] from day -2. (B), Representative immunoblots and quantification of aP2, PPAR $\gamma$  and UCP1 after chronic treatment of BA with CYM 5520 [specific S1PR2-Agonist, 10  $\mu\text{M}$ ] from day -2. T-test, \*\*  $p < 0.01$ , \*  $p < 0.05$ .

To evaluate the effects of S1PR3 agonism on BAs, the specific S1PR3 allosteric agonist CYM 5541 was used in a concentration of 10  $\mu\text{M}$  from the day of confluency (day -2) to accompany the differentiation process of BAs (Figure 20). The ORO staining indicates that the CYM 5541 treatment gives rise to more lipid droplets than the control treatment (Figure 20A). The protein levels of aP2 and UCP1 increase by 1,8 and 3fold in Western blot experiments, however these changes are not significant. PPAR $\gamma$  protein levels remain unaltered (Figure 20B).

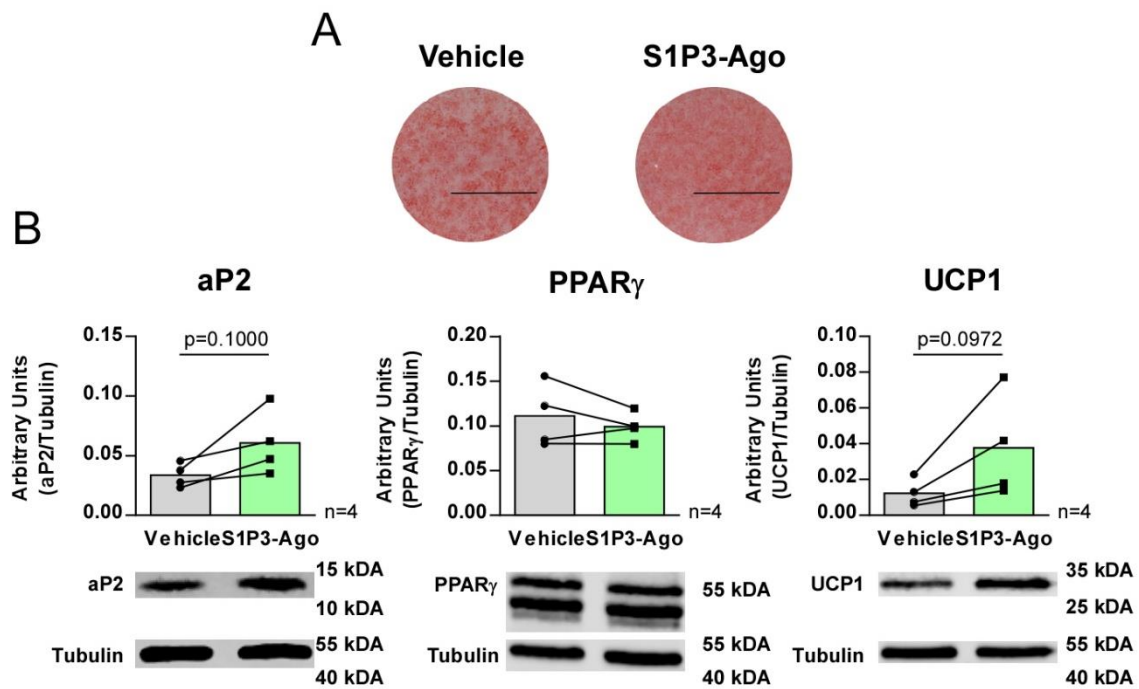


**Figure 20 | Agonism of S1PR3 does not influence differentiation of brown adipocytes**

(A) ORO of brown adipocytes treated chronically with CYM 5541 [specific S1PR3-Agonist, 10  $\mu$ M] from day -2. (B), Representative immunoblots and quantification of aP2, PPAR $\gamma$  and UCP1 after chronic treatment of BA with CYM 5541 [specific S1PR3-Agonist, 10  $\mu$ M] from day -2. T-test, \*\*  $p < 0.01$ , \*  $p < 0.05$ .

#### 4.4.2 The role of Sphingosine-1-phosphate receptors in calcium signaling in brown adipocytes

For further investigation of the S1PR responsible for the S1P-driven intracellular calcium increase in BAs (Figure 14) calcium measurements were performed in the presence of different S1PR antagonists. Therefore, preBAs were loaded with the fluorescent calcium dye Fluo-4 Direct™ and the change in fluorescence, corresponding to the change in  $[Ca^{2+}]_i$  was measured acutely. W 146, a specific S1PR1 antagonist, was not able to abolish the S1P-mediated  $[Ca^{2+}]_i$  increase (Figure 21). Instead, the antagonism of S1PR1 leads to a 12% increase in  $[Ca^{2+}]_i$  ( $p=0.0498$ ). This result suggests that the S1PR1-mediated inhibition of differentiation is presumably not due to an increase in  $[Ca^{2+}]_i$ .

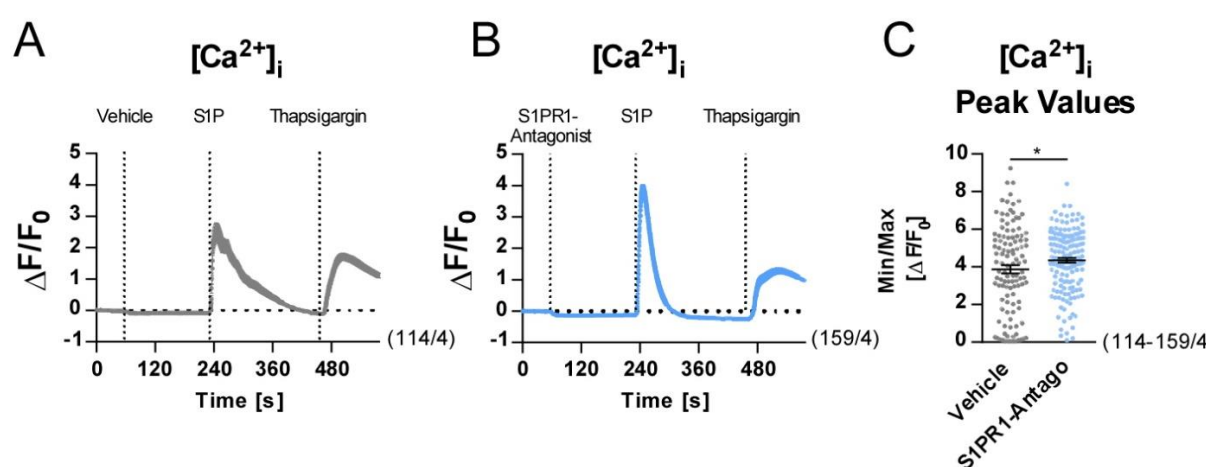


**Figure 21 | S1P mediated intracellular  $Ca^{2+}$  increase in preBA is further enhanced by S1PR1-Antagonist**

Measurement of intracellular calcium changes in preBAs acutely stimulated with either Vehicle (A) or S1PR1-Antagonist [W 146, 10  $\mu$ M] (B) followed by stimulation with S1P [1  $\mu$ M] and Thapsigargin [1  $\mu$ M]. (C) Min/Max Peak ratio of S1P peak. C: T-test. All data are represented as means  $\pm$  s.e.m. of n cells from x experiments (n/x).

Literature reveals that S1PR2 and S1PR3 can be coupled to  $G_q$  (Adada et al., 2013; Blaho et al., 2019). Hence, I investigated whether the S1P mediated  $[Ca^{2+}]_i$  increase could be blocked or diminished by addition of either the specific S1PR2 antagonist JTE 013 or the specific S1PR3 antagonist TY 52156 prior to S1P stimulation (Figure 22). In the presence of the S1PR2 antagonist the S1P-mediated  $[Ca^{2+}]_i$  peak is not significantly reduced. However, the addition of the S1PR3 antagonist attenuates the S1P-mediated  $[Ca^{2+}]_i$  increase significantly (Figure 22C, reduction of approximately 26%).

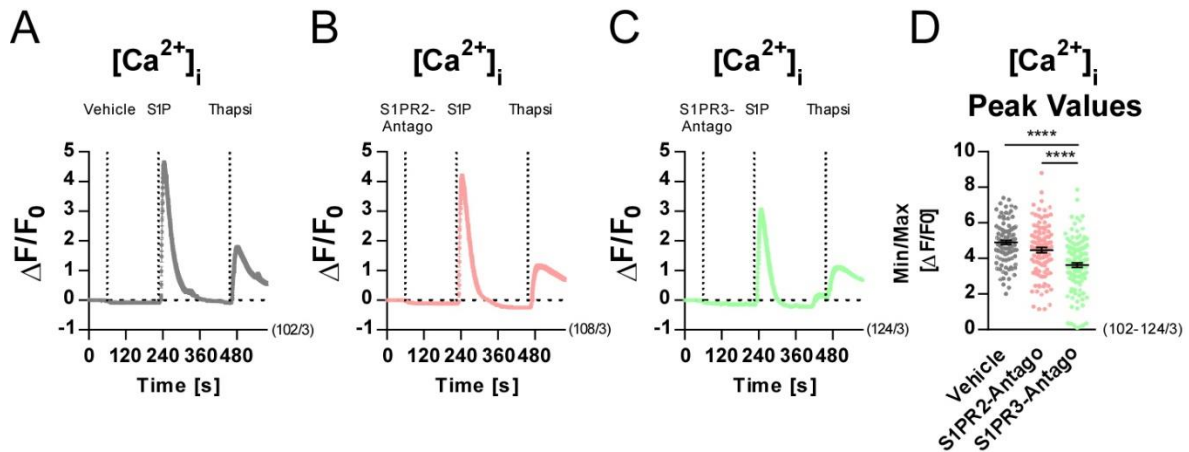


**Figure 22 | S1P mediated intracellular  $Ca^{2+}$  increase in preBA is decreased by S1PR3-Antagonist but not by S1PR2-Antagonist**

Measurement of intracellular calcium changes in preBAs acutely stimulated with either Vehicle (A), S1PR2-Antagonist [JTE 013, 10  $\mu$ M] (B) or S1PR3-Antagonist [TY 52156, 10  $\mu$ M] (C) followed by stimulation with S1P [1  $\mu$ M] and Thapsigargin [1  $\mu$ M]. (D) Min/Max Peak ratio of S1P peak. D: One-way ANOVA, post-hoc test: Tukey. All data are represented as means  $\pm$  s.e.m. of n cells from x experiments (n/x).

In order to test whether S1P receptors work synergistically to increase  $[Ca^{2+}]_i$  in preBAs upon S1P stimulation, S1P-mediated  $[Ca^{2+}]_i$  signals were analyzed in the presence of all three S1PR antagonists (Figure 23). Indeed, the combination of all three antagonists diminished the S1P-induced  $[Ca^{2+}]_i$  peak by 78%, significantly (Figure 23C). In summary, it can be stated that the S1P-mediated  $[Ca^{2+}]_i$  response in preBAs is mainly mediated by S1PR3 with some contribution of S1PR2.

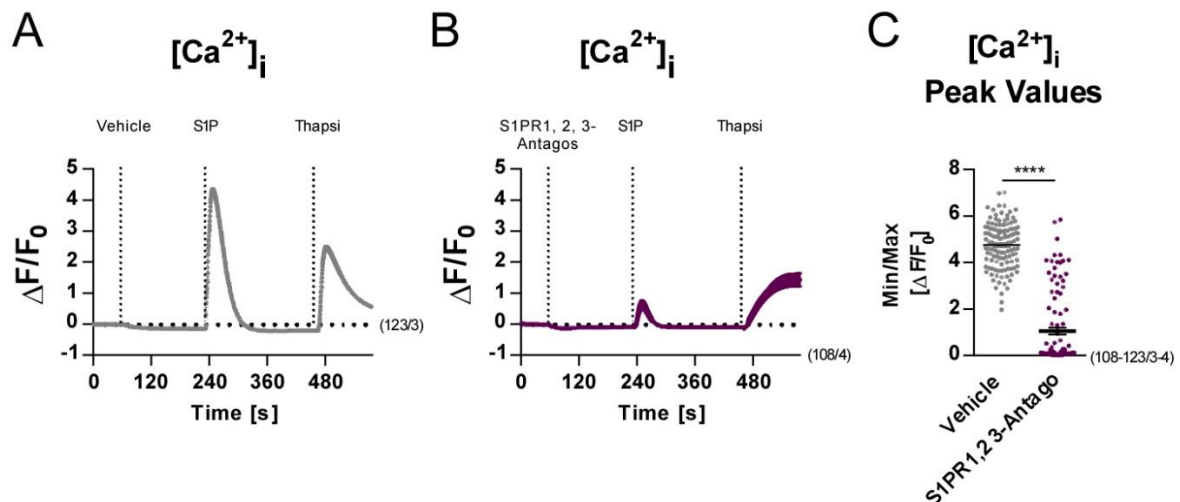


**Figure 23 | S1P mediated intracellular  $Ca^{2+}$  increase in preBA is diminished after addition of S1PR1, 2 and 3-Antagonists together**

Measurement of intracellular calcium changes in preBAs acutely stimulated with either Vehicle (A) or S1PR1-Antagonist [W 146, 10  $\mu$ M], S1PR2-Antagonist [JTE 013, 10  $\mu$ M] and S1PR3-Antagonist [TY 52156, 10  $\mu$ M] together (B) followed by stimulation with S1P [1  $\mu$ M] and Thapsigargin [1  $\mu$ M]. (C) Min/Max Peak ratio of S1P peak. C: T-test, \*\*\*\* $p < 0.0001$ . All data are represented as means  $\pm$  s.e.m. of n cells from x experiments (n/x).

#### 4.5 Sphingosine-1-phosphate in white adipocytes

It is of special interest whether the findings from chapters 4.3 and 4.4 are unique to BAs or if S1P plays a role in WAs as well. Therefore, the expression levels of S1PRs and SphKs were examined in WAs. For this purpose, mRNA of preWAs on day -2 which marks the day of confluency and of mature WAs on day 8 was analysed (Figure 24). S1PR1 and S1PR2 mRNA levels [ $2^{-\Delta\text{ct}}$ ] are significantly diminished in mature WAs compared to preWAs. The overall mRNA levels of S1PR1, S1PR2 and S1PR3 in preWAs as well as in mature WAs are of similar magnitude. In comparison to S1PR1, S1PR2 and S1PR3, the receptors S1PR4 and S1PR5 are considerably lower expressed. Similar to S1PR1 and S1PR2 also the Shk1 and Shk2 mRNA levels are significantly higher in preWAs than in mature WAs. Conclusively, the S1PR and SphK expression patterns are similar in BAs and WAs.

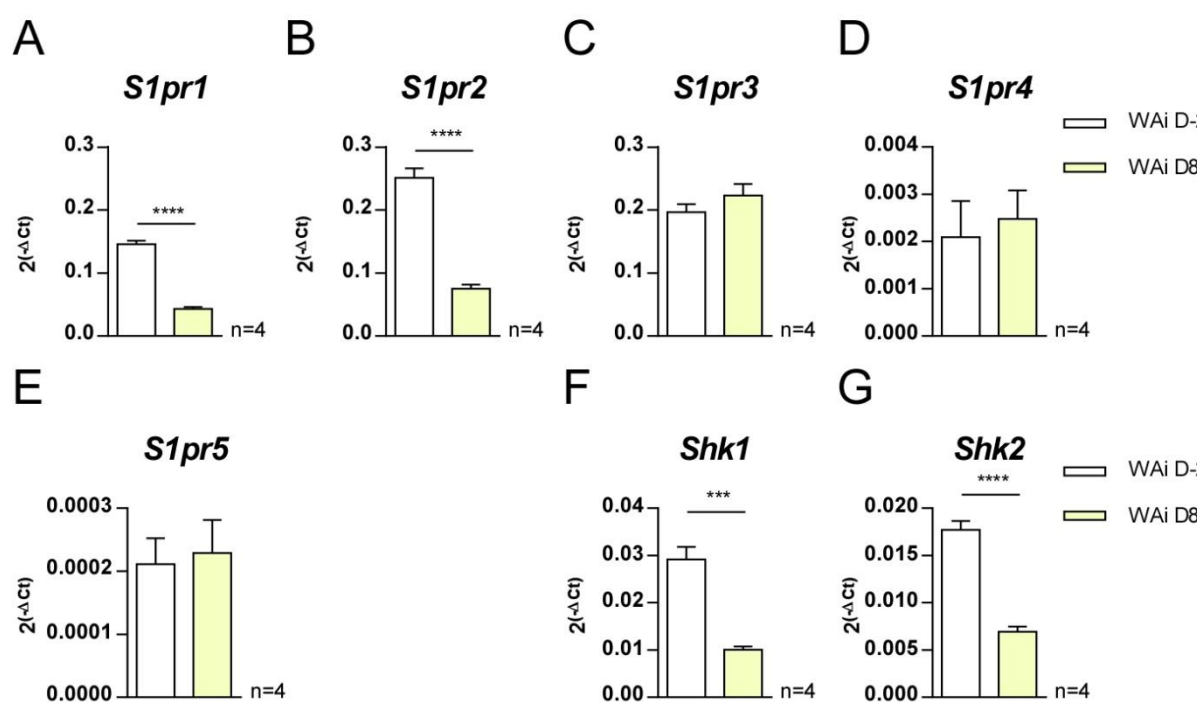


**Figure 24 | Expression of S1PRs and Sphks in WAs**

mRNA expression of *S1pr1* (A), *S1pr2* (B), *S1pr3* (C), *S1pr4* (D), *S1pr5* (E), *Shk1* (F), *Shk2* (G) in murine WAs at preadipocyte (D-2) and mature adipocyte (D8) state. Expression data are normalized to *Hprt*. T-test, \*\*\*\*  $p < 0.0001$ , \*\*\*  $p < 0.001$ . All data are represented as means  $\pm$  s.e.m.

The data from Figure 10 reveal that chronic S1P treatment of BAs inhibits their differentiation. WAs which were chronically treated with 1  $\mu\text{M}$  of S1P from day of confluency (day-2) exhibit significantly decreased  $\alpha\text{P2}$  and  $\text{PPAR}\gamma$  protein (Figure 25A) and mRNA (Figure 25B) levels. The ORO staining of WAs reveals a fewer lipid droplet accumulation when cells are treated chronically with S1P compared to the control group. To investigate whether S1P influences the ability of WAs to assume a more “brown-like” phenotype, WAs were treated for 16 hours either with S1P or vehicle in presence and absence of the

positive control NE. Afterwards the mRNA expression of the thermogenic marker UCP1 was measured in these cells. As anticipated the NE treatment leads to a significant rise of UCP1 mRNA in both, vehicle and S1P, treated cells. Upon S1P treatment the UCP1 mRNA levels remain unchanged independent of the co-treatment with or without NE. On the basis of this experiment I conclude that S1P decreases differentiation not only in BAs, but also in WAs.

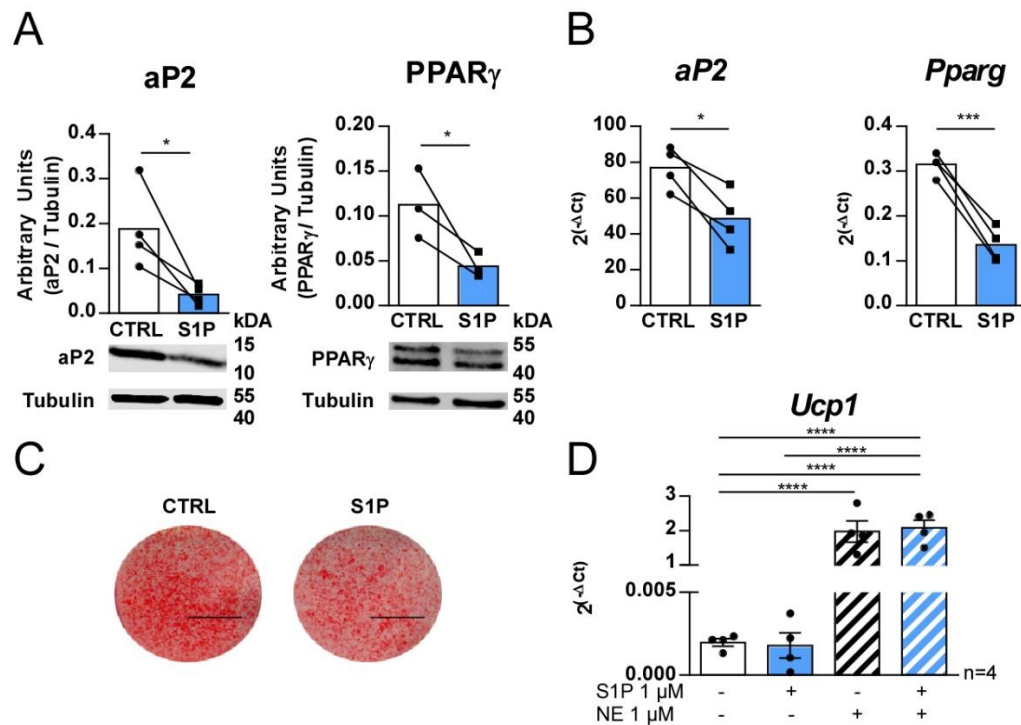


**Figure 25 | S1P decreases differentiation of white adipocytes**

(A) Representative immunoblots and quantification of aP2 (n=4) and PPAR $\gamma$  (n=3) after chronic treatment of WA with S1P [1 $\mu$ M] from day -2. (B) Relative mRNA expression of aP2 and Pparg after chronic treatment of WA with S1P [1 $\mu$ M] from day -2. (C) ORO of white adipocytes treated chronically with S1P [1 $\mu$ M] from day -2. (D) Relative mRNA expression of Ucp1 after a 16-hour treatment of WA with S1P [1 $\mu$ M] and / or NE [1  $\mu$ M] on day 9. Expression data are normalized to Hprt. A-B: t-test, D: one-way ANOVA, post-hoc test: Tukey, \*\*\* p < 0.001, \* p < 0.05. All data are represented as means  $\pm$  s.e.m.

#### 4.6 The role of S1P and S1PRs in mice and humans

To gain an insight into the regulation of S1PR1 and S1PR2, as well as of the SphKs in obesity, WT C57Bl/6J mice were fed either a CD or a HFD for twelve weeks, afterwards tissues were excised and mRNA was isolated (Figure 26). The mRNA levels of S1PR1 and SphK2 are significantly decreased in WATg after feeding an HFD. The S1PR2 mRNA expression is significantly increased in BAT when fed a HFD compared to the CD group. In comparison to S1PR2, S1PR1 mRNA levels tend to be higher, however when comparing two different genes quantitatively the primer efficiency has to be considered.

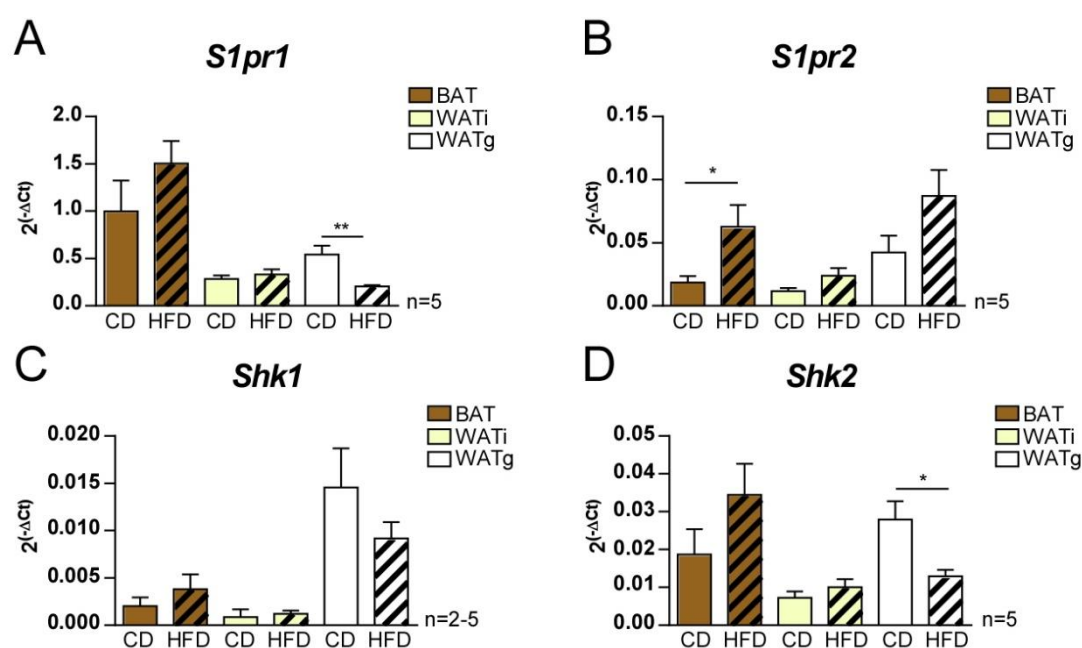


**Figure 26 | Expression of S1PRs and Sphks in fat tissues of mice fed a CD or a HFD**

mRNA expression of *S1pr1* (A), *S1pr2* (B), *Shk1* (C) and *Shk2* (D) in BAT, WATi and WATg of C57Bl/6J mice fed either a control diet (CD) or a high fat diet (HFD) for twelve weeks. Expression data are normalized to *Hprt*. T-test, \*\*  $p < 0.01$ , \*  $p < 0.05$ . All data are represented as means  $\pm$  s.e.m.

In order to find out whether S1PR1 and S1PR2 are differentially regulated *in vivo* during cold exposure of mice, WT C57Bl/6J mice were exposed either to 23°C for one week or to 16°C for three days following 4°C for one week. Fat tissues were excised and mRNA levels of S1PR1, S1PR2, SphK1 and SphK2 were measured (Figure 27). S1PR1 mRNA levels do not differ substantially between the different groups of fat BAT, WATi and WATg. The maximum difference accounts for 0,5fold. S1PR1 expression in BAT of mice housed at 4°C is 23% higher than in the 23°C group, however with a p- value of 0.054 this is not significant (Figure 27A). S1PR2 mRNA expression in BAT and WATi of mice kept at 4°C is significantly lower compared to housing animals at 23°C (Figure 27B). When mice are exposed to 4°C, SphK1 mRNA decreases significantly in BAT (Figure 27C). Contrary to these findings, Sphk2 levels increase significantly in the 4°C group in BAT and attenuate significantly in WATg at 4°C (Figure 27D).

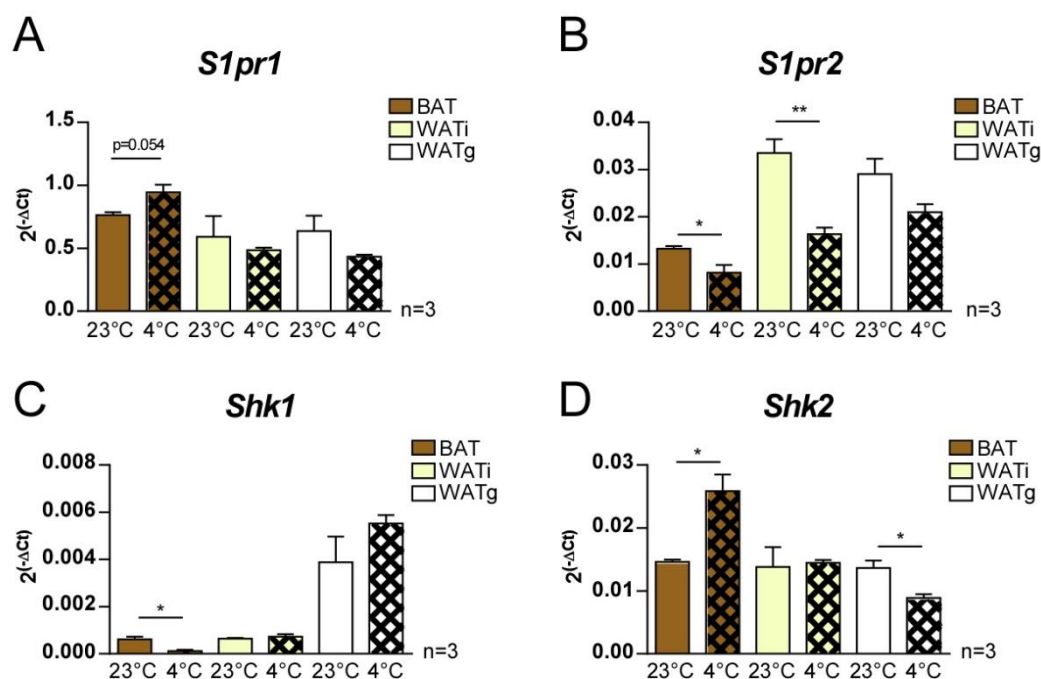


**Figure 27 | Expression of S1PRs and Sphks in fat tissues of mice exposed to 23°C or 4°C**

mRNA expression of *S1pr1* (A), *S1pr2* (B), *Shk1* (C) and *Shk2* (D) in BAT, WATi and WATg of C57Bl/6J mice housed either at 23°C or at 4°C for one week. Expression data are normalized to *Hprt*. T-test, \*\* p < 0.01, \*\*\*p < 0.05. All data are represented as means ± s.e.m.

An important question which has not been addressed yet is how S1P serum and tissue levels are regulated during cold adaptation, as well as during thermoneutrality in mice. To obtain a comprehensive overview of S1P metabolism, precursors of S1P, namely sphingomyelin and its metabolites phosphatidylcholine and lysophosphatidylcholine, sphingosine and C-16-ceramide (Albi et al., 2008; Law et al., 2019) were measured in serum whereas S1P was measured in serum and tissue samples. For this purpose, mice were housed either at 16°C for three days, followed by one week at 4°C, at 23°C or at 30°C for one week. Afterwards I have isolated blood and tissues of these mice. Following mass spectrometry analysis of these samples was performed by the working group of Professor Markus Gräler from the University Hospital in Jena, Germany (Figure 28). Among different weeklong housing temperatures the S1P levels in the serum remain constant (Figure 28A). Sphingosine, the unphosphorylated precursor of S1P, is significantly decreased at 4°C compared to 23°C (Figure 28B). Sphingomyelin serum concentrations are significantly higher in mice housed at 30°C compared to mice which were exposed to 4°C (Figure 28C). Albeit the exposure to different temperatures C16-Ceramide rates (Figure 28D) and Lysophosphatidylcholin levels (Figure 28F) remain unaltered. Phosphatidylcholin concentrations in the blood are significantly elevated at 4°C compared to 23°C and 30°C (Figure 28E). In BAT, there emerges a trend for increasing S1P levels at decreasing housing temperatures (Figure 28G). Conversely, it might be observed that with increasing housing

temperatures S1P levels elevate proportionally in WATi. However, these observations are not statistically significant. The latter is also true for S1P concentrations in WATg at different temperatures.

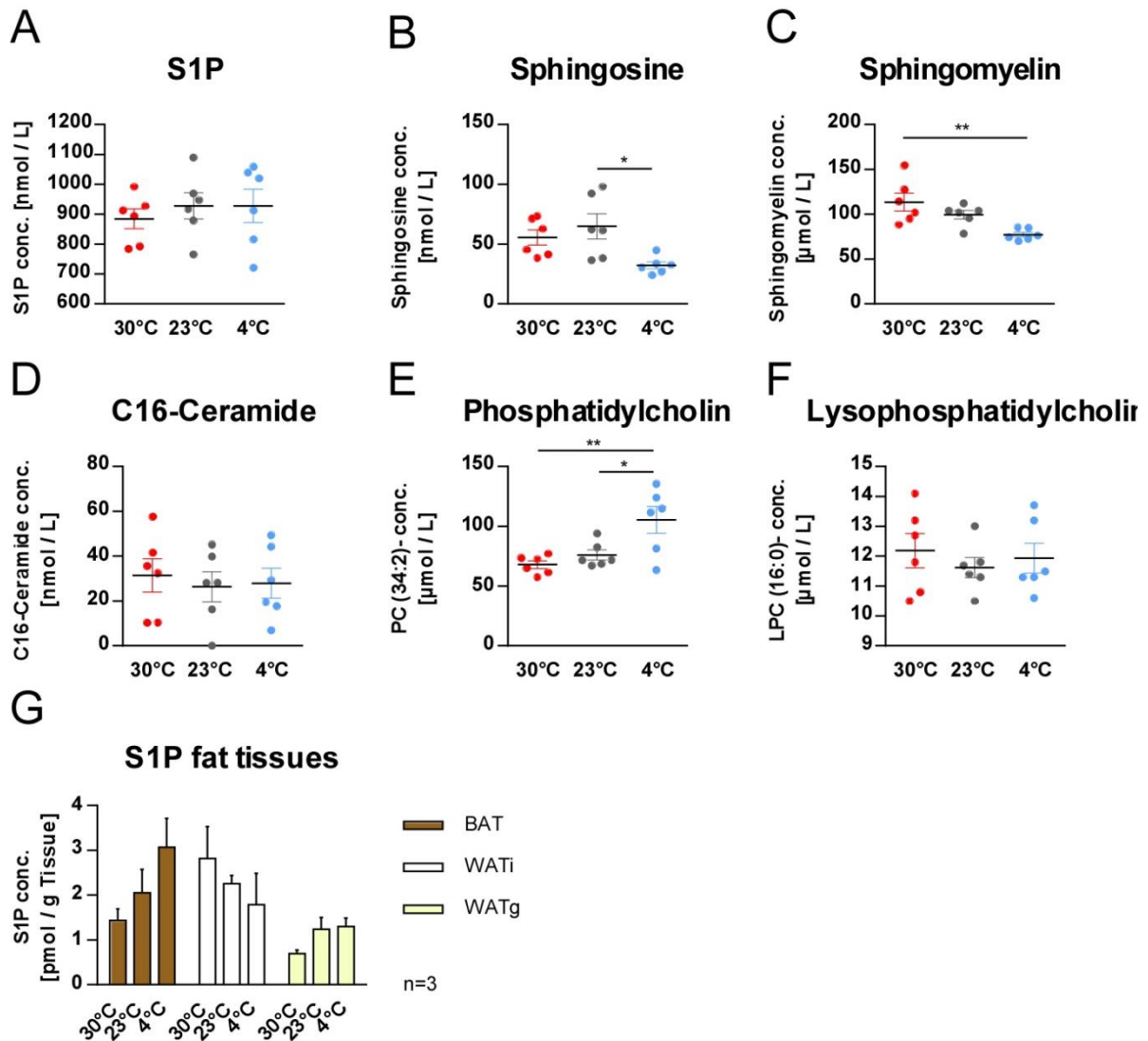


**Figure 28 | Spingolipids in serum and fat tissues after housing of mice at 30°C, 23°C or 4°C for one week**  
Plasma levels of S1P (A), Sphingosine (B), Sphingomyelin (C), C16-Ceramide (D), Phosphatidylcholin (E) and Lysophosphatidylcholin (F) of C57Bl6/J mice which were housed at 30°C, 23°C or 4°C for one week, n= 6 (G) S1P concentrations in brown adipose tissue [BAT], inguinal white adipose tissue [WATi] and gonadal white adipose tissue [WATg] of C57Bl6/J mice which were housed at 30°C, 23°C or 4°C for one week, n=3 (A-F): One-way ANOVA, post-hoc test: Tukey. (G) Two-way ANOVA, \*\* p < 0.01, \* p < 0.05. All data are represented as means ± s.e.m.

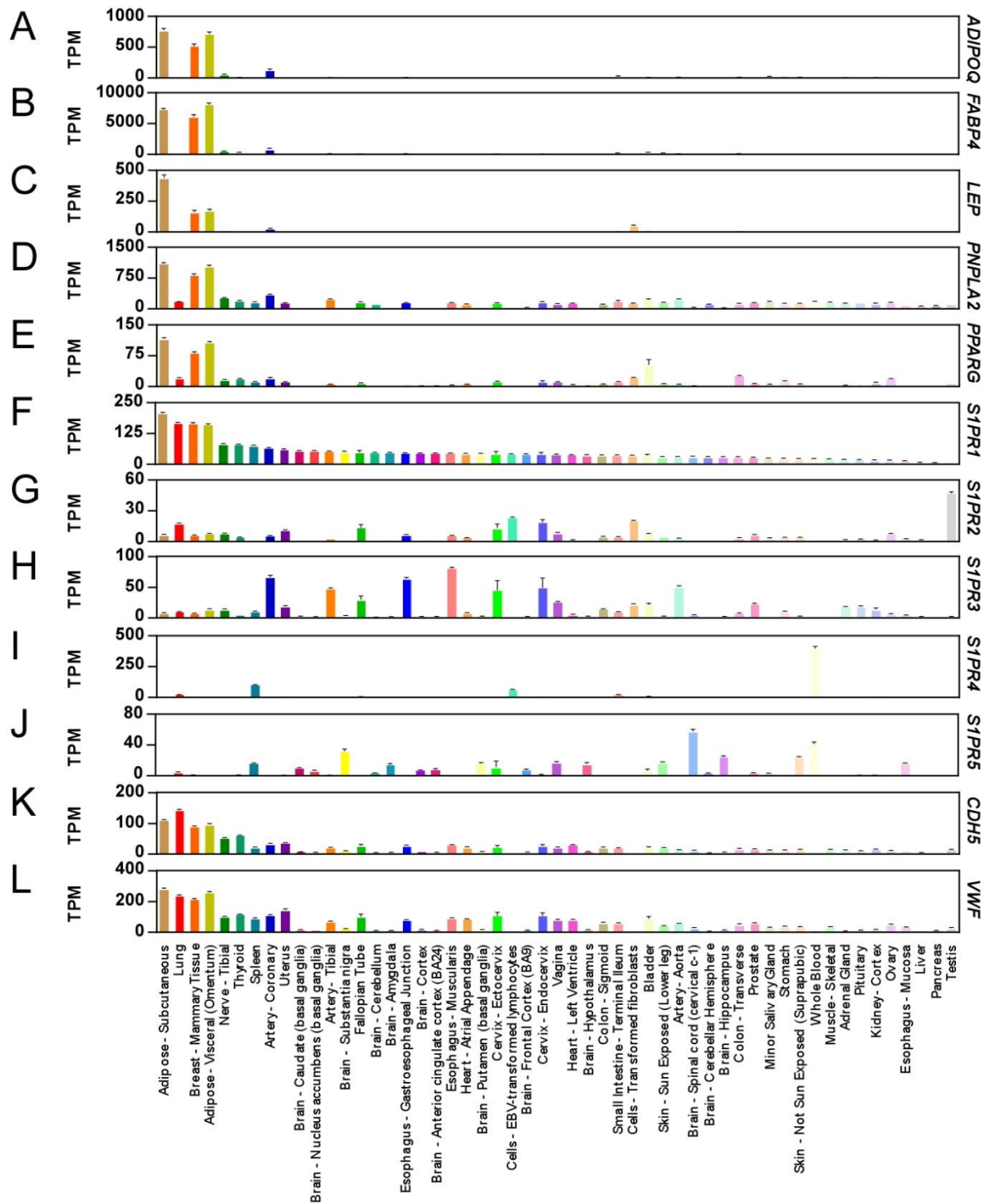


**Figure 29 | Analysis of S1PRs distribution in different human tissues**

RNA sequencing data presented as transcripts per million (TPM) of (A) Adiponectin (*ADIPOQ*), (B) Fatty acid binding protein 4 (*FABP4*), (C) Leptin (*LEP*), (D) Adipose triglyceride lipase (*PNPLA2*), (E) PPARgamma (*PPARG*), (F) *S1PR1*, (G) *S1PR2*, (H) *S1PR3*, (I) *S1PR4*, (J) *S1PR5*, (K) Cadherin 5 (*CDH5*), (L) Von Willebrand Factor (*VWF*) in various human tissues. Data are extracted from the data bank of the Genotype-Tissue Expression (GTEx) project. All data are represented as means  $\pm$  s.e.m.

Another tool to learn more about the role of S1PRs in human samples is the analysis of the open access Genotype-Tissue Expression (GTEx) project data bank (The Genotype-Tissue Expression (GTEx) project,

2013). The information provided by this data bank is based on a comprehensive RNA sequencing analysis performed in a plethora of different human tissues gathered from a multitude of donors. It occurs that S1PR1 distribution is highest in subcutaneous and visceral adipose tissue, as well as in breast tissue and lung. Adipose tissue markers such as adiponectin, fatty acid binding protein 4, leptin, patatin-like phospholipase domain-containing protein 2 and PPAR $\gamma$  are highest expressed in subcutaneous and visceral adipose tissue and breast tissue. The highest occurrence of the endothelial markers von Willebrand factor, as well as cadherin 5 resembles the organ distribution of S1PR1. S1PR2 expression is dominant in testis, lymphocytes and fibroblast cells whereas most transcripts of S1PR3 RNA are found in different tissue samples of esophagus and arteries. S1PR4 RNA appears predominantly in whole blood, spleen and lymphocyte samples. As S1PR4, S1PR5 is also highly present in whole blood, furthermore this receptor is predominantly found in several areas of the brain. The markers for endothelial cells von Willebrand factor (VWF) and Cadherin 5 (CDH5) are most abundantly detected in visceral and subcutaneous adipose tissues, lung and mammary tissue, similar to S1PR1 (Goncharov et al., 2017).

#### 4.7 *In vivo*: Injection of S1PR-Agonists and Antagonists in C57Bl/6J mice

A pharmacological approach deciphering the effects of specific S1PR agonists and antagonists is of great interest as drug application is until nowadays the method of choice when it comes to treatment of most chronic diseases. Thus, eight-week old C57Bl/6J mice were injected daily with either vehicle, the specific S1PR1 agonist SEW 2871 (Figure 30), the specific S1PR2 agonist CYM 5520 (Figure 31) or the specific S1PR2 antagonist JTE 013 (Figure 32). The mice were divided into two groups. One group was housed at 23°C accompanied by daily intraperitoneal (i.p.) injections of the latter mentioned compounds for one week. The other group was kept at 16°C for three days, followed by a one-week 4°C cold exposure accompanied by daily i.p. injections of the S1PR modulators.

When mice are injected with the S1PR1 agonist no effect in O<sub>2</sub> consumption occurs between the vehicle and the compound treated animals at 23°C as well as at 4°C (Figure 30A). The difference in O<sub>2</sub> consumption between both temperature groups is expected to emerge as the mice need more energy and thus O<sub>2</sub> to maintain their body temperature when they are exposed to 4°C. Body weight, as well as body composition remain unaffected by the weeklong SEW 2871 treatment when it is compared to vehicle exposure (Figure 30B, C). Among the S1PR1 agonist treated mice, animals of the 23°C group weigh significantly more after the seven injections than animals in the 4°C group. Significant differences in wet tissue weight can be detected in WAT<sub>i</sub> and WAT<sub>g</sub>. The weight of these fat tissues is significantly decreased in cold exposed mice (4°C treatment) compared to 23°C housed animals independent of the treatment regime (Figure 30E, F). For BAT (Figure 30D) and liver no influence of either treatment or temperature is detectable. Among one treatment group the histology of WAT<sub>i</sub> shows more adipocytes with multilocular lipid droplets at 4°C compared to 23°C (Figure 30H). The occurrence of smaller lipid droplets after 4°C cold exposure is a sign for browning of the WAT<sub>i</sub> (Paschos et al., 2018). However, no histological difference neither at 23°C nor at 4°C occurs between the vehicle and the S1PR1 agonist treated group.

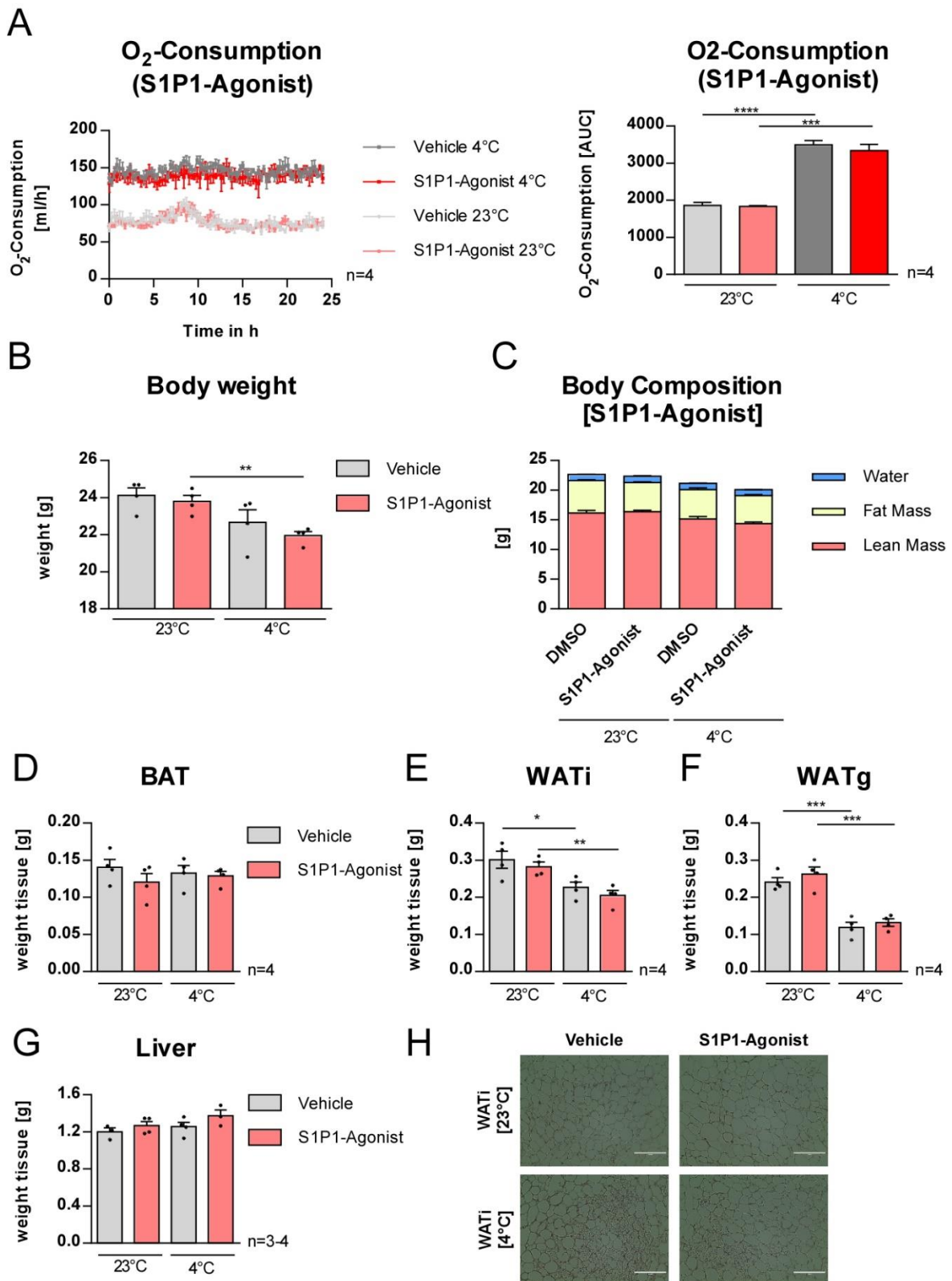


**Figure 30 | One-week daily i.p. injections of S1PR1-Agonist SEW 2871 in C57Bl/6J mice during 23°C and 4°C**

(A) O<sub>2</sub>-consumption, (B) body weight, (C) body composition, weight of BAT (D), WATi (E), WATg (F), Liver (G), (H) representative HE stainings (40x) of WATi of C57Bl/6J mice housed either at 23°C or at 4°C for one week while being daily i.p. injected with either Vehicle or SEW 2871 [5mg/kg/d]. **A, C:** Two-way ANOVA, **B, D-I:** T-test, \*\*\*\*p < 0.0001, \*\*\*p < 0.001, \*\*p < 0.01, \*p < 0.05. All data are represented as means ± s.e.m.

**Note:** In accordance with the '3 R principle of humane animal research' (Russell and Burch, 1992) there is no separate, independent Vehicle control group for each of the three figures (Figure 30, Figure 31, Figure 32). Instead, we reduced the animal numbers by showing the same Vehicle animals in all three figures!

The injection of the specific S1PR2 agonist CYM 5520 does not lead to changes in O<sub>2</sub> consumption between vehicle and agonist treated mice (Figure 31A). As anticipated a significant increase in O<sub>2</sub> consumption is observed in mice kept at 4°C for one week compared to the 23°C exposed animals. No alterations in body weight (Figure 31B) and body composition (Figure 31C) subject to treatment with vehicle or S1PR2 agonist are observed. At a housing temperature of 23°C, the wet weight of BAT (Figure 31D), WAT<sub>i</sub> (Figure 31E) and WAT<sub>g</sub> (Figure 31F) is significantly lower in mice which have been treated for one week with CYM 5520 compared to the vehicle group. A significant decrease in WAT<sub>i</sub> and WAT<sub>g</sub> wet weight between the 23°C and the 4°C group among the same treatment is observed (Figure 31E, F). BAT and liver weight are unaltered by both temperature and treatment (Figure 32D, G).

Another cohort of mice was injected with the selective S1PR2 antagonist JTE 013 and was exposed to either 23°C or 4°C for seven days. The injection of the antagonist does not alter O<sub>2</sub> consumption of the mice neither at 23°C nor at 4°C compared to vehicle injections (Figure 32A). A significant decrease of body weight can be detected in mice injected with the specific S1PR2 antagonist at 4°C compared to the 23°C surrounding temperature group (Figure 32B). The overall body composition remains unaffected by the treatment (Figure 32C). The pharmacological blockade of S1PR2 results in significant lower BAT weights of mice housed at 4°C compared to the 23°C group (Figure 32D). At cold exposure (4°C) WAT<sub>i</sub> (Figure 32E) and WAT<sub>g</sub> (Figure 32F) wet weights are significantly decreased in both treatment groups -vehicle and S1PR2 antagonist- compared to animals housed at 23°C. HE stainings of WAT<sub>i</sub> show more multilocular cells at 4°C compared to 23°C (Figure 32H) whereas no difference is observable in the histology between vehicle and S1PR2 antagonist treated mice. The mass of the liver is independent of treatment or surrounding temperature (Figure 32G).

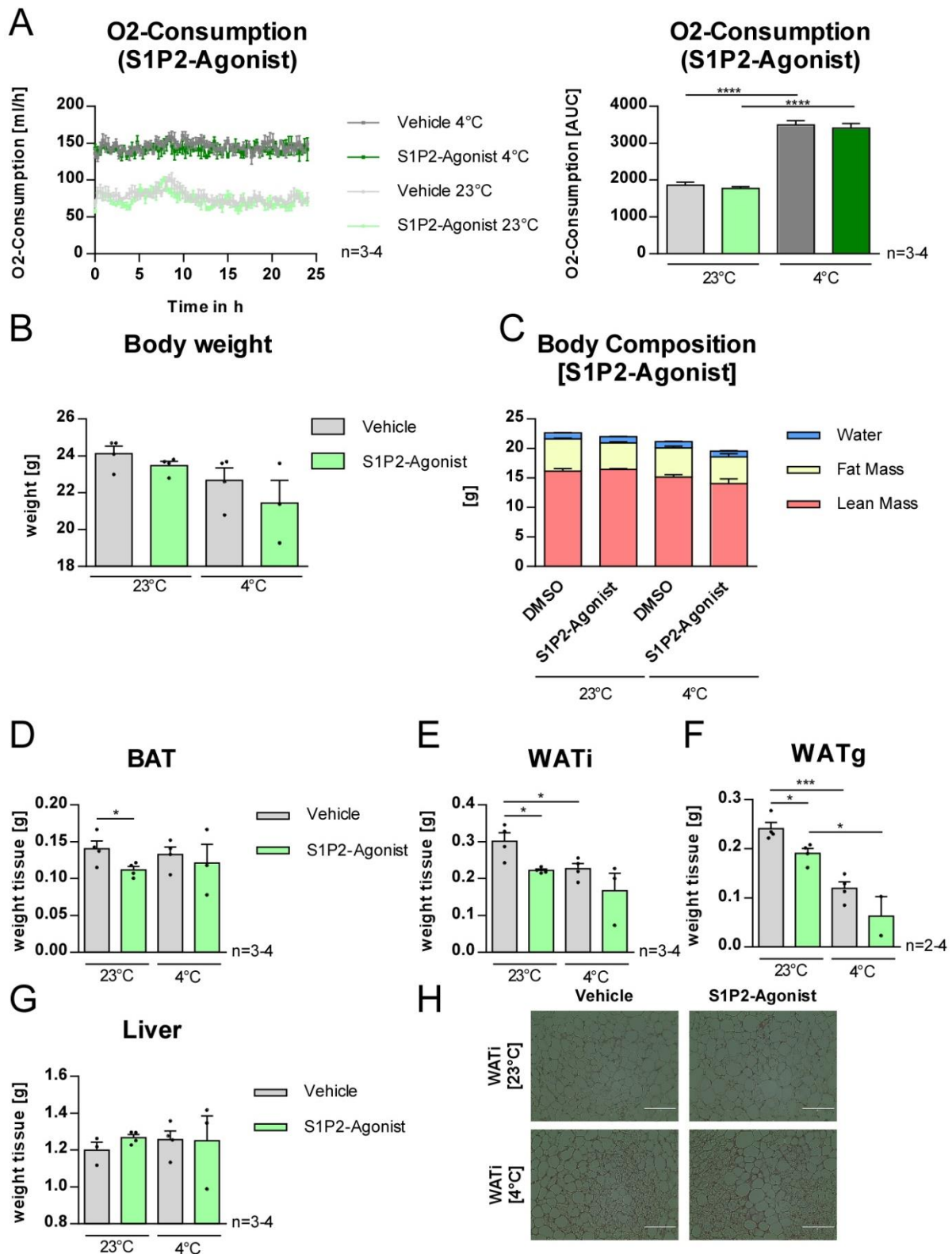


**Figure 31 | One-week daily i.p. injections of S1PR2-Agonist CYM 5520 in C57Bl/6J mice during 23°C and 4°C**

(A) O<sub>2</sub>-consumption, (B) body weight, (C) body composition, weight of BAT (D), WATi (E), WATg (F), Liver (G), (H) representative HE stainings (40x) of WATi of C57Bl/6J mice house either at 23°C or at 4°C for one week while being daily i.p. injected with either Vehicle or CYM 5520 [5mg/kg/d]. A, C: Two-way ANOVA, B, D-I: T-test, \*\*\*\*p < 0.0001, \*\*\*p < 0.001, \*\* p < 0.01, \* p < 0.05. All data are represented as means ± s.e.m.

**Note:** In accordance with the '3 R principle of humane animal research' (Russell and Burch, 1992) there is no separate, independent Vehicle control group for each of the three figures (Figure 30, Figure 31, Figure 32). Instead, we reduced the animal numbers by showing the same Vehicle animals in all three figures!

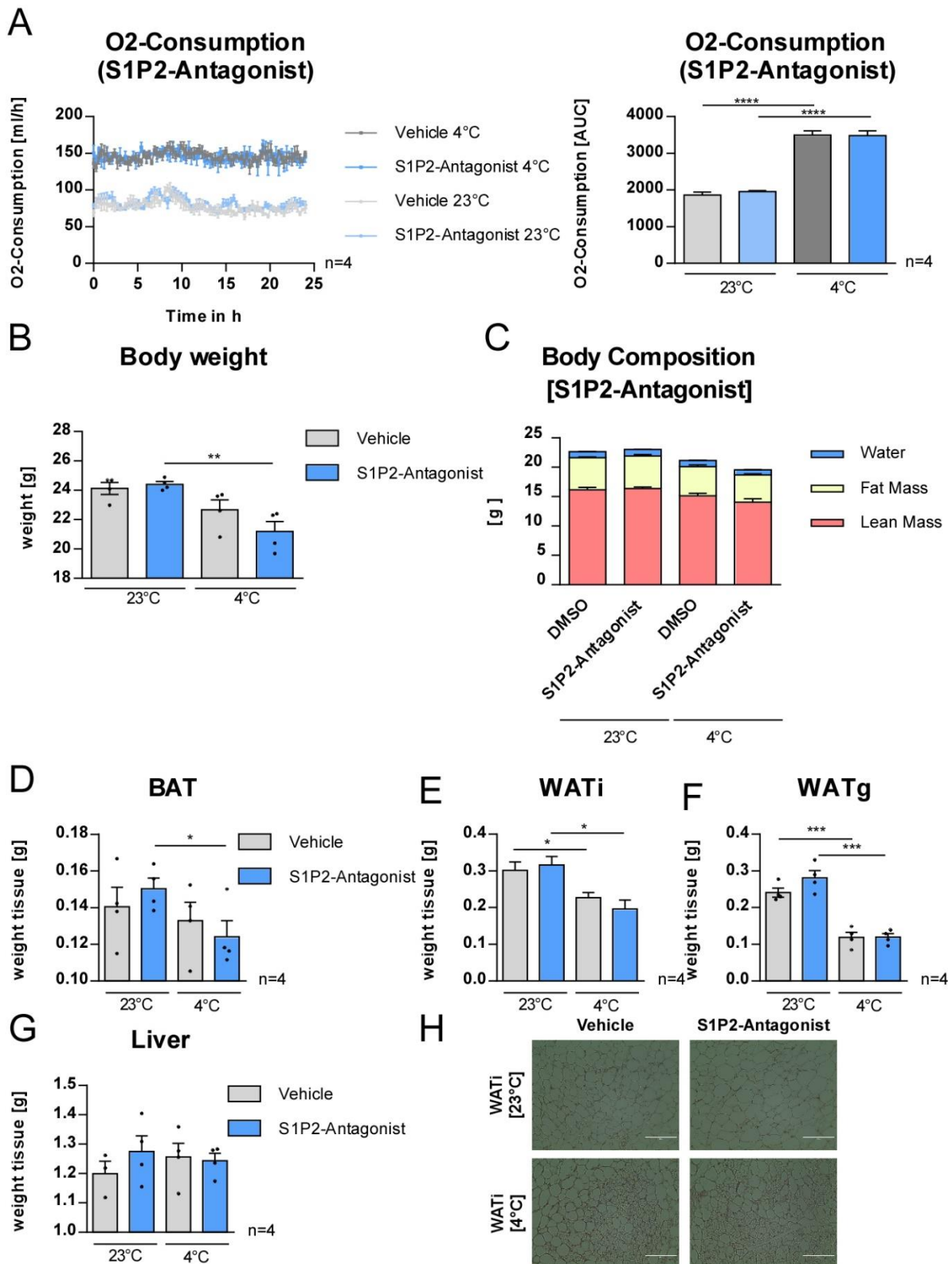


**Figure 32 | One-week daily i.p. injections of S1PR2-Antagonist JTE 013 in C57Bl/6J mice during 23°C and 4°C**

(A) O<sub>2</sub>-consumption, (B) body weight, (C) body composition, weight of BAT (D), WAT<sub>i</sub> (E), WAT<sub>g</sub> (F), Liver (G), (H) representative HE stainings (40x) of WAT<sub>i</sub> of C57Bl/6J mice housed either at 23°C or at 4°C for one week while being daily i.p. injected with either Vehicle or JTE 013 [4mg/kg/d]. A, C: Two-way ANOVA, B, D-I: T-test, \*\*\*\*p < 0.0001, \*\*\*p < 0.001, \*\*p < 0.01, \*p < 0.05. All data are represented as means ± s.e.m.

**Note:** In accordance with the '3 R principle of humane animal research' (Russell and Burch, 1992) there is no separate, independent Vehicle control group for each of the three figures (Figure 30, Figure 31, Figure 32). Instead, we reduced the animal numbers by showing the same Vehicle animals in all three figures!

## 5 Discussion

The research about the role of S1P in adipocytes conducted to date allows an interesting insight into functional aspects of S1P in obesity and adipose tissues, however many questions remain still unaddressed. Coherent so far is the finding that chronic S1P treatment impairs adipogenesis of 3T3-L1 and 3T3-F442A cells (chapter 1.4.3). These cell lines are used to investigate effects in white adipocytes (Ruiz-Ojeda et al., 2016). Besides two recently published papers there is no other literature found investigating the role of S1P in brown adipocytes (Christoffersen et al., 2018; Gohlke et al., 2019). With the prevalence of obesity on the rise and an estimated increase of 300% of obese patients in 2050 compared to 2007 new targets for the treatment of adiposity are desperately needed (Agha and Agha, 2017). The exploration of S1P and its receptors could lead to promising new targets to combat obesity in a pharmacological manner.

### 5.1 Sphingosine-1-phosphate in brown adipocytes

The analysis of S1PR mRNA expression in brown adipocytes (Figure 8) reveals a relatively high level of S1PR1, S1PR2 and S1PR3 mRNA. Even though to a lower extend, S1PR4 and S1PR5 are also expressed in BAs.

Interestingly, S1PR1 expression is induced when cells are treated with IBMX leading to the conclusion that a possible intracellular cAMP or cGMP increase promotes S1PR1 expression (Diederens et al., 2006; Kraynik et al., 2013). Both second messengers are required to induce differentiation of brown adipocytes (Jennissen et al., 2011). Moreover, the intracellular cAMP elevation upon sympathetic NE stimulation of  $\beta$ -3 adrenergic receptors is crucial for the induction of thermogenesis (Cannon and Nedergaard, 2004). The cyclic nucleotide cGMP leads to an increased adipogenesis of brown adipocytes (Haas et al., 2009; Mitschke et al., 2013; Hoffmann et al., 2015). The upregulation of S1PR1 mRNA upon IBMX treatment is possibly attributed to an intracellular increase of cAMP or cGMP. Taken these findings together S1PR1 expression might be influenced by these two second messengers in brown adipocytes. To further elucidate the regulation of S1PR1 expression, brown adipocytes could be treated on the day of induction with either IBMX, cAMP, cGMP or a combination of both cyclic nucleotides to narrow down the main regulator of S1PR1 expression. S1PR3, as well as Shk1 also have enhanced mRNA expression after brown adipocyte induction. The compound responsible for this effect has still to be evaluated.

In the lysophospholipid field it is matter of discussion which S1P concentration mimics adequately physiological circumstances in *in vitro* cellular culture systems as S1P levels in blood and interstitium differ (Cyster and Schwab, 2012). We found in our cell culture medium 10 nM S1P which is unavoidably

introduced by the requirement of fetal bovine serum (FBS). Therefore, we decided to use low micromolar concentrations of S1P. This further enables the comparability of our results to those described in the literature as a low micromolar concentration of S1P is commonly used (Moon et al., 2014; Moon et al., 2015; Kitada et al., 2016b; Weske et al., 2018; Gohlke et al., 2019). Noteworthy, S1P can be bound to both albumin and apoM *in vivo* (Christoffersen et al., 2011; Wilkerson et al., 2012). Commonly, albumin-bound S1P is used for cellular treatments. When translating *in vitro* experiments to possible *in vivo* effects, it has to be considered that apoM-bound S1P may exert slightly different effects than albumin-bound S1P which is used in our system (Ruiz et al., 2017). Even though *in vitro* studies bear some limitations, the *in vitro* research is a highly valuable tool for investigation of underlying mechanistic pathways, to obtain an idea of physiologic occurrences and for reduction of laboratory animal numbers.

In mature brown adipocytes S1P treatment does not exhibit major impact on lipolysis (Figure 9). However, when brown adipocytes are treated during differentiation with S1P a decrease in aP2, PPAR $\gamma$  and UCP1 mRNA and protein expression is observed (Figure 10). Hence S1P has the potential to attenuate adipogenesis of brown adipocytes. These results are in congruence with data obtained by other research groups in 3T3-L1 and 3T3-F442A cells (Moon et al., 2014; Moon et al., 2015; Kitada et al., 2016b; Weske et al., 2018). When Gohlke et al. treated brown adipocytes chronically with S1P no changes in UCP1 and PGC1 $\alpha$  mRNA levels were observed. Merely a four-hour long NE stimulation following the chronic S1P treatment lead to a reduction of UCP1 and PGC1 $\alpha$  mRNA (Gohlke et al., 2019). Even though the trends are similar, these results differ slightly from observations made in our lab. It is worth mentioning that even though both groups investigate brown adipocytes, isolation protocols for these cells differ. Gohlke et al. isolate brown adipocyte precursor cells via FACS from adult mice. In contrast our group isolates brown preadipocytes from newborn pups and differentiates these cells after immortalization with a SV40 large T-antigen virus to mature adipocytes. Another noteworthy difference is that our immortalized preadipocytes do not require addition of the PPAR $\gamma$  activator Rosiglitazone – a strong stimulator of adipogenesis - for growing the brown adipocyte precursors to confluence (Jennissen et al., 2013; Gohlke et al., 2019). In our system we can robustly find that S1P decreases adipogenesis of brown adipocytes.

## 5.2 Downstream signaling of S1P in brown adipocytes

In 2016, our lab published that the activation of G $_q$  signaling leads to a decreased differentiation of brown adipocytes. When the G $_q$  signaling was blocked with the specific G $_q$  inhibitor FR brown adipocytes displayed an enhanced adipogenesis (Klepac et al., 2016). In brown adipocytes treated

chronically with S1P, I also observed an inhibition of differentiation (Figure 10). As S1PRs are reported to couple also to  $G_q$ , the question arose whether the S1P mediated decrease of brown adipocyte differentiation occurs via activation of the  $G_q$  signaling pathway. To test this hypothesis the chronic S1P treatment during brown adipocyte differentiation was accompanied by a treatment with FR. The  $G_q$  inhibitor was partially able to rescue the S1P mediated diminution of differentiation, however it was not able to rescue the effect completely, especially not for the proteins  $\alpha P2$  and UCP1 (Figure 11).

Interestingly, we found that S1P induces a  $Ca^{2+}$  release in brown preadipocytes (Figure 13). To evaluate whether the  $[Ca^{2+}]_i$  derives from intracellular stores or from the extracellular space a buffer without  $Ca^{2+}$  and enriched with the calcium chelator EGTA was used (Figure 13B). In a  $Ca^{2+}$  free buffer a signal is only expected upon  $Ca^{2+}$  release from intracellular stores. The S1P-induced calcium response observed in  $Ca^{2+}$ - free buffer was comparable to that seen with 1 mM  $[Ca^{2+}]_{ex}$ . thus we can conclude that S1P induces  $Ca^{2+}$  release from intracellular stores (Figure 13).

Moreover, acute  $Ca^{2+}$  signals induced by the addition of S1P were abolished by preincubation with the  $G_q$  inhibitor FR (Figure 14). These results lead to the conclusion that the S1P-triggered calcium response is rooted in  $G_q$ -signaling, most likely via the activation of  $IP_3$  receptors located at the endoplasmic reticulum, thereby leading to an increase in intracellular calcium. To further support the hypothesis of S1P mediated  $G_q$  signaling in BAi the  $IP_1$  assay was performed additionally. Surprisingly, no increase in  $IP_1$  was observable in contrast to the positive control ET-1 (Figure 15). This discrepancy between the calcium increase and the  $IP_1$  data is unexpected. A potential explanation for the absence of  $IP_1$  and respectively  $IP_3$  signal might be the simultaneous stimulation of all five S1PRs in the brown adipocytes upon S1P treatment and thereby an interference of different downstream signaling pathways. Noteworthy,  $[Ca^{2+}]_i$  imaging experiments result in an immediate single cell response, whereas the  $IP_1$  assay reflects the accumulation of  $IP_1$  over a time-window of two hours in a cell suspension. Moreover, detachment of cultured adhesive cells applying the protease trypsin can lead to cleavage of cell surface proteins (Huang et al., 2010). Possibly the S1PR responsible for  $G_q$  mediated  $Ca^{2+}$  signals might be affected by trypsin application which is required prior to  $IP_1$  assay. Therefore, live-cell calcium imaging might be a more robust and reliable option for our characterization of the S1P-mediated  $G_q$ -signaling pathway in preBAs.

In a recently published paper it is reported that S1P increases intracellular calcium and  $IP_3$  levels via PLC activation in pulmonary artery smooth muscle cells (PASMC) of rats resulting in an enhanced proliferation of these cells (Yan et al., 2019). In analogy to the effects observed in PASMCs, it would be of great interest to investigate whether the S1P-mediated intracellular calcium signal in preBAs might be inhibited similarly by the pretreatment with a PLC inhibitor, not at least to support the finding that S1P contributes to  $G_q$  signaling in preBAs. Moreover, Yan et al. found that S1P treatment induces the

calcineurin/nuclear factor of activated T cells (NFAT) pathway in PSMCs (Yan et al., 2019). In the early 2000s, it was reported that a sustained calcineurin activation impairs differentiation of 3T3-L1 adipocytes via reduction of PPAR $\gamma$  and C/EBP $\alpha$  and thus contributes to a calcium dependent inhibition of adipogenesis (Neal and Clipstone, 2002). Combining the latter mentioned findings and my results, it is conceivable that S1P activates the calcium calcineurin NFAT pathways in preBAs and thereby leading to an inhibition of the driver of adipogenesis PPAR $\gamma$  which results in an impaired adipocyte differentiation. However, future investigation of the chronic treatment of brown adipocytes with S1P in presence and absence of the calcineurin inhibitor cyclosporin A is required to test this hypothesis (Azzi et al., 2013).

DMR measurements were performed in brown preadipocytes to obtain a holistic, label free readout for S1P signaling. In these measurements a dose dependent S1P signal was still observed despite the addition of G $_i$ , G $_q$  and ROCK inhibitors, arguing for a further signaling pathway addressed by S1P (Figure 12). Overall, the S1P signaling in brown adipocytes seems to be versatile. A potential G $_{12/13}$  signaling component of S1P is revealed by real-time quantitative PCR analysis of CYR61 expression (Figure 16). S1P induces potently CYR61 mRNA levels, which can be significantly diminished by the Rho inhibitor C3 transferase but not by FR. Thus, the S1P mediated Rho activation is based on signaling of G $_{12/13}$  rather than signaling of G $_q$ .

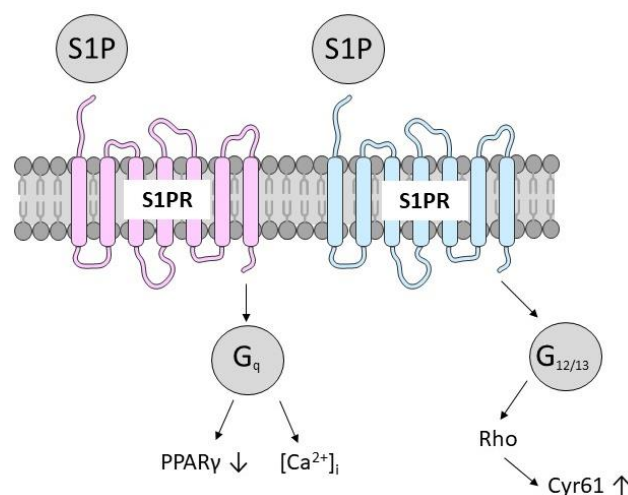


**Figure 33 | Model of S1P mediated downstream signaling in brown adipocytes**

This image was produced using templates of Servier Medical Art by Servier which are licensed under a Creative Commons Attribution 3.0 Unported License, <https://smart.servier.com>. (26.10.2019).

Conclusively the attenuated differentiation of brown adipocytes via S1P might be mediated by G $_q$  and G $_{12/13}$  signaling. Generally, it must be considered that S1P binds to its five different receptors which are all expressed in brown adipocytes. Therefore, whenever the lysophospholipid is utilized for treatments it can be assumed that several S1PRs, although differently expressed (Figure 7), are activated in parallel

and their different G protein-coupling moieties may lead to an interplay of various signaling pathways. Thus, the application of S1P does not always allow a clear conclusion regarding a specific signaling pathway.

### 5.3 The role of S1PRs in brown adipocytes

The chronic treatment of brown adipocytes with specific agonists reveals that S1PR1 and S1PR2 are responsible for the inhibition of brown adipogenesis (Figure 18, Figure 19). In literature it is already reported that S1P decreases differentiation of 3T3-L1 and 3T3-F442A cells, however there is still debate about the receptor mediating this effect. Moon et al. found in 3T3-L1 adipocytes that S1PR2 is mediating the abolishment of differentiation, whereas Kitada et al. postulate that in 3T3-F442A adipocytes S1PR1 and S1PR3 mediate the inhibition of adipogenesis (Moon et al., 2015; Kitada et al., 2016a). These discrepancies can also root in the use of relative, but still slightly different cell lines (Ruiz-Ojeda et al., 2016). In our model of immortalized brown adipocytes, activation of either S1PR1 or S1PR2 account for the attenuation of brown adipocyte differentiation.

In contrast to the earlier mentioned working groups who use antagonists to evaluate the influence of the single receptor, I took advantage of specific agonists. As mentioned previously all five S1PRs are present in brown adipocytes. When one receptor is blocked by its specific antagonist, the response investigated will be the one of the other four receptors. Therefore, the usage of the specific agonists appears to be more advantageous as the effect observed derives only from agonism of one single receptor.

S1PR1 is probably the best characterized of all S1PRs and consistently reported to be coupled to  $G_i$  (Spiegel and Milstien, 2003; O'Sullivan and Dev, 2013; Mendelson et al., 2014; Patmanathan et al., 2017). The impairment of adipogenesis upon S1PR1 agonism leads to the conclusion that besides the observed  $G_q$  and  $G_{12/13}$  signaling moieties (chapters 4.3 and 5.2) also a  $G_i$  downstream pathway is potentially triggered by S1P in adipocytes.

S1PR3 activation does not negatively affect the differentiation of brown adipocytes (Figure 20). In addition, preliminary data suggest a S1PR4-mediated increase of brown adipogenesis, whereas S1PR5 agonism does not seem to affect differentiation of brown adipocytes.

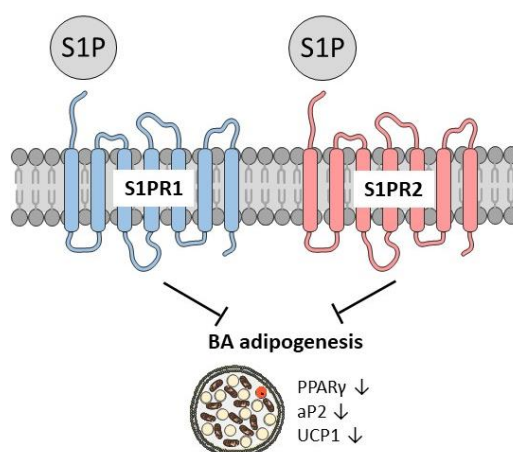


**Figure 34 | Model of S1P mediated inhibition of brown adipocyte differentiation**

This image was produced using templates of Servier Medical Art by Servier which are licensed under a Creative Commons Attribution 3.0 Unported License, <https://smart.servier.com>. (26.10.2019).

In chapters 4.3 and 5.2 an  $[Ca^{2+}]_i$  increase upon S1P stimulation of preBAs is described. Similar experiments were performed using specific S1PR antagonists to decipher the receptor responsible for this effect. The intracellular calcium increase is neither S1PR1- nor S1PR2-mediated as specific antagonists for S1PR1 or S1PR2 are unable to abolish this response (Figure 21, Figure 22). It even occurs that the antagonism of S1PR1 increases  $[Ca^{2+}]_i$  by 12% (Figure 21). In literature it is reported that an overexpression of S1PR1 in HEK 293 and rat hepatoma RH7777 cells inhibits  $Ca^{2+}$  signaling (Heringdorf et al., 2003). Thus, the data of Heringdorf et al. and our data suggest that S1PR1 signaling potentially lowers  $[Ca^{2+}]_i$  release. S1PR3 inhibition results in a significant decrease of the S1P mediated calcium response by 25% (Figure 22). These finding is congruent with the earlier mentioned study which reported that overexpression of S1PR3 leads to an intracellular calcium increase in RH7777 cells (Heringdorf et al., 2003). The combination of S1PR1, S1PR2 and S1PR3 antagonists decreases the  $Ca^{2+}$  response of about 78%. However, the S1P-mediated  $Ca^{2+}$  increase was not completely abolished even by the triple antagonist combination (Figure 22, Figure 23), suggesting the possible involvement of S1PR4 and S1PR5 or another unknown target within this signaling pathway.

The drug Fingolimod (FTY720) is known to target S1PR1, S1PR3, S1PR4 and S1PR5 and literature suggests that it also influences S1PR2 (Brinkmann et al., 2002; Al Alam and Kreydiyyeh, 2016). FTY720 is already clinically approved for the treatment of multiple sclerosis. Single case reports reveal that the intake of FTY720 resulted in tremendous weight loss in three different human patients (Kiyiloğlu, 2017). As an S1PR targeting drug is already clinically applied and possible weight related side effects were observed, it of interest whether FTY720 also affects the differentiation of brown adipocytes. Indeed, the phosphorylated form of FTY720 (FTY720-P) -which does not require the activation via Sphks- decreases adipogenesis of brown adipocytes, similarly to S1P and the S1PR1 and S1PR2 agonists

(Figure 17). Our findings regarding the influence of FTY720-P on brown adipocytes resemble the findings of Moon et al. that FTY720 inhibits differentiation of 3T3-L1 adipocytes (Moon et al., 2012). Moreover injection of FTY720 to mice fed a high fat diet over a time period of ten weeks resulted in lesser weight gain compared to the control group (Moon et al., 2012). Further investigation is required to find out if these FTY720 results could potentially explain side effects of this drug such as the observed weight loss in single cases. However, it is questionable whether FTY720 is a suitable candidate for a future pharmacological treatment of obesity. FTY720 is a potent drug used as escalation therapeutic in multiple sclerosis and can induce lymphopenia in patients. Furthermore, one contraindication for Fingolimod (FTY720) is the intake of  $\beta$  blockers which is quite common among obese patients with hypertension (Pischon and Sharma, 2001; Ayzenberg et al., 2016).

#### 5.4 Sphingosine-1-phosphate in white adipocytes

In congruence with prior studies, we found that S1PRs are not only present in brown but also in white adipocytes (Kitada et al., 2016a; Christoffersen et al., 2018). Interestingly S1PR1, S1PR2, Sphk1 and Sphk2 are significantly higher expressed in white preadipocytes compared to mature adipocytes (Figure 24). On the one hand these observations imply a potential importance of the mentioned receptors and kinases for the proliferation or differentiation of adipocytes rather than for their function. On the other hand it has to be stated that the remaining mRNA levels in mature adipocytes are still quite high especially compared to S1PR4 and S1PR5. Even though there is a difference in mRNA expression levels between mature adipocytes and preadipocytes the conclusions to be drawn from this observation are still limited. Similar to other research conducted in adipocyte cell lines our comprehensive analysis of S1P influence on adipocyte differentiation indicates that S1P does not uniquely influence brown adipocytes but it also decreases differentiation of primary white adipocytes (Figure 25). This allows the hypothesis that S1P is of overall importance for adipogenesis independent of the fat cell type (Moon et al., 2014; Moon et al., 2015; Weske et al., 2018).

#### 5.5 The role of S1P and S1PRs in mice and humans

In order to get an overview of S1P, S1PR and Sphk regulation during HFD and cold exposure, mRNA analysis, as well as lipidomics were performed.

As both, S1PR1 and S1PR2, decrease differentiation of brown adipocytes *in vitro*, an increase in differentiation is expected in knockout models of these two receptors *in vivo*. Both receptors were further characterized for choosing one of them in a knockout mouse model to investigate more in

depth in regards of obesity. S1PR1 and S1PR2 mRNA expression levels are regulated during a twelve-week long HFD. S1PR1 mRNA is decreased in WATg whereas S1PR2 mRNA is significantly increased in BAT compared to the CD group (Figure 26).

The exposure of mice to 4°C for seven days compared to housing these animals at 23°C leads to a significant reduction of S1PR2 mRNA in BAT and WATi. This finding points towards a less important role of S1PR2 at 4°C compared to room temperature (Figure 27). Sphk1 is generally lower expressed in adipose tissues than Sphk2. The expression patterns of S1PR1 and Sphk2 are very similar in both HFD and cold exposure leading to the hypothesis that sphingosine might be converted by Sphk2 to S1P for the purpose of activating S1PR1 which is for example the case for the synthetic compound FTY720 in lymphocytes (Brinkmann et al., 2004; Matloubian et al., 2004).

As far as we know previous research has only investigated S1P blood levels in obese humans and mice (Kowalski et al., 2013; Weske et al., 2018). However, there has no study been conducted so far investigating S1P levels in blood and adipose tissues in mice which were exposed to either 30°C, 23°C or 4°C for one week. Interestingly, when the latter mentioned experiment was performed (Figure 28), it is found that S1P blood levels remain constant between all three temperature groups. However, the S1P precursors sphingomyelin and sphingosine are significantly decreased in the murine plasma at 4°C compared to 30°C or respectively 23°C. Bartelt et al. found in 2011 that upon short term cold exposure triglyceride-rich lipoproteins (TRLs) are taken up by BAT and thereby cleared from the blood (Bartelt et al., 2011). Possibly due to cold exposure the S1P precursors are preferentially taken up by BAT and are converted to S1P by Sphk2 which is significantly upregulated upon 4°C housing (Figure 27). S1P levels increase gradually in BAT the colder the surrounding temperatures of the mice get. However, the observation is after analysis of three biological replicates not yet significant. It is of great interest to investigate whether adipose tissues express functional S1P transporters which could export S1P to the extracellular space or interstitium acting in an autocrine or paracrine manner to activate S1PRs (Kawahara et al., 2009; Fukuhara et al., 2012; Vu et al., 2017; Kobayashi et al., 2018).

The GTEX project data bank analysis and correlation study of the different S1PRs in various human tissues and organs reveals that the quantitative distribution pattern of S1PR1 RNA throughout human organs is very similar to the quantitative distribution of different adipose tissue (ADIPOQ, FABP4, LEP, PNPLA2, PPARG) and endothelial markers (VWF, CDH5) (Figure 29). S1PR1 RNA is most abundant in subcutaneous and visceral fat tissues, as well as in breast tissue and lung. According to these data we hypothesize that S1PR1 can assume an important role in adipose tissue or in endothelial cells within the adipose tissue.

## 5.6 *In vivo*: Injection of S1PR-Agonists and Antagonists in C57Bl/6J mice

The one-week long injection of the S1PR1 agonist SEW 2871 and the S1PR2 antagonist JTE 013 during exposure to 23°C and 4°C do not reveal any effect on oxygen consumption, body and tissue weights and body composition (Figure 30, Figure 32). Interestingly, agonizing the S1PR2 pharmacologically with injections of CYM 5520 lead to a significant decrease of BAT, WAT<sub>i</sub> and WAT<sub>g</sub> weight of mice housed at 23°C (Figure 31). This observation is interesting as Kitada et al. report that S1PR2 knockout mice have generally a lower body weight and improved insulin sensitivity in HFD (Kitada et al., 2016a). It remains to further investigate whether the pharmacological agonism of S1PR2 induces a healthy and sustainable fat loss and to decipher the underlying mechanism of the drastic fat loss. Therefore, it would be of great interest to investigate the effect of S1PR2 agonist treatment on already manifested obesity and to evaluate whether the compound also decreases fat mass in obese mice in a healthy manner.

## 5.7 Outlook: Fat tissue specific knockout of S1PR1 *in vitro* and *in vivo*

We decided to further investigate the fat tissue specific deletion of S1PR1 in the mouse model because we discovered that S1PR1 agonism decreases differentiation of brown adipocytes *in vitro* (Figure 18). S1PR1 is found in both murine brown and white adipocytes and adipose tissues. Among all S1PRs, S1PR1 is the most highly expressed receptor in human adipose tissues. Besides in human lung tissue, S1PR1 RNA transcripts are most abundant in human adipose and breast tissue similarly to adipocyte markers such as aP2 and PPAR $\gamma$ . According to our data, genetical deletion of S1PR2 is also an interesting model for further metabolic investigation, however the study of S1PR1 is of higher novelty because Kitada et al. have already conducted a comprehensive metabolic HFD study in S1PR2 knockout mice (Kitada et al., 2016a).

We are currently crossing S1PR1<sup>fl/fl</sup> mice with adiponectin Cre mice. Expression of Cre recombinase under adiponectin promotor leads to a recombination in brown and white adipocytes (Kong et al., 2017). Further we plan to breed the S1PR1<sup>fl/fl</sup> mice with other Cre expressing mouse lines all targeting adipocytes, however in a different manner: The crossing of a floxed line with UCP1-Cre mice results in BAT specific deletion of the respective gene (Emmett et al., 2017). PDGFR $\alpha$  is broadly present in adipocyte progenitor cells, therefore the PDGFR $\alpha$  Cre model is suitable for the investigation of the ablation of a specific gene on the development of adipocytes (Berry and Rodeheffer, 2013; Krueger et al., 2014; Shao et al., 2016).

The global S1PR1 knockout as well as the non-inducible Tie2-Cre S1PR1<sup>fl/fl</sup> mouse model lead to embryonic lethality due to haemorrhage between E12.5 and E14.5 and therefore cannot be used for investigation of global S1PR1 effects on metabolism (Liu et al., 2000; Allende et al., 2003).

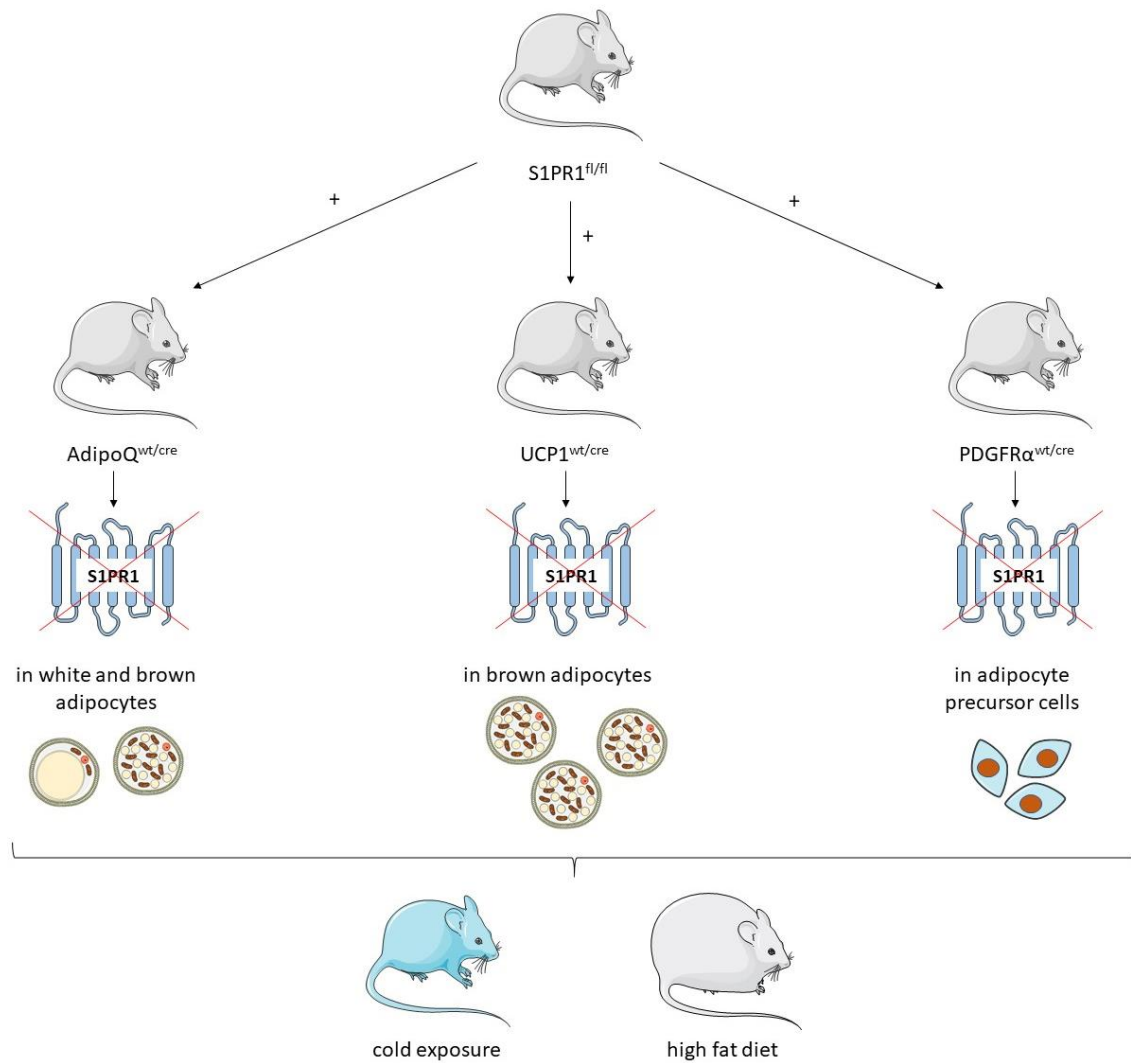


**Figure 35 | Plan for adipose tissue specific S1PR1 deletion**

S1PR1<sup>fl/fl</sup> mice are planned to be bred with mice expressing the enzyme Cre recombinase under the control of either adiponectin (AdipoQ<sup>wt/cre</sup>), uncoupling protein 1 (UCP1<sup>wt/cre</sup>) or platelet-derived growth factor receptor α (PDGFRα<sup>wt/cre</sup>) promoter control. Cold exposure and high fat diet (HFD) experiments are planned. This image was produced using templates of Servier Medical Art by Servier which are licensed under a Creative Commons Attribution 3.0 Unported License, <https://smart.servier.com>. (26.10.2019).

## 6 References

- Abdelaal, M., Le Roux, C.W., and Docherty, N.G. (2017). Morbidity and mortality associated with obesity. *Annals of Translational Medicine* 5.
- Adada, M., Canals, D., Hannun, Y.A., and Obeid, L.M. (2013). Sphingosine-1-phosphate receptor 2. *The FEBS journal* 280, 6354-6366.
- Agha, M., and Agha, R. (2017). The rising prevalence of obesity: part A: impact on public health. *International Journal of Surgery. Oncology* 2, e17.
- Al Alam, N., and Kreydiyyeh, S.I. (2016). FTY720P inhibits hepatic Na<sup>(+)</sup>-K<sup>(+)</sup> ATPase via S1PR2 and PGE2. *Biochemistry and cell biology = Biochimie et biologie cellulaire* 94, 371-377.
- Albi, E., Lazzarini, R., and Viola Magni, M. (2008). Phosphatidylcholine/sphingomyelin metabolism crosstalk inside the nucleus. *The Biochemical journal* 410, 381-389.
- Al-Goblan, A.S., Al-Alfi, M.A., and Khan, M.Z. (2014). Mechanism linking diabetes mellitus and obesity. *Diabetes, Metabolic Syndrome and Obesity: Targets and Therapy* 7, 587-591.
- Allende, M.L., Yamashita, T., and Proia, R.L. (2003). G-protein-coupled receptor S1P1 acts within endothelial cells to regulate vascular maturation. *Blood* 102, 3665-3667.
- Ayzenberg, I., Hoepner, R., and Kleiter, I. (2016). Fingolimod for multiple sclerosis and emerging indications: appropriate patient selection, safety precautions, and special considerations. *Therapeutics and Clinical Risk Management* 12, 261-272.
- Azzi, J.R., Sayegh, M.H., and Mallat, S.G. (2013). Calcineurin inhibitors: 40 years later, can't live without. *Journal of immunology (Baltimore, Md. : 1950)* 191, 5785-5791.
- Bartelt, A., Bruns, O.T., Reimer, R., Hohenberg, H., Ittrich, H., Peldschus, K., Kaul, M.G., Tromsdorf, U.I., Weller, H., and Waurisch, C., et al. (2011). Brown adipose tissue activity controls triglyceride clearance. *Nature medicine* 17, 200-205.
- Bartelt, A., and Heeren, J. (2014). Adipose tissue browning and metabolic health. *Nature reviews. Endocrinology* 10, 24-36.
- Basith, S., Cui, M., Macalino, S.J.Y., Park, J., Clavio, N.A.B., Kang, S., and Choi, S. (2018). Exploring G Protein-Coupled Receptors (GPCRs) Ligand Space via Cheminformatics Approaches: Impact on Rational Drug Design. *Frontiers in pharmacology* 9, 128.
- Becher, T., Palanisamy, S., Kramer, D.J., Marx, S.J., Wibmer, A.G., Del Gaudio, I., Butler, S.D., Jiang, C.S., Vaughan, R., and Schöder, H., et al. (2020). Brown Adipose Tissue is Associated with Improved Cardiometabolic Health and Regulates Blood Pressure.
- Berdyshev, E.V., Gorshkova, I., Skobeleva, A., Bittman, R., Lu, X., Dudek, S.M., Mirzapooiazova, T., Garcia, J.G.N., and Natarajan, V. (2009). FTY720 inhibits ceramide synthases and up-regulates dihydrosphingosine 1-phosphate formation in human lung endothelial cells. *The Journal of biological chemistry* 284, 5467-5477.
- Berry, R., and Rodeheffer, M.S. (2013). Characterization of the adipocyte cellular lineage in vivo. *Nature cell biology* 15, 302-308.
- Blackburn, S. (2011). Brown adipose tissue. *The Journal of perinatal & neonatal nursing* 25, 222-223.
- Blaho, V., Chun, J., Jonnalagadda, D., Kihara, Y., Mizuno, H., Mpamhanga, C., Spiegel, S., and Tan, V. (2019). Lysophospholipid (S1P) receptors (version 2019.4) in the IUPHAR/BPS Guide to Pharmacology Database. *GtoPdb CITE* 2019.
- Bode, C., and Gräler, M.H. (2012). Quantification of sphingosine-1-phosphate and related sphingolipids by liquid chromatography coupled to tandem mass spectrometry. *Methods in molecular biology (Clifton, N.J.)* 874, 33-44.
- Brinkmann, V., Cyster, J.G., and Hla, T. (2004). FTY720: sphingosine 1-phosphate receptor-1 in the control of lymphocyte egress and endothelial barrier function. *American journal of transplantation : official journal of the American Society of Transplantation and the American Society of Transplant Surgeons* 4, 1019-1025.
- Brinkmann, V., Davis, M.D., Heise, C.E., Albert, R., Cottens, S., Hof, R., Bruns, C., Prieschl, E., Baumruker, T., and Hiestand, P., et al. (2002). The immune modulator FTY720 targets sphingosine 1-phosphate receptors. *The Journal of biological chemistry* 277, 21453-21457.

- Buhl, A.M., Johnson, N.L., Dhanasekaran, N., and Johnson, G.L. (1995). G alpha 12 and G alpha 13 stimulate Rho-dependent stress fiber formation and focal adhesion assembly. *The Journal of biological chemistry* 270, 24631-24634.
- Cannon, B., and Nedergaard, J. (2004). Brown adipose tissue: function and physiological significance. *Physiological reviews* 84, 277-359.
- Christoffersen, C., Federspiel, C.K., Borup, A., Christensen, P.M., Madsen, A.N., Heine, M., Nielsen, C.H., Kjaer, A., Holst, B., and Heeren, J., et al. (2018). The Apolipoprotein M/S1P Axis Controls Triglyceride Metabolism and Brown Fat Activity. *Cell reports* 22, 175-188.
- Christoffersen, C., Obinata, H., Kumaraswamy, S.B., Galvani, S., Ahnström, J., Sevana, M., Egerer-Sieber, C., Muller, Y.A., Hla, T., and Nielsen, L.B., et al. (2011). Endothelium-protective sphingosine-1-phosphate provided by HDL-associated apolipoprotein M. *Proceedings of the National Academy of Sciences of the United States of America* 108, 9613-9618.
- Chun, J., Goetzl, E.J., Hla, T., Igarashi, Y., Lynch, K.R., Moolenaar, W., Pyne, S., and Tigyi, G. (2002). International Union of Pharmacology. XXXIV. Lysophospholipid receptor nomenclature. *Pharmacological reviews* 54, 265-269.
- Coelho, M., Oliveira, T., and Fernandes, R. (2013). Biochemistry of adipose tissue: an endocrine organ. *Archives of medical science : AMS* 9, 191-200.
- Cohen, P., Levy, J.D., Zhang, Y., Frontini, A., Kolodin, D.P., Svensson, K.J., Lo, J.C., Zeng, X., Ye, L., and Khandekar, M.J., et al. (2014). Ablation of PRDM16 and beige adipose causes metabolic dysfunction and a subcutaneous to visceral fat switch. *Cell* 156, 304-316.
- Csige, I., Ujvárosy, D., Szabó, Z., Lőrincz, I., Paragh, G., Harangi, M., and Somodi, S. (2018). The Impact of Obesity on the Cardiovascular System. *Journal of diabetes research* 2018, 3407306.
- Cyster, J.G., and Schwab, S.R. (2012). Sphingosine-1-phosphate and lymphocyte egress from lymphoid organs. *Annual review of immunology* 30, 69-94.
- Diederer, R.M.H., La Heij, E.C., Ittersum, M.M.-v., Kijlstra, A., Hendrikse, F., and Vente, J. de (2006). Selective blockade of phosphodiesterase types 2, 5 and 9 results in cyclic 3'5' guanosine monophosphate accumulation in retinal pigment epithelium cells. *The British Journal of Ophthalmology* 91, 379-384.
- Donati, C., and Bruni, P. (2006). Sphingosine 1-phosphate regulates cytoskeleton dynamics: implications in its biological response. *Biochimica et biophysica acta* 1758, 2037-2048.
- D'Orléans-Juste, P., Davenport, A.P., Godfraind, T., Maguire, J.J., Ohlstein, E.H., and Ruffolo, R.R. (2019). Endothelin receptors (version 2019.4) in the IUPHAR/BPS Guide to Pharmacology Database. *GtoPdb CITE* 2019.
- Emmett, M.J., Lim, H.-W., Jager, J., Richter, H.J., Adlanmerini, M., Peed, L.C., Briggs, E.R., Steger, D.J., Ma, T., and Sims, C.A., et al. (2017). Histone deacetylase 3 prepares brown adipose tissue for acute thermogenic challenge. *Nature* 546, 544-548.
- Farmer, S.R. (2006). Transcriptional control of adipocyte formation. *Cell metabolism* 4, 263-273.
- Fenzl, A., and Kiefer, F.W. (2014). Brown adipose tissue and thermogenesis. *Hormone molecular biology and clinical investigation* 19, 25-37.
- Floresta, G., Pistarà, V., Amata, E., Dichiara, M., Marrazzo, A., Prezzavento, O., and Rescifina, A. (2017). Adipocyte fatty acid binding protein 4 (FABP4) inhibitors. A comprehensive systematic review. *European journal of medicinal chemistry* 138, 854-873.
- Frayn, K.N., Karpe, F., Fielding, B.A., Macdonald, I.A., and Coppack, S.W. (2003). Integrative physiology of human adipose tissue. *International journal of obesity and related metabolic disorders : journal of the International Association for the Study of Obesity* 27, 875-888.
- Fukuhara, S., Simmons, S., Kawamura, S., Inoue, A., Orba, Y., Tokudome, T., Sunden, Y., Arai, Y., Moriwaki, K., and Ishida, J., et al. (2012). The sphingosine-1-phosphate transporter Spns2 expressed on endothelial cells regulates lymphocyte trafficking in mice. *The Journal of clinical investigation* 122, 1416-1426.
- Furuhashi, M., Saitoh, S., Shimamoto, K., and Miura, T. (2015). Fatty Acid-Binding Protein 4 (FABP4): Pathophysiological Insights and Potent Clinical Biomarker of Metabolic and Cardiovascular Diseases. *Clinical Medicine Insights. Cardiology* 8, 23-33.

- Gnad, T., Scheibler, S., Kügelgen, I. von, Scheele, C., Kilić, A., Glöde, A., Hoffmann, L.S., Reverte-Salisa, L., Horn, P., and Mutlu, S., et al. (2014). Adenosine activates brown adipose tissue and recruits beige adipocytes via A2A receptors. *Nature* *516*, 395-399.
- Gohlke, S., Zagoriy, V., Cuadros Inostroza, A., Méret, M., Mancini, C., Japtok, L., Schumacher, F., Kuhlow, D., Graja, A., and Stephanowitz, H., et al. (2019). Identification of functional lipid metabolism biomarkers of brown adipose tissue aging. *Molecular Metabolism* *24*, 1-17.
- Goncharov, N.V., Nadeev, A.D., Jenkins, R.O., and Avdonin, P.V. (2017). Markers and Biomarkers of Endothelium: When Something Is Rotten in the State. *Oxidative Medicine and Cellular Longevity* *2017*.
- Gonzalez-Cabrera, P.J., Hla, T., and Rosen, H. (2007). Mapping pathways downstream of sphingosine 1-phosphate subtype 1 by differential chemical perturbation and proteomics. *The Journal of biological chemistry* *282*, 7254-7264.
- Gosejacob, D., Jäger, P.S., Vom Dorp, K., Frejno, M., Carstensen, A.C., Köhnke, M., Degen, J., Dörmann, P., and Hoch, M. (2016). Ceramide Synthase 5 Is Essential to Maintain C16:0-Ceramide Pools and Contributes to the Development of Diet-induced Obesity. *The Journal of biological chemistry* *291*, 6989-7003.
- Graeler, M., and Goetzl, E.J. (2002). Activation-regulated expression and chemotactic function of sphingosine 1-phosphate receptors in mouse splenic T cells. *FASEB journal : official publication of the Federation of American Societies for Experimental Biology* *16*, 1874-1878.
- Gräler, M.H., Bernhardt, G., and Lipp, M. (1998). EDG6, a novel G-protein-coupled receptor related to receptors for bioactive lysophospholipids, is specifically expressed in lymphoid tissue. *Genomics* *53*, 164-169.
- Grundmann, M., Merten, N., Malfacini, D., Inoue, A., Preis, P., Simon, K., Rüttiger, N., Ziegler, N., Benkel, T., and Schmitt, N.K., et al. (2018). Lack of beta-arrestin signaling in the absence of active G proteins. *Nature communications* *9*, 341.
- Haas, B., Mayer, P., Jennissen, K., Scholz, D., Berriel Diaz, M., Bloch, W., Herzig, S., Fässler, R., and Pfeifer, A. (2009). Protein kinase G controls brown fat cell differentiation and mitochondrial biogenesis. *Science signaling* *2*, ra78.
- Heringdorf, D.M. zu, Vincent, M.E.M., Lipinski, M., Danneberg, K., Stropp, U., Wang, D.-a., Tigyi, G., and Jakobs, K.H. (2003). Inhibition of Ca(2+) signalling by the sphingosine 1-phosphate receptor S1P(1). *Cellular signalling* *15*, 677-687.
- Herr, D.R., Grillet, N., Schwander, M., Rivera, R., Müller, U., and Chun, J. (2007). Sphingosine 1-phosphate (S1P) signaling is required for maintenance of hair cells mainly via activation of S1P2. *The Journal of neuroscience : the official journal of the Society for Neuroscience* *27*, 1474-1478.
- Hla, T., and Dannenberg, A.J. (2012). Sphingolipid signaling in metabolic disorders. *Cell metabolism* *16*, 420-434.
- Hla, T., and Maciag, T. (1990). An abundant transcript induced in differentiating human endothelial cells encodes a polypeptide with structural similarities to G-protein-coupled receptors. *The Journal of biological chemistry* *265*, 9308-9313.
- Hla, T., Venkataraman, K., and Michaud, J. (2008). The vascular S1P gradient-cellular sources and biological significance. *Biochimica et biophysica acta* *1781*, 477-482.
- Hoffmann, L.S., Etzrodt, J., Willkomm, L., Sanyal, A., Scheja, L., Fischer, A.W.C., Stasch, J.-P., Bloch, W., Friebe, A., and Heeren, J., et al. (2015). Stimulation of soluble guanylyl cyclase protects against obesity by recruiting brown adipose tissue. *Nature communications* *6*, 7235.
- Holland, W.L., Miller, R.A., Wang, Z.V., Sun, K., Barth, B.M., Bui, H.H., Davis, K.E., Bikman, B.T., Halberg, N., and Rutkowski, J.M., et al. (2011). Receptor-mediated activation of ceramidase activity initiates the pleiotropic actions of adiponectin. *Nature medicine* *17*, 55-63.
- Hotamisligil, G.S., and Bernlohr, D.A. (2015). Metabolic functions of FABPs--mechanisms and therapeutic implications. *Nature reviews. Endocrinology* *11*, 592-605.
- Huang, H.-L., Hsing, H.-W., Lai, T.-C., Chen, Y.-W., Lee, T.-R., Chan, H.-T., Lyu, P.-C., Wu, C.-L., Lu, Y.-C., and Lin, S.-T., et al. (2010). Trypsin-induced proteome alteration during cell subculture in mammalian cells. *Journal of Biomedical Science* *17*, 36.
- Ibrahim, M.M. (2010). Subcutaneous and visceral adipose tissue: structural and functional differences. *Obesity reviews : an official journal of the International Association for the Study of Obesity* *11*, 11-18.

- Im, D.S., Heise, C.E., Ancellin, N., O'Dowd, B.F., Shei, G.J., Heavens, R.P., Rigby, M.R., Hla, T., Mandala, S., and McAllister, G., et al. (2000). Characterization of a novel sphingosine 1-phosphate receptor, Edg-8. *The Journal of biological chemistry* *275*, 14281-14286.
- Imasawa, T., Koike, K., Ishii, I., Chun, J., and Yatomi, Y. (2010). Blockade of sphingosine 1-phosphate receptor 2 signaling attenuates streptozotocin-induced apoptosis of pancreatic  $\beta$ -cells. *Biochemical and biophysical research communications* *392*, 207-211.
- Inagaki, T., Sakai, J., and Kajimura, S. (2016). Transcriptional and epigenetic control of brown and beige adipose cell fate and function. *Nature reviews. Molecular cell biology* *17*, 480-495.
- Jennissen, K., Haas, B., Kunz, W.S., and Pfeifer, A. (2011). cGMP and cAMP differentially regulate differentiation and function of brown adipocytes. *BMC Pharmacol* *11*, ra78.
- Jennissen, K., Haas, B., Mitschke, M.M., Siegel, F., and Pfeifer, A. (2013). Analysis of cGMP signaling in adipocytes. *Methods in molecular biology (Clifton, N.J.)* *1020*, 175-192.
- Jéquier, E., and Schutz, Y. (1988). Energy expenditure in obesity and diabetes. *Diabetes Metab. Rev.* *4*, 583-593.
- Jiang, L.I., Collins, J., Davis, R., Fraser, I.D., and Sternweis, P.C. (2008). Regulation of cAMP responses by the G12/13 pathway converges on adenylyl cyclase VII. *The Journal of biological chemistry* *283*, 23429-23439.
- Jiang, L.I., Collins, J., Davis, R., Lin, K.-M., DeCamp, D., Roach, T., Hsueh, R., Rebres, R.A., Ross, E.M., and Taussig, R., et al. (2007). Use of a cAMP BRET Sensor to Characterize a Novel Regulation of cAMP by the Sphingosine 1-Phosphate/G13 Pathway\**S*. *The Journal of biological chemistry* *282*, 10576-10584.
- Jolly, P.S., Rosenfeldt, H.M., Milstien, S., and Spiegel, S. (2002). The roles of sphingosine-1-phosphate in asthma. *Molecular immunology* *38*, 1239-1245.
- Kao, J.P.Y., Li, G., and Auston, D.A. (2010). Practical aspects of measuring intracellular calcium signals with fluorescent indicators. *Methods in cell biology* *99*, 113-152.
- Kawahara, A., Nishi, T., Hisano, Y., Fukui, H., Yamaguchi, A., and Mochizuki, N. (2009). The sphingolipid transporter spns2 functions in migration of zebrafish myocardial precursors. *Science (New York, N.Y.)* *323*, 524-527.
- Kershaw, E.E., and Flier, J.S. (2004). Adipose tissue as an endocrine organ. *The Journal of clinical endocrinology and metabolism* *89*, 2548-2556.
- Keul, P., Lucke, S., Wnuck Lipinski, K. von, Bode, C., Gräler, M., Heusch, G., and Levkau, B. (2011). Sphingosine-1-phosphate receptor 3 promotes recruitment of monocyte/macrophages in inflammation and atherosclerosis. *Circulation research* *108*, 314-323.
- Khaodhiar, L., McCowen, K.C., and Blackburn, G.L. (1999). Obesity and its comorbid conditions. *Clinical cornerstone* *2*, 17-31.
- Kim, S.-N., Jung, Y.-S., Kwon, H.-J., Seong, J.K., Granneman, J.G., and Lee, Y.-H. (2016). Sex differences in sympathetic innervation and browning of white adipose tissue of mice. *Biology of Sex Differences* *7*.
- Kim, Y.M., Lim, S.-C., Han, C.Y., Kay, H.Y., Cho, I.J., Ki, S.H., Lee, M.Y., Kwon, H.M., Lee, C.H., and Kim, S.G. (2011). G(alpha)12/13 induction of CYR61 in association with arteriosclerotic intimal hyperplasia: effect of sphingosine-1-phosphate. *Arteriosclerosis, thrombosis, and vascular biology* *31*, 861-869.
- King, L.K., March, L., and Anandacoomarasamy, A. (2013). Obesity & osteoarthritis. *The Indian Journal of Medical Research* *138*, 185-193.
- Kitada, Y., Kajita, K., Taguchi, K., Mori, I., Yamauchi, M., Ikeda, T., Kawashima, M., Asano, M., Kajita, T., and Ishizuka, T., et al. (2016a). Blockade of Sphingosine 1-Phosphate Receptor 2 Signaling Attenuates High-Fat Diet-Induced Adipocyte Hypertrophy and Systemic Glucose Intolerance in Mice. *Endocrinology* *157*, 1839-1851.
- Kitada, Y., Kajita, K., Taguchi, K., Mori, I., Yamauchi, M., Ikeda, T., Kawashima, M., Asano, M., Kajita, T., and Ishizuka, T., et al. (2016b). Blockade of Sphingosine 1-Phosphate Receptor 2 Signaling Attenuates High-Fat Diet-Induced Adipocyte Hypertrophy and Systemic Glucose Intolerance in Mice. *Endocrinology* *157*, 1839-1851.
- Kiyloğlu, N. (2017). Weight Loss and Fingolimod. *tnd* *23*, 250-251.

- Klepac, K., Kilić, A., Gnad, T., Brown, L.M., Herrmann, B., Wilderman, A., Balkow, A., Glöde, A., Simon, K., and Lidell, M.E., et al. (2016). The Gq signalling pathway inhibits brown and beige adipose tissue. *Nature communications* 7, 10895.
- Kobayashi, N., Kawasaki-Nishi, S., Otsuka, M., Hisano, Y., Yamaguchi, A., and Nishi, T. (2018). MFS2B is a sphingosine 1-phosphate transporter in erythroid cells. *Scientific reports* 8, 4969.
- Kong, X., Williams, K.W., and Liu, T. (2017). Genetic Mouse Models: The Powerful Tools to Study Fat Tissues. *Methods in molecular biology* (Clifton, N.J.) 1566, 99-107.
- Kono, M., Belyantseva, I.A., Skoura, A., Frolenkov, G.I., Starost, M.F., Dreier, J.L., Lidington, D., Bolz, S.-S., Friedman, T.B., and Hla, T., et al. (2007). Deafness and stria vascularis defects in S1P2 receptor-null mice. *The Journal of biological chemistry* 282, 10690-10696.
- Kowalski, G.M., Carey, A.L., Selathurai, A., Kingwell, B.A., and Bruce, C.R. (2013). Plasma sphingosine-1-phosphate is elevated in obesity. *PLoS one* 8, e72449.
- Kraynik, S.M., Miyaoka, R.S., and Beavo, J.A. (2013). PDE3 and PDE4 isozyme-selective inhibitors are both required for synergistic activation of brown adipose tissue. *Molecular pharmacology* 83, 1155-1165.
- Krueger, K.C., Costa, M.J., Du, H., and Feldman, B.J. (2014). Characterization of Cre Recombinase Activity for In Vivo Targeting of Adipocyte Precursor Cells. *Stem Cell Reports* 3, 1147-1158.
- Law, S.-H., Chan, M.-L., Marathe, G.K., Parveen, F., Chen, C.-H., and Ke, L.-Y. (2019). An Updated Review of Lysophosphatidylcholine Metabolism in Human Diseases. *International journal of molecular sciences* 20.
- Lee, M.J., van Brocklyn, J.R., Thangada, S., Liu, C.H., Hand, A.R., Menzeleev, R., Spiegel, S., and Hla, T. (1998). Sphingosine-1-phosphate as a ligand for the G protein-coupled receptor EDG-1. *Science (New York, N.Y.)* 279, 1552-1555.
- Lefterova, M.I., Zhang, Y., Steger, D.J., Schupp, M., Schug, J., Cristancho, A., Feng, D., Zhuo, D., Stoeckert, C.J., and Liu, X.S., et al. (2008). PPARgamma and C/EBP factors orchestrate adipocyte biology via adjacent binding on a genome-wide scale. *Genes & development* 22, 2941-2952.
- Lindström, P. (2007). The physiology of obese-hyperglycemic mice ob/ob mice. *TheScientificWorldJournal* 7, 666-685.
- Liu, L., and Shi, G.-P. (2012). CD31: beyond a marker for endothelial cells. *Cardiovascular research* 94, 3-5.
- Liu, Y., Wada, R., Yamashita, T., Mi, Y., Deng, C.X., Hobson, J.P., Rosenfeldt, H.M., Nava, V.E., Chae, S.S., and Lee, M.J., et al. (2000). Edg-1, the G protein-coupled receptor for sphingosine-1-phosphate, is essential for vascular maturation. *The Journal of clinical investigation* 106, 951-961.
- Lobstein, T., Jackson-Leach, R., Moodie, M.L., Hall, K.D., Gortmaker, S.L., Swinburn, B.A., James, W.P.T., Wang, Y., and McPherson, K. (2015). Child and adolescent obesity: part of a bigger picture. *Lancet (London, England)* 385, 2510-2520.
- Loncar, D. (1991). Convertible adipose tissue in mice. *Cell and tissue research* 266, 149-161.
- Lovren, F., Teoh, H., and Verma, S. (2015). Obesity and atherosclerosis: mechanistic insights. *The Canadian journal of cardiology* 31, 177-183.
- Matloubian, M., Lo, C.G., Cinamon, G., Lesneski, M.J., Xu, Y., Brinkmann, V., Allende, M.L., Proia, R.L., and Cyster, J.G. (2004). Lymphocyte egress from thymus and peripheral lymphoid organs is dependent on S1P receptor 1. *Nature* 427, 355-360.
- Mendelson, K., Evans, T., and Hla, T. (2014). Sphingosine 1-phosphate signalling. *Development (Cambridge, England)* 141, 5-9.
- Michaud, J., Im, D.-S., and Hla, T. (2010). Inhibitory role of sphingosine 1-phosphate receptor 2 in macrophage recruitment during inflammation. *Journal of immunology* (Baltimore, Md. : 1950) 184, 1475-1483.
- Mitschke, M.M., Hoffmann, L.S., Gnad, T., Scholz, D., Kruithoff, K., Mayer, P., Haas, B., Sassmann, A., Pfeifer, A., and Kilic, A. (2013). Increased cGMP promotes healthy expansion and browning of white adipose tissue. *FASEB journal : official publication of the Federation of American Societies for Experimental Biology* 27, 1621-1630.
- Moon, M.H., Jeong, J.K., Lee, J.H., Park, Y.G., Lee, Y.J., Seol, J.W., and Park, S.Y. (2012). Antiobesity activity of a sphingosine 1-phosphate analogue FTY720 observed in adipocytes and obese mouse model. *Experimental & molecular medicine* 44, 603-614.

- Moon, M.-H., Jeong, J.-K., Lee, Y.-J., Seol, J.-W., and Park, S.-Y. (2014). Sphingosine-1-phosphate inhibits the adipogenic differentiation of 3T3-L1 preadipocytes. *International journal of molecular medicine* *34*, 1153-1158.
- Moon, M.-H., Jeong, J.-K., and Park, S.-Y. (2015). Activation of S1P2 receptor, a possible mechanism of inhibition of adipogenic differentiation by sphingosine 1-phosphate. *Molecular medicine reports* *11*, 1031-1036.
- Neal, J.W., and Clipstone, N.A. (2002). Calcineurin Mediates the Calcium-dependent Inhibition of Adipocyte Differentiation in 3T3-L1 Cells. *J. Biol. Chem.* *277*, 49776-49781.
- Neeland, I.J., Ayers, C.R., Rohatgi, A.K., Turer, A.T., Berry, J.D., Das, S.R., Vega, G.L., Khera, A., McGuire, D.K., and Grundy, S.M., et al. (2013). Associations of visceral and abdominal subcutaneous adipose tissue with markers of cardiac and metabolic risk in obese adults. *Obesity (Silver Spring, Md.)* *21*, E439-47.
- Neves, S.R., Ram, P.T., and Iyengar, R. (2002). G protein pathways. *Science (New York, N.Y.)* *296*, 1636-1639.
- Obinata, H., and Hla, T. (2012). Sphingosine 1-phosphate in coagulation and inflammation. *Seminars in immunopathology* *34*, 73-91.
- Okamatsu-Ogura, Y., Fukano, K., Tsubota, A., Uozumi, A., Terao, A., Kimura, K., and Saito, M. (2013). Thermogenic ability of uncoupling protein 1 in beige adipocytes in mice. *PLoS one* *8*, e84229.
- O'Sullivan, C., and Dev, K.K. (2013). The structure and function of the S1P1 receptor. *Trends in pharmacological sciences* *34*, 401-412.
- Ouakinin, S.R.S., Barreira, D.P., and Gois, C.J. (2018). Depression and Obesity: Integrating the Role of Stress, Neuroendocrine Dysfunction and Inflammatory Pathways. *Frontiers in endocrinology* *9*.
- Parham, K.A., Zebol, J.R., Tooley, K.L., Sun, W.Y., Moldenhauer, L.M., Cockshell, M.P., Gliddon, B.L., Moretti, P.A., Tigyi, G., and Pitson, S.M., et al. (2015). Sphingosine 1-phosphate is a ligand for peroxisome proliferator-activated receptor- $\gamma$  that regulates neoangiogenesis. *FASEB journal : official publication of the Federation of American Societies for Experimental Biology* *29*, 3638-3653.
- Paschos, G.K., Tang, S.Y., Theken, K.N., Li, X., Verginadis, I., Lekkas, D., Herman, L., Yan, W., Lawson, J., and FitzGerald, G.A. (2018). Cold-Induced Browning of Inguinal White Adipose Tissue Is Independent of Adipose Tissue Cyclooxygenase-2. *Cell reports* *24*, 809-814.
- Patmanathan, S.N., Wang, W., Yap, L.F., Herr, D.R., and Paterson, I.C. (2017). Mechanisms of sphingosine 1-phosphate receptor signalling in cancer. *Cellular signalling* *34*, 66-75.
- Pergola, G. de, and Silvestris, F. (2013). Obesity as a Major Risk Factor for Cancer. *Journal of Obesity* *2013*.
- Pfeifer, A., and Hoffmann, L.S. (2015). Brown, beige, and white: the new color code of fat and its pharmacological implications. *Annual review of pharmacology and toxicology* *55*, 207-227.
- Pischon, T., and Sharma, A.M. (2001). Use of beta-blockers in obesity hypertension: potential role of weight gain. *Obesity Reviews* *2*, 275-280.
- Poti, J.M., Braga, B., and Qin, B. (2017). Ultra-processed Food Intake and Obesity: What Really Matters for Health – Processing or Nutrient Content? *Current obesity reports* *6*, 420-431.
- Proia, R.L., and Hla, T. (2015). Emerging biology of sphingosine-1-phosphate: its role in pathogenesis and therapy. *The Journal of clinical investigation* *125*, 1379-1387.
- Quintanilla Rodriguez, B.S., and Correa, R. (2019). StatPearls. Rosiglitazone (Treasure Island (FL)).
- Ramstedt, B., and Slotte, J.P. (2002). Membrane properties of sphingomyelins. *FEBS Letters* *531*, 33-37.
- Ravichandran, S., Finlin, B.S., Kern, P.A., and Özcan, S. (2019). Sphk2<sup>-/-</sup> mice are protected from obesity and insulin resistance. *Biochimica et biophysica acta. Molecular basis of disease* *1865*, 570-576.
- Rivera, R., and Chun, J. (2008). Biological effects of lysophospholipids. *Reviews of physiology, biochemistry and pharmacology* *160*, 25-46.
- Ruiz, M., Okada, H., and Dahlbäck, B. (2017). HDL-associated ApoM is anti-apoptotic by delivering sphingosine 1-phosphate to S1P1 & S1P3 receptors on vascular endothelium. *Lipids in Health and Disease* *16*.

- Ruiz-Ojeda, F.J., Rupérez, A.I., Gomez-Llorente, C., Gil, A., and Aguilera, C.M. (2016). Cell Models and Their Application for Studying Adipogenic Differentiation in Relation to Obesity: A Review. *International journal of molecular sciences* *17*.
- Russell, W.M.S., and Burch, R.L. (1992). *The principles of humane experimental technique* (Potters Bar, Herts: Universities Federation for Animal Welfare).
- Salviato Balbão, M., Cecílio Hallak, J.E., Arcoverde Nunes, E., Homem de Mello, M., Triffoni-Melo, A.d.T., Ferreira, F.I.d.S., Chaves, C., Durão, A.M.S., Ramos, A.P.P., and Souza Crippa, J.A. de, et al. (2014). Olanzapine, weight change and metabolic effects: a naturalistic 12-month follow up. *Therapeutic Advances in Psychopharmacology* *4*, 30-36.
- Sanchez, T., Skoura, A., Wu, M.T., Casserly, B., Harrington, E.O., and Hla, T. (2007). Induction of vascular permeability by the sphingosine-1-phosphate receptor-2 (S1P2R) and its downstream effectors ROCK and PTEN. *Arteriosclerosis, thrombosis, and vascular biology* *27*, 1312-1318.
- Sánchez-Fernández, G., Cabezudo, S., García-Hoz, C., Benincá, C., Aragay, A.M., Mayor, F., and Ribas, C. (2014). Gαq signalling: the new and the old. *Cellular signalling* *26*, 833-848.
- Sanyal, A., Naumann, J., Hoffmann, L.S., Chabowska-Kita, A., Ehrlund, A., Schlitzer, A., Arner, P., Blüher, M., and Pfeifer, A. (2017). Interplay between Obesity-Induced Inflammation and cGMP Signaling in White Adipose Tissue. *Cell reports* *18*, 225-236.
- Sanyal, D., and Raychaudhuri, M. (2016). Hypothyroidism and obesity: An intriguing link. *Indian Journal of Endocrinology and Metabolism* *20*, 554-557.
- Sarwar, R., Pierce, N., and Koppe, S. (2018). Obesity and nonalcoholic fatty liver disease: current perspectives. *Diabetes, Metabolic Syndrome and Obesity: Targets and Therapy* *11*, 533-542.
- Schrage, R., Schmitz, A.-L., Gaffal, E., Annala, S., Kehraus, S., Wenzel, D., Büllsbach, K.M., Bald, T., Inoue, A., and Shinjo, Y., et al. (2015). The experimental power of FR900359 to study Gq-regulated biological processes. *Nature communications* *6*, 10156.
- Schröder, R., Schmidt, J., Blättermann, S., Peters, L., Janssen, N., Grundmann, M., Seemann, W., Kaufel, D., Merten, N., and Drewke, C., et al. (2011). Applying label-free dynamic mass redistribution technology to frame signaling of G protein-coupled receptors noninvasively in living cells. *Nature protocols* *6*, 1748-1760.
- Seale, P., Bjork, B., Yang, W., Kajimura, S., Chin, S., Kuang, S., Scimè, A., Devarakonda, S., Conroe, H.M., and Erdjument-Bromage, H., et al. (2008). PRDM16 controls a brown fat/skeletal muscle switch. *Nature* *454*, 961-967.
- Shao, M., Hepler, C., Vishvanath, L., MacPherson, K.A., Busbuso, N.C., and Gupta, R.K. (2016). Fetal development of subcutaneous white adipose tissue is dependent on Zfp423. *Molecular Metabolism* *6*, 111-124.
- Shao, M., Wang, Q.A., Song, A., Vishvanath, L., Busbuso, N.C., Scherer, P.E., and Gupta, R.K. (2019). Cellular Origins of Beige Fat Cells Revisited. *Diabetes* *68*, 1874-1885.
- Sharma, A.M., and Padwal, R. (2010). Obesity is a sign - over-eating is a symptom: an aetiological framework for the assessment and management of obesity. *Obesity reviews : an official journal of the International Association for the Study of Obesity* *11*, 362-370.
- Shin, W., Okamatsu-Ogura, Y., Matsuoka, S., Tsubota, A., and Kimura, K. (2019). Impaired adrenergic agonist-dependent beige adipocyte induction in obese mice. *The Journal of veterinary medical science* *81*, 799-807.
- Smith, N.J., and Milligan, G. (2010). Allosteric at G protein-coupled receptor homo- and heteromers: uncharted pharmacological landscapes. *Pharmacological reviews* *62*, 701-725.
- Spiegel, S., Maczys, M.A., Maceyka, M., and Milstien, S. (2019). New insights into functions of the sphingosine-1-phosphate transporter SPNS2. *Journal of lipid research* *60*, 484-489.
- Spiegel, S., and Milstien, S. (2003). Sphingosine-1-phosphate: an enigmatic signalling lipid. *Nature reviews. Molecular cell biology* *4*, 397-407.
- Sriram, K., and Insel, P.A. (2018). G Protein-Coupled Receptors as Targets for Approved Drugs: How Many Targets and How Many Drugs? *Molecular pharmacology* *93*, 251-258.
- Steinhilber, D., Schubert-Zsilavecz, M., and Roth, H.J. (2010). *Medizinische Chemie* (Stuttgart: Dt. Apotheker-Verl.).

- Sun, W., Dong, H., Becker, A.S., Dapito, D.H., Modica, S., Grandl, G., Opitz, L., Efthymiou, V., Straub, L.G., and Sarker, G., et al. (2018). Cold-induced epigenetic programming of the sperm enhances brown adipose tissue activity in the offspring. *Nature medicine* *24*, 1372-1383.
- Sun, X., Singleton, P.A., Letsiou, E., Zhao, J., Belvitch, P., Sammani, S., Chiang, E.T., Moreno-Vinasco, L., Wade, M.S., and Zhou, T., et al. (2012). Sphingosine-1-phosphate receptor-3 is a novel biomarker in acute lung injury. *American journal of respiratory cell and molecular biology* *47*, 628-636.
- Terai, K., Soga, T., Takahashi, M., Kamohara, M., Ohno, K., Yatsugi, S., Okada, M., and Yamaguchi, T. (2003). Edg-8 receptors are preferentially expressed in oligodendrocyte lineage cells of the rat CNS. *Neuroscience* *116*, 1053-1062.
- (2013). The Genotype-Tissue Expression (GTEx) project. *Nature genetics* *45*, 580-585.
- Trayhurn, P., and Beattie, J.H. (2001). Physiological role of adipose tissue: white adipose tissue as an endocrine and secretory organ. *The Proceedings of the Nutrition Society* *60*, 329-339.
- Trinquet, E., Fink, M., Bazin, H., Grillet, F., Maurin, F., Bourrier, E., Ansanay, H., Leroy, C., Michaud, A., and Durroux, T., et al. (2006). D-myo-inositol 1-phosphate as a surrogate of D-myo-inositol 1,4,5-tris phosphate to monitor G protein-coupled receptor activation. *Analytical biochemistry* *358*, 126-135.
- Trzaskowski, B., Latek, D., Yuan, S., Ghoshdastider, U., Debinski, A., and Filipek, S. (2012). Action of molecular switches in GPCRs--theoretical and experimental studies. *Current medicinal chemistry* *19*, 1090-1109.
- Tukijan, F., Chandrakanthan, M., and Nguyen, L.N. (2018). The signalling roles of sphingosine-1-phosphate derived from red blood cells and platelets. *British journal of pharmacology* *175*, 3741-3746.
- Venkataraman, K., Lee, Y.-M., Michaud, J., Thangada, S., Ai, Y., Bonkovsky, H.L., Parikh, N.S., Habrukowich, C., and Hla, T. (2008). Vascular endothelium as a contributor of plasma sphingosine 1-phosphate. *Circulation research* *102*, 669-676.
- Vijgen, G.H.E.J., Bouvy, N.D., Teule, G.J.J., Brans, B., Schrauwen, P., and van Marken Lichtenbelt, W.D. (2011). Brown adipose tissue in morbidly obese subjects. *PLoS one* *6*, e17247.
- Virtanen, K.A., Lidell, M.E., Orava, J., Heglind, M., Westergren, R., Niemi, T., Taittonen, M., Laine, J., Savisto, N.-J., and Enerbäck, S., et al. (2009). Functional brown adipose tissue in healthy adults. *The New England journal of medicine* *360*, 1518-1525.
- Vu, T.M., Ishizu, A.-N., Foo, J.C., Toh, X.R., Zhang, F., Whee, D.M., Torta, F., Cazenave-Gassiot, A., Matsumura, T., and Kim, S., et al. (2017). Mfsd2b is essential for the sphingosine-1-phosphate export in erythrocytes and platelets. *Nature* *550*, 524-528.
- Walsh, C.T., Stupack, D., and Brown, J.H. (2008). G protein-coupled receptors go extracellular: RhoA integrates the integrins. *Molecular interventions* *8*, 165-173.
- Watters, R.J., Wang, H.-G., Sung, S.-S., Loughran, T.P., and Liu, X. (2011). Targeting Sphingosine-1-Phosphate Receptors in Cancer. *Anti-cancer agents in medicinal chemistry* *11*, 810-817.
- Weske, S., Vaidya, M., Reese, A., Wnuck Lipinski, K. von, Keul, P., Bayer, J.K., Fischer, J.W., Flögel, U., Nelsen, J., and Epple, M., et al. (2018). Targeting sphingosine-1-phosphate lyase as an anabolic therapy for bone loss. *Nature medicine* *24*, 667-678.
- Wilkerson, B.A., Grass, G.D., Wing, S.B., Argraves, W.S., and Argraves, K.M. (2012). Sphingosine 1-phosphate (S1P) carrier-dependent regulation of endothelial barrier: high density lipoprotein (HDL)-S1P prolongs endothelial barrier enhancement as compared with albumin-S1P via effects on levels, trafficking, and signaling of S1P1. *The Journal of biological chemistry* *287*, 44645-44653.
- World Health Organization (WHO) (2020). Fact sheet - Obesity and overweight. <https://www.who.int/news-room/fact-sheets/detail/obesity-and-overweight>. 27.04.2020.
- Yan, X., Wang, J., Zhu, Y., Feng, W., Zhai, C., Liu, L., Shi, W., Wang, Q., Zhang, Q., and Chai, L., et al. (2019). S1P induces pulmonary artery smooth muscle cell proliferation by activating calcineurin/NFAT/OPN signaling pathway. *Biochemical and biophysical research communications* *516*, 921-927.
- Yoneshiro, T., Aita, S., Matsushita, M., Kameya, T., Nakada, K., Kawai, Y., and Saito, M. (2011). Brown adipose tissue, whole-body energy expenditure, and thermogenesis in healthy adult men. *Obesity (Silver Spring, Md.)* *19*, 13-16.

Yu, W.-H., Li, F.-G., Chen, X.-Y., Li, J.-T., Wu, Y.-H., Huang, L.-H., Wang, Z., Li, P., Wang, T., and Lahn, B.T., et al. (2012). PPAR $\gamma$  suppression inhibits adipogenesis but does not promote osteogenesis of human mesenchymal stem cells. *The international journal of biochemistry & cell biology* *44*, 377-384.

Yupanqui-Lozno, H., Bastarrachea, R.A., Yupanqui-Velazco, M.E., Alvarez-Jaramillo, M., Medina-Méndez, E., Giraldo-Peña, A.P., Arias-Serrano, A., Torres-Forero, C., García-Ordoñez, A.M., and Mastronardi, C.A., et al. (2019). Congenital Leptin Deficiency and Leptin Gene Missense Mutation Found in Two Colombian Sisters with Severe Obesity. *Genes* *10*.

Zondag, G.C., Postma, F.R., Etten, I.V., Verlaan, I., and Moolenaar, W.H. (1998). Sphingosine 1-phosphate signalling through the G-protein-coupled receptor Edg-1. *The Biochemical journal* *330* ( Pt 2), 605-609.

## Summary

Obesity is a worldwide health issue with increasing numbers of patients every year. Moreover, the prevalence of obesity gives rise to related cardiovascular diseases and various other comorbidities influencing quality of life and burdening the healthcare systems. To date no pharmacological therapy exists to treat obesity. Therefore, new biological targets for therapy of the obesity pandemic are extensively searched for. In recent years brown adipose tissue has attracted attention in the scientific community due to its ability to burn calories in form of fat and transform them into heat. Activation of brown adipocytes or transformation of white adipocytes into 'brown-like' beige adipocytes could be a new way of treating excess overweight.

Sphingosine-1-phosphate (S1P) is a versatile biological messenger involved in a plethora of physiological functions. It agonizes five different G protein-coupled Sphingosine-1-phosphate receptors (S1PRs) which are broadly expressed throughout human and murine tissues. The role of S1P in the immune system is already quite well elucidated whereas the knowledge about the role of S1P in obesity is still in its infancy.

This study broadly investigates the role of S1P and S1PRs in brown and white adipocytes, as well as in adipose tissues and attempts to give an overview of the different most important S1PRs, their function and their downstream signaling moieties.

In this work it was found that all known five Sphingosine-1-phosphate receptors (S1PRs) are expressed in murine brown and white adipocytes.

*In vitro*, chronic S1P treatment decreases adipogenesis of brown and white adipocytes. Signaling not only via Sphingosine-1-phosphate receptor 2 (S1PR2) but also via Sphingosine-1-phosphate receptor 1 (S1PR1) inhibits the differentiation of brown adipocytes. Putative underlying downstream signaling mechanisms of S1P might include activation of  $G_i$ ,  $G_q$  and  $G_{12/13}$  pathways. Furthermore, S1P potently increases intracellular calcium in brown preadipocytes in a  $G_q$  dependent manner.

The expression of S1PR1 and S1PR2 in adipose tissues is differentially regulated during high fat diet or cold exposure. To evaluate if pharmacological modulation of S1PR1 or S1PR2 has therapeutic potential, mice were injected for one week with compounds targeting S1PR1 and S1PR2. Agonism of S1PR2 diminishes fat tissue mass presenting S1PR2 agonism as a potential treatment against obesity.

Overall, this thesis reveals that S1P imposes promising actions on adipose tissues. It is of value to uncover the full potential of S1P receptor modulation as a novel target for combating obesity.

## Abstracts

The 2019 FASEB Science Research Conference on Lysophospholipid and Related Mediators: From Bench to Clinic, Lisbon, Portugal, poster presentation “The role of Sphingosine-1-phosphate (S1P) receptors in brown adipocytes”

International Symposium of the DFG Research Training Group 1873, 2019, pharmacology of 7-TM receptors and downstream signaling pathways, Bonn, Germany, poster presentation “The role of Sphingosine-1-phosphate (S1P) receptors in adipocytes and adipose tissue (Poster)”